A Framework for Dissecting and Applying Bacterial Antibiotic Responses

by

Hannah Ruth Brittany Meredith

Department of Biomedical Engineering
Duke University

Date:_____

Approved:

_____
Lingchong You, Supervisor

_____
Deverick Anderson

_____
Lawrence David

_____
Charles Gersbach

_____
Brenton Hoffman

Dissertation submitted in partial fulfillment of
the requirements for the degree of Doctor
of Philosophy in the Department of
Biomedical Engineering in the Graduate School
of Duke University

2017

ABSTRACT

A Framework for Dissecting and Applying Bacterial Antibiotic Responses

by

Hannah Ruth Brittany Meredith

Department of Biomedical Engineering
Duke University

Date:_____

Approved:

_____
Lingchong You, Supervisor

_____
Deverick Anderson

_____
Lawrence David

_____
Charles Gersbach

_____
Brenton Hoffman

An abstract of a dissertation submitted in partial fulfillment of the requirements for the degree of Doctor of Philosophy in the Department of Biomedical Engineering in the Graduate School of Duke University

2017

Abstract

An essential property of microbial communities is the ability to survive a disturbance. This is readily observed in bacteria, which have developed the ability to survive every antibiotic treatment at an alarming rate, considering the timescale at which new antibiotics are developed. Thus, there is a critical need to use antibiotics more effectively, extend the shelf life of existing antibiotics and minimize their side effects. This requires understanding the mechanisms underlying bacterial drug responses. Past studies have focused on survival in the presence of antibiotics by individual cells, such as genetic mutants. Also important, however, is the fact that a population of bacterial cells can collectively survive antibiotic treatments lethal to individual cells. This tolerance can arise by diverse mechanisms, including resistance-conferring enzyme production, titration-mediated bistable growth inhibition, swarming and interpopulation interactions. These strategies can enable rapid population recovery after antibiotic treatment and provide a time window during which otherwise susceptible bacteria can acquire inheritable genetic resistance.

To further explore bacterial antibiotic responses, I focused on bacteria producing β-lactamase, an enzyme that has drastically limited the use of our most commonly prescribed antibiotics: β-lactams. Through the characterization of clinical isolates and a computational model, my Ph.D. thesis has three implications:

First, survival can be achieved through *resistance*, the ability to absorb effects of a disturbance without a significant change, or *resilience*, the ability to recover after being perturbed by a disturbance. Current practices for determining the antibiotic sensitivity of bacteria do not characterize a population as resistant and/or resilient, they only report whether the bacteria can survive the antibiotic exposure. As resistance and resilience often depend on different attributes, distinguishing between these two modes of survival could inform treatment strategies. These concepts have long been applied to the analysis of ecological systems, though their interpretations are often subject to debate. This framework readily lends itself to the dissection of the bacterial response to antibiotic treatment, where both terms can be unambiguously defined.

Second, the ability to tolerate the antibiotic treatment in the short term corresponds to resistance, which primarily depends on traits associated with individual cells. In contrast, the ability to recover after being perturbed by an antibiotic corresponds to resilience, which primarily depends on traits associated with the population.

And finally, understanding the temporal dynamics of an antibiotic response could guide the design of a dosing protocol to optimize treatment efficiency for any antibiotic-pathogen combination. Ultimately, optimized dosing protocols could allow reintroduction of a repertoire of first-line antibiotics with improved treatment outcomes and preserve last-resort antibiotics.

Dedication

To Dr. Ruth Clemo and Dr. Alex Meredith, who are not only my parents, but also my colleagues, best friends, supporters, and role models. They pushed me to reach heights I did not know I could attain, encouraged me patiently while I searched for my passion, and celebrated when I took off on my own. Thank you for showing me the world, cultivating my love for interesting conversations, and telling me all those bedtime biology stories.

Contents

List of Tables

List of Figures

Acknowledgements

I would like to thank Dr. Lingchong You for inviting me to join his lab and for his continued support over the past 5 years. His optimism, critical thinking, knack for telling a compelling scientific story, and sense of humor have kept me going through the thick and thin of grad school. When work was difficult and confusing, he would crack a joke about my "recovery time" getting shorter as I got better at processing the situation and plotting a new research path forward. He has given me the freedom, the encouragement, and the tools to explore my passion: tackling antibiotic resistance. I am incredibly grateful for his mentorship and consider this only the beginning of what I hope to be a life-long collaboration and friendship.

I could not have dreamed of having a better collaborator than Virgile Andreani. We formed a collaboration to work on my thesis project about 3.5 years into my PhD. At that point, I had hit rock-bottom in terms of motivation and was having trouble seeing a way forward with my work. Virgile's genuine curiosity, logical way of thinking things through, and incredible ability for computational modeling really lifted me out of doldrums of grad school and breathed life back into my own passion for research. He has made himself available practically around the clock to discuss ideas, give me second opinions on methods, and provide feedback on anything from my modeling to my manuscripts. I am eternally grateful for Virgile's commitment to this work.

When I signed up to be a teaching assistant for Dr. Lisa Satterwhite, I had no idea I would also be getting a friend, role model, and mentor. Lisa's outlook and passion for

her research is contagious and inspiring. After TAing for her twice, Lisa and I continued to get together to talk about my research progress, career aspirations, and personal well-being. Lisa is one of the most motivated, curious, kind, caring, and smart people I have had the privilege of getting to know while at Duke.

Dr. Deverick Anderson has played a crucial role in facilitating my passion for public health. I first met Dev when I was seeking an MD's perspective for my antibiotic resistance computational model. As head of the Antimicrobial Stewardship Team at Duke Hospital, he helped ground my research and make it (somewhat) more clinically translational. After expressing my interest in working with the Center for Disease Control (CDC) to improve the way we use antibiotics, Dev introduced me to someone at the CDC who completely revolutionized my career goals. I am grateful for Dev's mentoring and network, which helped me discover how to apply my engineering background in a public health arena.

Joining the Duke Global Health Institute for a doctoral certificate was one of the best decisions I made during my PhD. The department was welcoming beyond belief and became like a second academic family for me. The classes opened my eyes to global health issues beyond antibiotic resistance as well as the wide array of approaches used to tackle them. Through the certificate program, I had the opportunity to complete 4 weeks of field work in Sri Lanka under the mentorship of Dr. Gayani Tillekeratne. These 4 weeks were transformative, confirming my desire to work in the field on urgent health

issues. It gave me the experience of working in a foreign country, under very different lab/work conditions, and helped me form some lifelong friendships and memories.

I am forever grateful for the support of my family and all the friends I have formed during grad school. My parents, Ruth and Alex, have both gone through grad school and could relate to my successes, pitfalls, and frustrations. They were always there for me, ready to comfort, celebrate, and encourage. I am so lucky that my siblings, Sam and Kate, have also become some of my best friends. It has been an incredible journey growing up together and I love that we continue to keep each other involved in our lives, despite being in completely different parts of the country. Thank you for always being ready to goof off, go on adventures, and be there when I need you.

My dad always advised me to surround myself with brilliant people, because it would help me achieve things I could not imagine doing otherwise. I could not have been luckier to have Allison Loptakin and Will Cao as my labmates. They turned out to be some of my closest friends and colleagues. When Allie and I get together, we dive into intense conversations that span everything from hair-brained science ideas to religion to cooking to the subjective meaning of taking a risk. Allie is one of the most brilliant, motivated, and selfless scientists that I have had the pleasure of working with. She inspires me to set my expectations higher and push myself to excel. I predict that she will go on to do remarkable things, wherever she decides to go. Will and I started in Lingchong's lab at the same time and her humor, cleverness, and thoughtfulness were apparent from the start. We have experienced a lot together- whether it is toughing it out

in lab when nothing seems to work, learning to define who we are and what we want out of life, or traveling around the world. Will's curiosity and sense of adventure have helped keep my love for trying new things alive.

Last but not least, I could not have made it through without my best friends: Lauren Czaplicki, Nikki Pelot, and Manu Raghavan. Lauren and I met in our first year at Duke and have been inseparable ever since, cooking for each other frequently, going on runs, and exploring Durham together. We have celebrated each other's successes and supported each other through setbacks, both in lab and in life. She has taught me how to speak my mind, be more self-confident, and recognize and uphold personal standards. Thank you, Lauren, for making me mature into the researcher, and friend I am today. Your passion, opinions, and tenacity have always been and continue to inspire me.

The friendship I have with Nikki is one of my oldest and strongest from Duke. When we met on our recruitment weekend, her personal drive caught my attention. Time and time again, I have been motivated by the way Nikki gives 110% of her efforts in lab, to the community, and to her friends and family. I was fortunate to have Nikki's support, compassion, and pragmatism to help me navigate my time in grad school. I am so grateful, especially, for the way she made me feel less alone and daunted during the final weeks leading up to my defense.

Manu has been a constant source of logic, encouragement, and humor for me. He has seen me at my lowest, but never lost faith in my potential as a researcher and a person. His love for science, current events, books, and music has been a constant

reminder for me to keep seeking out knowledge in all forms. Manu's uncanny ability to diffuse my stressful situations through teasing has also helped me start to look at research and life in a new light.

I cannot help but make a corny reference to my thesis: I am where I am today because of collective tolerance. With the support of all my family, friends, and mentors, I can achieve so much more than I could on my own.

1. Introduction

Currently, bacterial antibiotic responses are categorized as sensitive, intermediate, or resistant based on the absence or presence of growth after a set exposure time to a set antibiotic dose. However, temporal dynamics reveal that antibiotic responses are more complex, involving varying degrees of resistance and resilience. The ability to quantify and identify the determinants for these differing responses is crucial for predicting how bacteria will respond to a treatment. Although resistance and resilience have been defined in the literature for decades, the resistance-resilience framework has not been widely applied. This is partially because it is often difficult to determine the pre-disturbance state of a population, the definitions vary, and there is a lack of quantitative studies demonstrating how to implement these terms.

To quantify these responses, we developed and applied metrics using clinical isolates producing β-lactamase and a kinetic model. These metrics can be used to dissect the responses of other systems and guide the optimization of treatment strategies.

1.1 Objectives

The objectives of my thesis are to (1) develop a resistance-resilience framework for dissecting bacterial antibiotic responses and (2) demonstrate how capturing the temporal dynamics of an antibiotic response can guide the optimization of multi-dose treatments. Specifically:

Objective 1: Develop a resistance-resilience framework for antibiotic responses

This includes: characterizing the antibiotic response of clinical isolates producing β-lactamase; developing a kinetic model to further explore the effectors of resistance and resilience; apply resistance-resilience framework in dissecting antibiotic responses to identify optimal treatment strategies.

Objective 2: Use temporal dynamics of the antibiotic response to optimize multi-dosing protocols

This includes: developing a kinetic model that captures the characteristic response of isolates producing β-lactamase (Bla) exposed to a β-lactam; formulating a metric that captures the temporal dynamics of an antibiotic response; using the metric to predict the outcome of a multi-dose treatment.

1.2 Organization of the objectives

This dissertation is divided into three chapters:

Chapter 2 discusses the different mechanisms bacteria use to survive antibiotic exposure. In particular, this chapter focuses on collective antibiotic tolerance, its underlying mechanisms, and how this knowledge can be used to inform bacterial treatment strategies.

Chapter 3 develops a resistance-resilience framework for dissecting bacterial antibiotic responses. Our analysis reveals that the antibiotic response is not absolute, but rather a dynamic response that shifts from depending on resistance and resilience to different degrees, depending on the concentration of antibiotic applied and the underlying mechanisms of the population. To this end, resistance is reflective of the short-term antibiotic response and primarily dependent on single cell traits, whereas resilience reflects a long-term response and primarily depends on population-level traits. Ultimately, this chapter provides a

quantitative framework that can be used to dissect other systems' responses and guide the formulation of improved treatment strategies.

Chapter 4 demonstrates how the antibiotic response to a single dose can predict the outcome of a multi-dose regimen. The analysis of this chapter revealed how the temporal dynamics of antibiotic responses could be used to identify a window of increased antibiotic susceptibility. To capture this window of susceptibility, we used the metric recovery time, or the amount of time a population needs to recover to its initial density prior to the addition of an antibiotic. Using a kinetic model, we demonstrated how a population of bacteria producing low-to-intermediate amounts of β-lactamase could be effectively eradicated if antibiotic doses were applied at time intervals shorter than 1 recovery time. If the time between doses was greater than 1 recovery time or the population was made up of highly resistant bacteria, then the treatment would fail.

2. Collective antibiotic tolerance: mechanisms, dynamics and intervention[1]

Bacteria have developed resistance against every antibiotic at an alarming rate, considering the timescale at which new antibiotics are developed. Thus, there is a critical need to use antibiotics more effectively, extend the shelf life of existing antibiotics and minimize their side effects. This requires understanding the mechanisms underlying bacterial drug responses. Past studies have focused on survival in the presence of antibiotics by individual cells, as genetic mutants or persisters. Also important, however, is the fact that a population of bacterial cells can collectively survive antibiotic treatments lethal to individual cells. This tolerance can arise by diverse mechanisms, including resistance-conferring enzyme production, titration-mediated bistable growth inhibition, swarming and interpopulation interactions. These strategies can enable rapid population recovery after antibiotic treatment and provide a time window during which otherwise susceptible bacteria can acquire inheritable genetic resistance. Here, we emphasize the potential for targeting collective antibiotic tolerance behaviors as an antibacterial treatment strategy.

[1] The content of this chapter has been published. Meredith H.R.*, Srimani J.K.*, Lee A.J., Lopatkin A.J., & You L. Collective antibiotic tolerance: mechanisms, dynamics and intervention. Nature Chemical Biology. 2015 Feb 17; 11:182-8. (* Equal contributions).
Author contributions: HRM, JKS, AJL, AJL, and LY wrote the manuscript.

2.1 Introduction

Antibiotic-resistant bacteria have emerged as a global crisis, resulting in increased morbidity rates, mortality rates, and healthcare costs. The time interval between the introduction of a new antibiotic and the emergence of resistance has rapidly decreased since the 1930s, largely due to antibiotic overuse and misuse[1]. Concurrently, a lack of financial incentive has led pharmaceutical companies to decrease antibiotic research and development[2]. Given the drying antibiotic pipeline, it is critical to develop a detailed understanding of how bacteria survive antibiotic treatment. Doing so can uncover new treatment strategies and enable us to use existing antibiotics more effectively[3].

Bacteria can survive antibiotics via many different mechanisms (**Figure 1a**). Genetic resistance can arise from *de novo* mutations or horizontal gene transfer[4]. Expression of resistance proteins can allow individual bacteria to survive antibiotic treatment by deactivating the antibiotic, altering the antibiotic's target, or preventing its intracellular accumulation[1,4].

Bacteria can also exhibit *phenotypic tolerance*, whereby they survive antibiotic treatment without acquiring new mutations[5]. For example, a predominantly sensitive population often has a very small fraction of non- or slow-growing bacteria (persisters). These persisters may emerge stochastically, in response to stress, or due to errors in replication and cell metabolism[6,7]. They are genetically identical to susceptible cells, but are tolerant to antibiotics[7,8]. In the absence of antibiotics, persisters can switch back to the growing state, leading to population recovery. As a result, persisters can cause post-

treatment relapses and enable development of genetic resistance[8]. Unlike genetic resistance, persistence is non-inheritable, though the frequency of persisters in a population can be genetically determined[8,9].

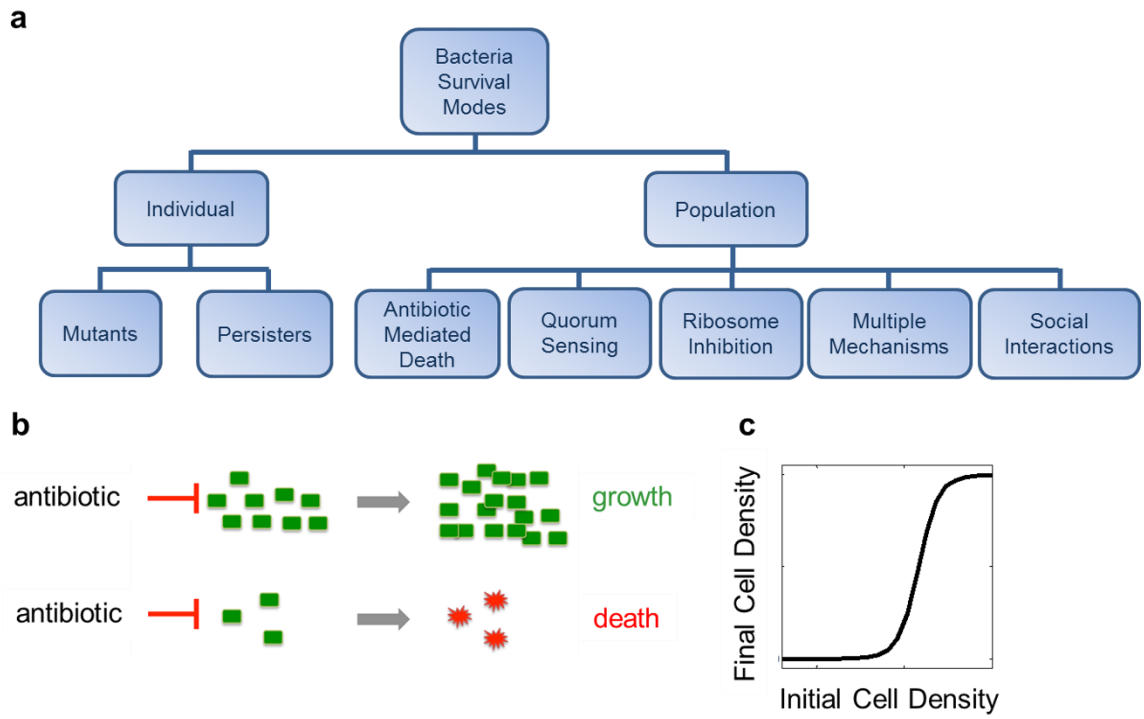

Figure 1: Bacterial survival modes. (a) Bacterial survival modes can be at the individual or population level. Populations can use different mechanisms to survive antibiotics collectively. **(b) Collective antibiotic tolerance** emerges when a population at a sufficiently high density can survive an antibiotic dose that would be lethal to a low density population. **(c) Initial cell density** determines the outcome of a population treated by an antibiotic. For each antibiotic concentration, there is a critical initial density above which the population will recover; below this, the population will die.

In contrast, a population at a sufficiently high density can survive an antibiotic dose that is lethal to a low-density population **(Figure 1b&c)**. This *collective antibiotic tolerance* (CAT) can arise from diverse mechanisms, including collective synthesis of resistance-conferring enzymes, antibiotic titration, and social interactions within and

between populations[10-12]. CAT enables a population to recover faster than persisters, and provides a time window for otherwise susceptible bacteria to acquire genetic resistance[12] (**Figure 2**). Here, we review mechanisms underlying CAT, their characteristic dynamics, and potential strategies to inhibit or exploit these mechanisms for antibacterial treatment.

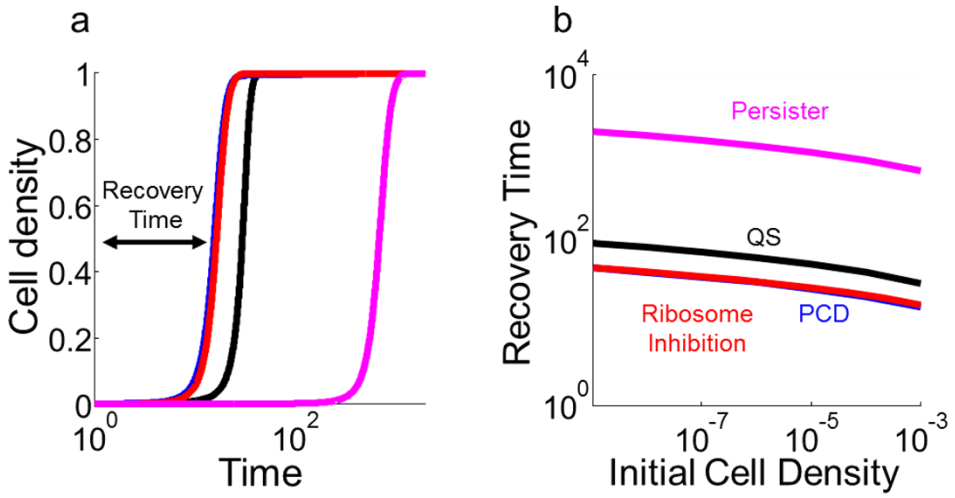

Figure 2: Comparison of population level responses due to different forms of CAT or persistence. The mechanism by which bacteria survive antibiotic treatment can significantly influence the speed of their recovery. Here, we use previously published models to compare the recoveries of populations dependent on different forms of CAT or persistence [9,10,13,14]. **(a) Time course simulations**. After being treated with an antibiotic, the bacteria actively tolerating antibiotics through bistable ribosome inhibition, programmed cell death (PCD), or quorum sensing (QS) recover much faster than persisters. **(b) Recovery times**. For persisters and CAT bacteria alike, increasing the initial cell density decreases the time it takes for a population to recover from antibiotic treatment.

2.2 Mechanisms underlying CAT

2.2.1 Antibiotic-mediated altruistic death

Genetic antibiotic resistance arises from the expression of resistance-conferring proteins, which often degrade or modify the antibiotic[4]. However, expression levels of the resistance protein may be insufficient to provide single-cell level protection,

depending on the antibiotic concentration. If so, the fate of a bacterial population will depend on its density **(Figure 3a):** population survival is determined by the relative rates of antibiotic-mediated killing and population-mediated antibiotic degradation. The population will initially decline due to antibiotic-mediated killing of some bacteria. This death is altruistic because the subsequent release of resistance proteins will benefit the surviving cells by contributing to antibiotic degradation[15,16]. If the initial population density is too low, the population will be eradicated before the antibiotic is degraded to a sub-lethal level. Conversely, if the initial population density is sufficiently high, the total resistance protein can clear the antibiotic before complete eradication of the population, allowing the survivors to repopulate. The interplay between cell growth, antibiotic-mediated killing, and antibiotic degradation by the resistance protein from cells (live or dead) will result in CAT. Indeed, smaller inocula of pathogens expressing β-lactamases (Bla) are more susceptible to β-lactams than larger inocula[17]. Such CAT often arises from constitutive expression of Bla and other resistance proteins[18]. Alternatively, many pathogens' Bla expression is up-regulated through the induction of *ampC* in the presence of β-lactam antibiotics[18].

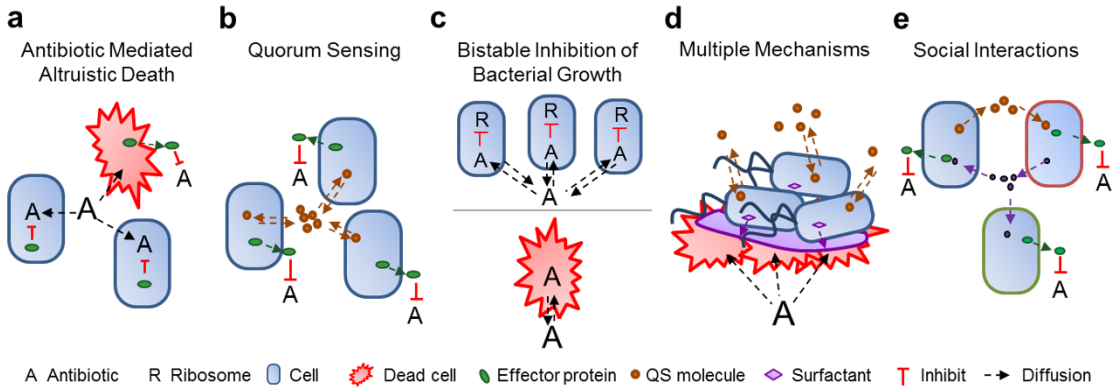

Figure 3: Underlying mechanisms of CAT. (a) Antibiotic mediated altruistic death involves a subpopulation lysing to release effector proteins that benefit the remainder of the population. CAT can only emerge if the population is large enough to generate a collective effector protein concentration sufficient to inhibit the antibiotic before the antibiotic kills all of the population. **(b) Quorum sensing** is often involved in regulating the expression of effector proteins or the maturation of biofilm formation, both of which can lead to CAT. **(c) Bistable inhibition** of bacterial growth arises as a function of intracellular antibiotic concentration and bistable ribosome inhibition. Sufficiently dense populations can titrate the antibiotic such that the intracellular concentration does not inhibit ribosome synthesis. However, low density populations cannot titrate the antibiotic to a sublethal level, thus, ribosome synthesis will be inhibited. **(d) Multiple mechanisms** can be used by a clonal population to survive antibiotic treatment. For example, swarming is a function of phenotype, QS, and PCD that confers antibiotic tolerance. **(e) Social interactions** can facilitate the survival of multiple subpopulations (denoted by different colored cell outlines). For instance, one subpopulation can produce a signaling molecule necessary to upregulate a second subpopulation's resistance mechanism and vice versa. There are also situations where one subpopulation donates a signaling molecule that protects a second population, without deriving any benefit in return.

Partial population death is a natural consequence of bactericidal antibiotic action. In other contexts, antibiotic-mediated death is genetically programmed[15]. For example, some antibiotics affect bacterial death by interfering with toxin-antitoxin systems[19]. The *mazEF* system can result in programmed cell death (PCD) when an antibiotic, such as chloramphenicol, inhibits the transcription/translation of the MazE antitoxin[20]. Without the labile MazE antitoxin, the stable MazF toxin accumulates and triggers PCD. Other antibiotics, such as fluoroquinolones, trigger PCD by inducing an SOS response[21].

During a stress response, PCD can benefit survivors by directly or indirectly relieving stress[15,16]. When this occurs, the use of antibiotic can promote the survival of a pathogen and aggravate its virulence. For instance, antibiotics induce PCD in Shiga toxin (Stx)-producing *Escherichia coli* (STEC) O157:H7. Encoded in a bacteriophage[22], Stx is assembled and released upon cell lysis. Stx kills nearby eukaryotic predators, thereby enabling STEC growth and survival[23]. Death here is altruistic and required for the release of Stx. The population must be large enough to afford the cost of lysing the bacteria necessary to release sufficient Stx for survival.

2.2.2 Quorum Sensing and Biofilm Formation

If a resistance protein's production is costly, it may be advantageous to delay synthesis until the cell density is high enough so the overall benefit of the protein outweighs its production cost. This delay can be realized by quorum sensing (QS), which enables bacteria to coordinate gene expression in a density-dependent manner[24,25]. In QS, individual cells produce a signaling molecule that increases in extracellular concentration with cell density. By sensing the signal concentration, bacteria can coordinate gene expression according to their density[24]. Using a synthetic gene circuit, QS has been demonstrated to represent an optimal strategy for controlling the expression of a costly protein that benefits the entire population[13].

QS could control the expression of resistance-conferring enzymes **(Figure 3b)**. In *Providencia stuartii*, a Gram-negative pathogen that causes urinary catheter infections, QS controls the expression of an acetyltransferase, which inactivates aminoglycoside

antibiotics[26,27]. Low-density populations express minimal levels of acetyltransferase, rendering them sensitive to aminoglycosides; high cell density triggers acetyltransferase expression, yielding CAT.

QS can also contribute to CAT by modulating biofilm formation, which enhances antibiotic tolerance[28]. Although the specifics of biofilm formation vary by species, the general steps are similar[25,29]. Planktonic bacteria first attach to a surface at a low density and begin to form microcolonies, while producing basal levels of QS signals. Once the population reaches a sufficiently high density, the accumulated QS signals activate genes involved in biofilm formation[24]. Depending on the antibiotic and bacterial specie, the surface layer of biofilms may serve as a protective barrier for resident bacteria by reducing the penetration rate of some antibiotics[30,31]. Moreover, some antibiotics, such as piperacillin or ampicillin, can induce antibiotic-deactivating enzymes in biofilms, which can further reduce antibiotic penetration and the killing of biofilm-residing bacteria[32,33]. Biofilms also have limited nutrients at their core, which diminishes internal cell growth. These slow growing cells tend to be less sensitive to certain antibiotics[34].

2.2.3 Bistable inhibition of the replication machinery

When bacterial populations produce a resistance-conferring protein, density-dependence may be intuitive: increasing cell density increases total protein production, thus increasing the likelihood that a population will survive treatment[35]. However, CAT has also been observed in response to antibiotics that inhibit ribosome activity and protein synthesis (e.g. gentamicin) without requiring production of degrading enzymes[36].

A previous study has established a mechanism for CAT in the absence of active antibiotic degradation: intra-population antibiotic titration coupled with bistable ribosome inhibition[10] **(Figure 3c)**. In each cell, ribosome synthesis is controlled by positive feedback: ribosomes translate mRNA into proteins, including ribosome components, resulting in ribosome synthesis[37]. This feedback can be inhibited by intracellular antibiotic, resulting in a bistable response[38].

Within a population, the extracellular antibiotic is allocated to individual cells according to the import and export rates across the cell membrane. When import is faster than export, the intracellular antibiotic will be higher than the extracellular concentration, and will decrease slightly with increasing cell density. This decrease is amplified by ribosomal positive feedback, leading to bistable growth inhibition: at high cell densities, the average intracellular antibiotic concentration is relatively low (below minimum inhibitory concentrations), positive feedback overcomes antibiotic inhibition and enables population survival. Modeling suggests that density dependence can be modulated by altering various processes, such as drug uptake and binding. However, the critical condition required for CAT in this scenario is the rapid degradation of ribosomes, which can be triggered by antibiotics that target ribosomal components. These antibiotics induce heat-shock response[39], which leads to upregulation of proteases and faster degradation of ribosomal components[40]. If the ribosome degradation rate remains slow, as with chloramphenicol treatment, the population fate is density-independent: populations either grow (low antibiotic concentrations) or die (high antibiotic concentrations). When

coupled with direct induction of heat shock, however, these antibiotics can also cause bistable inhibition of population growth, leading to CAT.

2.2.4 Mixed strategies

In nature, CAT often arises from traits that are controlled by combinations of the mechanisms discussed above. For example, when PCD is coupled with density-dependent gene expression in *Staphylococcus aureus*, lysis is tightly controlled and can result in CAT through biofilm formation. CidA and LrgA expressions turn lysis ON and OFF at specified stages of cell growth, respectively[41]. Lysis releases genomic DNA, resulting in enhanced biofilm formation[42,43]. These genes have been linked to regulation of antibiotic tolerance: mutations disrupting CidA or LrgA enhance or reduce population survival, respectively[41,44].

Another strategy to survive antibiotic treatment involves a combination of phenotypically shifting from a "swimming" state (planktonic growth) to a “swarming” state (surface growth), QS, and altruistic death **(Figure 3d)**. Swarming is flagella-driven group-migration of bacteria over a semi-solid surface and happens exclusively at the leading edge of a population[45,46]. Although the underlying mechanisms are species dependent and not fully elucidated, some swarming species have been observed to rely on QS to upregulate the production of biosurfactants, such as rhamnolipids, which are necessary for reducing surface tension[45]. Swarmers exhibit increased tolerance to a variety of antibiotics, including aminoglycosides and fluoroquinolones[46,47]. Altruistic death may contribute to this survival advantage. It is speculated that cells dying from

prolonged direct contact with the antibiotic form a protective platform that prevents other swarmers from coming into direct contact[46]. Thus, the population has to have a high enough density to upregulate QS-mediated swarming genes[46] and afford the cost of individuals that are directly exposed to the antibiotic. While swarming and biofilm formation involve similar mechanisms, such as altruistic death and QS, the two states are inversely regulated[48,49]. As a result, biofilms contain a population of sessile cells while swarms disperse a population of active cells[49].

The mechanisms underlying swarming-mediated motility and density-dependent survival appear to vary between species; QS has been implicated in *Pseudomonas aeruginosa*[45], but not in *Salmonella*[46]. Other studies have examined the impact of biofilm creation[46] and increased efflux pump expression[50]. Swarming motility has been observed to strongly correlate with the expression of the *pmrHFIJKLM* operon[47]. This operon encodes the lipid A portion of LPS, which reduces the binding strength of various antimicrobial peptides[51]. A previous study shows *pmrK* expression is upregulated in conditions that promote swarming. Expression decreases as cells de-differentiate from the swarming phenotype, and knockout results in the loss of swarming ability[47].

2.2.5 Social interactions

In a mixed population, CAT can be facilitated by "charitable" actions, wherein one subpopulation produces a product that helps another subpopulation, without receiving any benefit from the latter **(Figure 3e)**. For example, a recent study demonstrated how a population of drug sensitive *E. coli* can tolerate antibiotic with the

aid of a few highly resistant population members[52]. In the absence of antibiotic, the entire population produces indole, a signaling molecule generated by growing bacteria. In the presence of an antibiotic, however, only a subpopulation with mutated efflux pumps has the resistance necessary to continue producing large amounts of indole. The released indole upregulates efflux pump expression and oxidative-stress mechanisms, thus enabling the entire population to tolerate the antibiotic. This survival tactic will fail if the fraction of mutant indole producers is too small to support a large population of sensitive cells or if the metabolic cost of production is too high.

CAT can also arise from *mutualistic* interactions, where two or more bacterial populations depend on one another to survive. For instance, an engineered system can demonstrate how two populations can collaborate to survive different antibiotics[12]. Each engineered population produced the QS signal molecule needed by the other to upregulate the production of a resistance protein. Increasing either population's initial density increased QS signal accumulation, resulting in higher final densities following antibiotic treatment.

Similarly, multispecies swarms can arise due to the communal nature of QS signals. For example, *Serratia ficaria* do not produce biosurfactants, but they do produce QS signals necessary for S. *liquefaciens* QS-deficient mutants to upregulate their own biosurfactant production. Once sufficient signaling molecules accumulate, *S. liquefaciens'* biosurfactant production facilitates the swarming[53] and, presumably, the CAT of both populations.

Another example of mutualism-mediated CAT can be found in multi-species biofilms[54]. For example, species can work together to decrease antibiotic penetration of biofilms. *Burkhodia cepacia* and *P. aeruginosa*, both associated with cystic fibrosis, produce polysaccharides that interact to increase biofilm viscosity and decrease antibiotic activity[55].

2.3 Implications for antimicrobial treatment strategies

The diverse mechanisms underlying CAT have implications for developing new treatment strategies. In particular, different mechanisms can lead to unique population and evolutionary dynamics that can be exploited for better treatment efficacy or serve as a cautionary tale against simplistic treatment strategies.

2.3.1 Timing in antibiotic dosing

A common property of CAT mechanisms is that a bacterial population is most vulnerable at low densities. This suggests the potential to inhibit bacterial growth by controlling the timing of antibiotic doses[56]. One method would be to detect and treat infections at earlier stages of development, when insufficient bacteria are present to realize CAT (**Figure 4a**). A mouse study on treating STEC infections showed early treatment (1-3 days after infection) with a lysis-inducing antibiotic resulted in zero mortality, while late treatment (3-5 days) resulted in 95% mortality[57]. The improved outcome by early treatment may have resulted from suppression of bacterial growth or virulence factor production. Targeting early stage infections is also effective in treating

biofilms; studies have demonstrated that immature biofilms are more susceptible to antibiotic treatment[58,59].

Timing control is intrinsic in the design of periodic antibiotic dosing protocols, which can be determined by the dynamic response of a population exhibiting CAT. A previous study demonstrated that different periodic dosing frequencies have drastically different outcomes when treating a population capable of generating CAT due to bistable ribosome inhibition[10]. When antibiotic doses were delivered at high frequency, populations had insufficient time to recover. Conversely, when doses were delivered at low frequency, the antibiotic eradicated the population to such an extent that it could not recover. For intermediate frequencies, however, treatment was ineffective; populations recovered between doses. Furthermore, the frequency range over which populations were able to survive can be modulated by changing the fraction of each period spent at a high antibiotic concentration. In general, the optimal dosing protocol will likely depend on the specific types of mechanisms by which CAT arises, representing a significant direction for quantitative biology research.

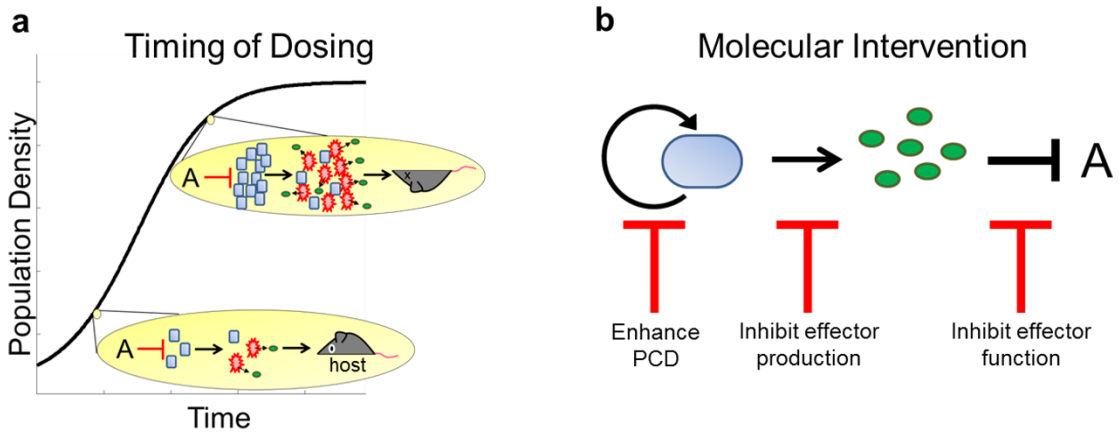

Figure 4: Inhibition strategies. (a) Timing control of antibiotic dosing is critical for optimizing efficacy of periodic antibiotic treatments. By timing the application of antibiotic doses with when the population is at a low density, the amount of public good and/or toxin released would be insufficient to allow the population to recover or harm the host. **(b) Molecular-level interventions of CAT** could be used to trigger PCD and inhibit the production and/or the function of an effector protein.

2.3.2 Molecular interventions to Disrupt CAT

Different mechanisms underlying CAT also suggest potential targets for molecular-level intervention (**Figure 4b**). CAT facilitated by enzyme expression can be reduced by inhibiting either the production or the action of the enzyme. These strategies are often adopted for treating bacteria that produce Bla. Weak inducers of AmpC Bla production, e.g. cefepimes and piperacillin, have been shown to have lower MICs when treating inducible pathogens[60]. Alternatively, a Bla-inhibitor, such as clavulanic acid, sulbactam, and tazobactam, is frequently used in conjuction with a β-lactam antibiotic to treat Bla-producing bacteria[61]. It should be noted that some bacteria have already evolved resistant mechanisms to Bla inhibitors[62].

This strategy can also be applied to target CAT resulting from PCD. Studies have begun to screen antimicrobial peptides that have increased efficacy in activating killing by triggering bacterial toxin-antitoxin systems[63,64]. For some pathogens, however, activation of PCD alone may be undesirable as it can enhance bacterial survival and virulence. Instead, PCD inhibition can reduce virulence by suppressing the release of effectors that promote bacterial survival or virulence. For example, in *Streptococcus pneumoniae*, release of a virulence factor to extracellular space is mediated by autolysis of a subpopulation of cells[65], which in turn can benefit survivors. Serum from mice immunized with autolysin inhibited autolysis and reduced bacterial virulence[65]. It will be interesting to examine how such strategies will impact overall bacterial survival. As demonstrated using synthetic gene circuits[14], reduced lysis can paradoxically lead to overall worse bacterial survival.

Similar strategies that inhibit either the production or the action of an enzyme have been applied to target QS pathogens. Targeting QS is appealing as it can reduce virulence without directly targeting the immediate survival of cells. For example, azithromycin has been shown to inhibit QS signaling, leading to inhibition of biofilm formation and virulence in *P. aeruginosa*[66,67]. Likewise, enzymes, such as AiiA that hydrolyze QS signal molecules[68] and synthetic molecules that prevent AHL receptor activation[69], can also block QS signaling and lead to decreased virulence and increased susceptibility to antibiotic treatment in QS pathogens[70]. Drugs that target the function of QS-mediated proteins have also been studied. Oseltamivir is a drug originally developed

to inhibit viral production of neuraminidase. As neuraminidase is also a QS-mediated enzyme essential for *P. aeruginosa's* initial colonization process and subsequent biofilm formation, oseltamivir has been tested for its ability to inhibit biofilm formation. Indeed, a dose-dependent decrease in biofilm formation was observed when oseltamivir was applied [71].

Rapid ribosome turnover is a prerequisite to generate CAT against antibiotics that target ribosomes[10]. As the rate of ribosome turnover increases, the range of antibiotic concentrations over which CAT occurs shrinks and shifts towards lower values. To reduce or eliminate CAT, future drug development could focus on alternative avenues to disrupt ribosome efficacy, such as interfering with subunit assembly[72]. Targeting pathways involved in the stringent response could also eliminate CAT. In response to various stresses, many bacterial species reduce rRNA transcription and ribosome synthesis while up-regulating amino acid synthesis[73]. These metabolic shifts can promote bacterial survival and virulence[74]. Inhibition of such metabolic shifts could prevent CAT at high population densities. These pathways may thus represent potential targets for new drugs[75].

A prior study observed that a fundamental requirement for swarming is the production of extracellular surfactants, particularly lipopolysaccharides (LPS), which lubricate cells' local environment so they can "slide" past each other[47]. Therefore, the increased antibiotic tolerance exhibited by swarmers could be avoided by inhibiting LPS production[76]. Previous studies have shown that LPS inhibition by antimicrobial peptides

results in the loss of swarming motility[51]. A caveat is that inhibiting swarming motility could lead to increased biofilm formation[77], as these phenotypes are often linked.

Finally, mixed populations can be inhibited by targeting the keystone members. In the case of charitable interactions, treatments should target the subpopulation producing the resistant protein that protects producers and non-producers alike. For instance, penicillin treatment of tonsillitis is often ineffective due to mixed populations of Bla producing pathogens that protect *Streptococci*. However, the infections were effectively treated upon the introduction of a Bla inhibitor, clavulanic acid[78]. In a mutual relationship, such as in the aforementioned synthetic system[12], survival depends on both subpopulations being present. For such systems, a viable treatment strategy could be to disable one subpopulation such that all participating subpopulations are more susceptible to treatment. To this end, Clustered Regulatory Interspaced short palindromic repeats (CRISPR)-Cas systems could represent an ideal antimicrobial strategy to directly target the specific sub-populations that promote CAT. This genome-editing tool utilizes targeted guide RNA sequences that can be designed to recognize desired bacterial DNA and induce nucleic acid breaks, which can disrupt gene function in the target. Indeed, recent studies demonstrate the ability to customize antimicrobial treatments by the targeted inactivation or killing of specific bacteria within a population through CRISPR delivery[79,80].

2.3.3 Treatment Considerations

Depending on the underlying mechanisms, complex treatment responses could arise from populations capable of CAT. One counterintuitive response is the Eagle effect, a phenomenon wherein increasing antibiotic concentration promotes bacterial recovery[81]. Whether and to what extent the Eagle effect happens in the clinical setting remains to be tested; however, the Eagle effect has been observed to result from PCD-mediated tolerance *in vitro*[14].

Another example is the counterintuitive effect of inhibiting different aspects of QS. Inhibiting QS signal synthesis effectively increases the cell density threshold required to trigger downstream gene expression, such as virulence factor production[82]. However, QS inhibition also alleviates the metabolic burden placed on each cell, resulting in faster growth[13]. Despite this caveat, the overall outcome of QS signaling inhibition ultimately depends on bacterial survival and virulence development. The treatment would likely be considered successful if the target bacteria are rendered non-pathogenic[83].

While QS inhibition can attenuate virulence in the short term, it can promote the selection of more virulent pathogens in the long term[84]. For example, long-term inhibition of QS signaling in *P. aeruginosa* by azithromycin can select for more cooperative and virulent individuals[67,84]. Azithromycin inhibits general protein synthesis; however, it has been shown that QS-regulated genes are among the most severely inhibited by this drug[85]. Over an 11 day course of azithromycin in patients, a slight

decrease in the frequency of QS-deficient mutants was observed; the QS-deficient mutant frequency in the placebo group increased approximately 2-fold[84]. One possible explanation for this counterintuitive response is, when uninhibited, the cooperative nature of QS is prone to cheaters: cells that do not produce virulence factors exploit the benefit while avoiding the cost of public good production[86]. Cheaters, therefore, are less virulent, but have a fitness advantage. For instance, *P. aeruginosa* cheaters that are QS-deficient due to LasR mutations have a growth advantage over the wildtype[67,87]. When the QS signal is inhibited and no public goods are synthesized, the fitness advantage by the cheaters will be reduced, making it more difficult for them to outcompete cooperators. The negative consequences of direct inhibition of enzyme production may be avoided by inhibiting the enzyme after it is produced[88]. This strategy aims to maintain the cost of enzyme production while eliminating the benefits, leaving virulent bacteria at a metabolic disadvantage and more vulnerable to treatment. This method may also reduce the selective pressure induced by antibiotic treatment, slowing pathogens' adaptive response.

Although resistance has been well studied, predicting long term consequences on bacterial dynamics has proved elusive. Bacteria have already developed strategies to survive QS inhibition[84] and combination treatments involving Bla inhibitors[62] and will likely develop strategies to survive other inhibition methods. A better understanding of bacterial population and evolutionary dynamics under different treatment strategies can help us optimize treatment strategy. More quantitative studies are needed to better establish the evolutionary dynamics involved in QS-mediated cooperation and the impact

of inhibition on different aspects of QS. For instance, the discussion above only considers QS effectors that are public goods. The evolutionary outcomes can be significantly different if the effectors are private goods, which only benefit the cell that produces them,[89] or species-specific goods, which only benefit a particular population of cells[90]. The same challenge is applicable for the population and evolutionary dynamics of other mechanisms leading to CAT. To this end, the use of well-defined model systems[91], both natural[10,89,92,93] and engineered[13,14,90], will be valuable for the development of better quantitative understanding of a population's response to antibiotics. This understanding can serve as the critical foundation to design 'evolution proof' treatment strategies that select against resistance[94].

3. A resistance-resilience framework to dissect bacterial antibiotic responses[2]

An essential property of microbial communities is the ability to survive a disturbance. Survival can be achieved through *resistance*, the ability to absorb effects of a disturbance without a significant change, or *resilience*, the ability to recover after being perturbed by a disturbance. These concepts have long been applied to the analysis of ecological systems, though their interpretations are often subject to debate. Here we show that this framework readily lends itself to the dissection of the bacterial response to antibiotic treatment, where both terms can be unambiguously defined. The ability to tolerate the antibiotic treatment in the short term corresponds to resistance, which primarily depends on traits associated with individual cells. In contrast, the ability to recover after being perturbed by an antibiotic corresponds to resilience, which primarily depends on traits associated with the population. This framework effectively reveals the phenotypic signatures of bacterial pathogens expressing extended spectrum β-lactamases (ESBLs), when treated by a β-lactam antibiotic. Our analysis has implications for optimizing

[2] The content of this chapter has not yet been published. Meredith H.R., Andreani, V., Lopatkin A.J., Lee, A.J., Anderson D.J., Batt, G. & You L A resistance-resilience framework to dissect bacterial antibiotic responses. Currently submitted for review.
Author contributions: H.R.M. conceived the research, designed and performed both modeling and experimental analyses, interpreted the results, and wrote the manuscript. VA assisted in model development, simulations, data interpretation, and manuscript revision. A.J. Lopatkin and A.J. Lee assisted in data interpretation and manuscript revisions. D.J.A. contributed isolates and medical perspective on how the work would clinically translate. G.B. assisted in model development and manuscript revisions. L.Y. conceived the research, assisted in research design, data interpretation, and manuscript writing.

treatment of these pathogens using a combination of a β-lactam and a β-lactamase (Bla) inhibitor. In particular, our results underscore the need to dynamically optimize combination treatments based on the quantitative features of the bacterial response to the antibiotic or the Bla inhibitor.

3.1 Introduction

A disturbance is a biological, chemical, or physical event that affects a community[95]. Given that the environment is constantly changing, an essential property of a community is its ability to recover after being disturbed. Responses to a disturbance include resistance, the ability to withstand perturbation in the presence of a disturbance; resilience, the ability to recover after being perturbed by a disturbance; or sensitivity, the inability to withstand or recover from a disturbance[96-99]. Resistance and resilience have been documented in a range of systems and are often determined by different processes [95,96,99,100]. Specifically, resistance is associated with processes that enable the tolerance of, or adaptation to, a disturbance, whereas resilience is associated with recolonization, reproduction, or rapid regrowth[96]. The ability to identify the determinants for resistance versus resilience is crucial for predicting how a given community will respond to a disturbance as well as for designing strategies that will either preserve, change, or eliminate it [97,98,101]. Although resistance and resilience have been defined in the literature for decades[102], the resistance-resilience framework has not been widely applied. This is partially because it is often difficult to determine the pre-disturbance state of a population,

the definitions vary, and there is a lack of quantitative studies demonstrating how to implement these terms[96,98,103-106].

Yet, this resistance-resilience framework naturally lends itself to the analysis of bacterial responses to antibiotic treatment. When running susceptibility tests, it is possible to characterize a pre-disturbance state (i.e. no exposure to antibiotic) and there are many ways to quantify the bacterial antibiotic responses (i.e. agar plates, E-test, plate reader, microscopy)[9,13,107]. Until now, resistance and resilience have not been distinguished in the context of antibiotic responses. Instead, bacteria are classified as resistant if they survive exposure to a set concentration of antibiotic after a set amount of time[108,109] (**Figure 5**). However, the apparently similar survival can result from diverse underlying mechanisms[1,8,110-112] that can lead to the ability of individual cells to withstand the treatment or the ability of the population to recover from the initial disturbance. We term the former resistance and the latter resilience.

Here, we apply these concepts to the analysis of bacterial pathogens producing extended spectrum β-lactamases (ESBLs), which are becoming increasingly prevalent and can degrade most β-lactam antibiotics – the most widely used class of antibiotics in the clinics[113-117]. We show that the resistance-resilience framework effectively reveals the phenotypic signatures of different ESBL-producing bacteria, and underscores the critical need to implement adjustable formulations of combination treatments to combat these pathogens.

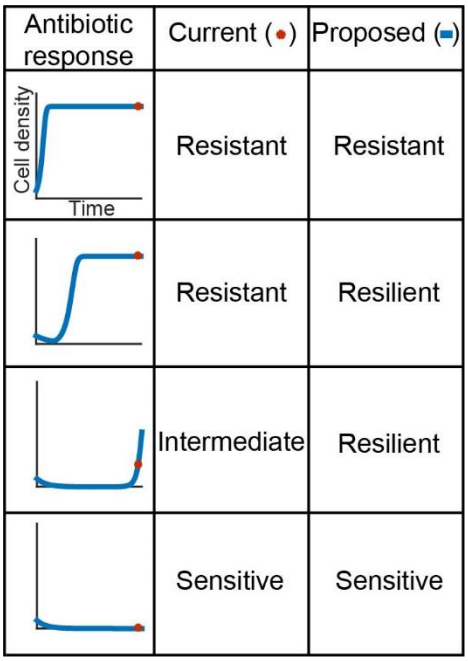

Figure 5. Defining antibiotic responses. Each panel represents a different response to an antibiotic delivered at time = 0. In the first row, the population grows up to carrying capacity, unperturbed. In the second row, the population is perturbed, but eventually recovers in the allotted time. A third population is perturbed and only partially recovers during the allotted time. In the final row, the population is perturbed and does not recover. Currently, antibiotic sensitivity analyses only consider whether bacteria can recover from a set dose of antibiotic in a standard period (red dot). Bacteria that display full recovery are considered resistant, partial recovery are intermediate, and no recovery are sensitive. However, temporal dynamics (blue curve) reveal differences in how a population recovers.

3.2 Results

3.2.1 Temporal dynamics of ESBL-producing bacteria in response to β-lactam treatment

The population grows at a rate dependent on the amount of nutrients available (**Figure 6a**). While the nutrients are mostly depleted by cell growth, they can be replenished to a degree by the nutrients released during cell lysis[118]. Gram-negative bacteria expressing a β-lactamase (Bla) harbor the enzyme in their periplasm, where it can degrade antibiotic that diffuses across the outer membrane [119]. Bla is released into the

environment due to membrane leakage or cell lysis[120]. Cell lysis occurs with the introduction of the β-lactam antibiotic, which interrupts the cell wall synthesis process and causes lysis[121]. When a high enough antibiotic concentration is added, there is a race between cell lysis and antibiotic degradation. When the population's lysis rate is greater than its growth rate, the population density crashes (**Figure 6b**). If sufficient Bla (periplasmic or extracellular) is present, then the antibiotic is degraded in time for the population to recover before it is completely lysed. A population's recovery depends on collective antibiotic tolerance (**Figure 11**): it must have a sufficiently high density when treated so enough Bla is collectively produced to remove the antibiotic before all bacteria are lysed. If the initial density is too low, then insufficient Bla will be produced to protect the population from antibiotic exposure.

Here, the population recovery was due to the Bla rapidly degrading the antibiotic, indicated by the level of antibiotic activity in the supernatant after 6 hours of exposure (**Figure 6c**). Sensitive bacteria do not produce Bla and cannot break down the antibiotic, thus the antibiotic remaining in the supernatant could inhibit the growth of sensitive bacteria. At a higher initial antibiotic concentration, the same amount of supernatant generated a larger zone of inhibition. In contrast, the bacteria producing ESBLs sufficiently degraded both antibiotic doses during the incubation period, as evidenced by the inability of the resulting supernatants to inhibit growth of sensitive cells.

To test if the population recovery was due to the selection of a more resistant or resilient subpopulation, we collected ESBL producing bacteria that had recovered from an

antibiotic treatment and re-exposed them to a range of antibiotic concentrations. The resulting antibiotic responses were similar, regardless of previous exposure concentrations (**Figure 6d**). This shows that the recovery was not due to the selection of a sub-population with enhanced tolerance, which is consistent with the notion of antibiotic degradation due to the Bla released from cell lysis.

We also tested if the antibiotic induced the production of Bla by using Fluorocillin, a substrate that fluoresces green when degraded by Bla, allowing for the real-time visualization of Bla activity. After incubating the isolate with different concentrations of cefotaxime for 3 hours, we added Fluorocillin to the sonicated culture to quantify the total Bla present. There was no significant increase in fluorescence as a function of antibiotic concentration (**Figure 6e)** at the $p < 0.05$ level [$F(1, 6) = 2.44$, $p = 0.17$] and [$F(1, 6) = 3.31$, $p = 0.12$] for A = 10 and 100 µg/mL, respectively. There was a slight, but significant, decrease in fluorescence for A= 1 µg/mL [$F(1, 6) = 6.68$, $p = 0.04$]. Overall, Bla production is not induced by exposure to this range of antibiotic concentrations.

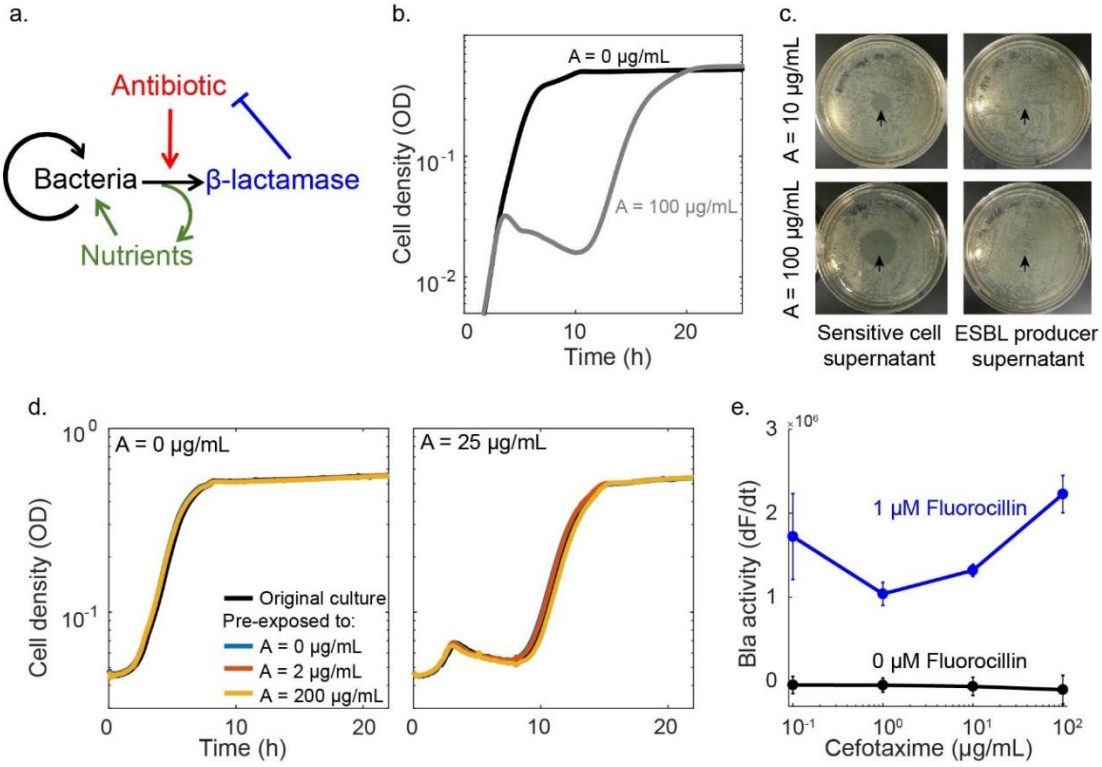

Figure 6. Response of an ESBL-producing population to cefotaxime, a β-lactam. (a) Schematic of antibiotic response of an ESBL-producing population. In the absence of antibiotic, bacteria reproduce and consume nutrients. Upon the introduction of an antibiotic, some of the bacteria undergo lysis and release β-lactamase and a small amount of recyclable nutrients into the environment. The released Bla degrades the antibiotic (blue inhibition arm). **(b) Time course of antibiotic response.** In the absence of an antibiotic (black curve), the bacteria grow to carrying capacity without any delay. In the presence of sufficient antibiotic (grey curve; A=100 μg/mL cefotaxime), the population displays the characteristic crash, as the cells lyse, and recovery after the Bla released from lysed cells degrades the antibiotic. **(c) ESBL significantly degraded cefotaxime in a short time window.** The supernatant from a culture of sensitive cells still contained significant concentrations of cefotaxime, as depicted by the zones of inhibition in the lawn of sensitive cells (strain MC4100, left column). The supernatant from the culture containing ESBL producing bacteria did not contain significant concentrations of cefotaxime, as depicted by the full lawns (right column). Arrowheads indicate where supernatant was placed on the agar plate. **(d) Populations previously exposed to cefotaxime exhibited the same temporal dynamics.** Culture was treated with a range of antibiotic concentrations. After 24 hours, bacteria from the recovered population were used to re-inoculate fresh media with or without 25μg/mL cefotaxime. During the 2nd round of treatment, the time courses from the populations previously exposed to 0, 2, or 200 μg/mL cefotaxime were identical, suggesting that the population recovery was unlikely due to mutants or phenotypic variants with increased tolerance. **(e) Bla production is not induced by cefotaxime.** We used Fluorocillin to determine that the isolate's Bla production is not significantly increased by the addition of antibiotic. Here, the Bla activity present in a population after 3 hours of exposure to a range of antibiotic concentrations was quantified by the rate at which Fluorocillin was hydrolyzed and produced green fluorescence. One way ANOVAs indicate that the increase in fluorescence recorded was insignificant when compared to the control.

3.2.2 Defining resistance and resilience

Borrowing concepts from ecology and the study of other microbial communities, a population can recover from a disturbance due to its resistance or resilience [95,96,103]. Here, we define resistance as the bacterial population's ability to withstand perturbation in the presence of antibiotic and resilience as the population's ability to recover following a perturbation once the antibiotic has been sufficiently degraded. Resistance is reflective of the short-term antibiotic response and primarily dependent on single cell traits: the ability for a single bacterium to withstand the effect of antibiotic determines the degree of perturbation displayed at the population level. Resilience reflects a long-term response and primarily depends on population-level traits: when a single bacterium can no longer survive the effects of antibiotic, the population is initially impacted; however, collective antibiotic tolerance allows for the population to outlast the disturbance and recover after being perturbed.

Here, we use the net growth rate to characterize a population's resistance. As the antibiotic concentration increases, more lysis will occur and the net growth rate decreases. Once the lysis rate is higher than the growth rate, the population will crash and the net growth rate will become negative. The more resistant a population is, the more antibiotic is needed to elicit a significant change in net growth rate, as compared to an untreated population. Mathematically, we define resistance at the time of maximum change in a treated population's net growth rate (ρ_A) normalized by the untreated population's net growth rate at the same point in time (ρ_0).

$$Resistance = \frac{\rho_A}{\rho_0} \quad (1)$$

The time needed for a population to reach 50% of its carrying capacity ($T^{50\%}$) was used to characterize a population's resilience. With increasing antibiotic concentration, more cells will lyse in the process of degrading the antibiotic, thus increasing the resulting recovery time. The more resilient a population is, the faster it can return to a normal state after being perturbed by an antibiotic. We define resilience as the inverse of the treated population's $T^{50\%}$ ($T_A^{50\%}$), normalized by the untreated population's $T^{50\%}$ ($T_0^{50\%}$) (**Figure 7a-b, Figure 12**)[95]. The inverse is taken to reflect the fact that increasing the recovery time corresponds to a decrease in resilience.

$$Resilience = \frac{T_0^{50\%},}{T_A^{50\%},} \quad (2)$$

Note that resistance and resilience are not absolute properties. Instead, for each bacterial strain, the degree of resistance or resilience depends on the type and dose of antibiotic used. At low antibiotic concentrations, the population experiences little or no disturbance and thus is characterized with relatively high resistance and resilience **(Figure 7c**). At intermediate concentrations (A=1.5 μg/mL), the population's recovery displays a decline in both resistance and resilience because the antibiotic concentration is high enough to induce some lysis and slow the net growth rate and delay the recovery time. Once the antibiotic concentration is high enough to induce a population crash (A>5 μg/mL), the recovery of the population shifts to being dominated by resilience. If the antibiotic concentration exceeds the threshold for population recovery, the resulting resilience and

resistance will be minimal. This resistance-resilience framework effectively reveals the phenotypic signature of each strain (**Figure 7d**) when treated by a β-lactam.

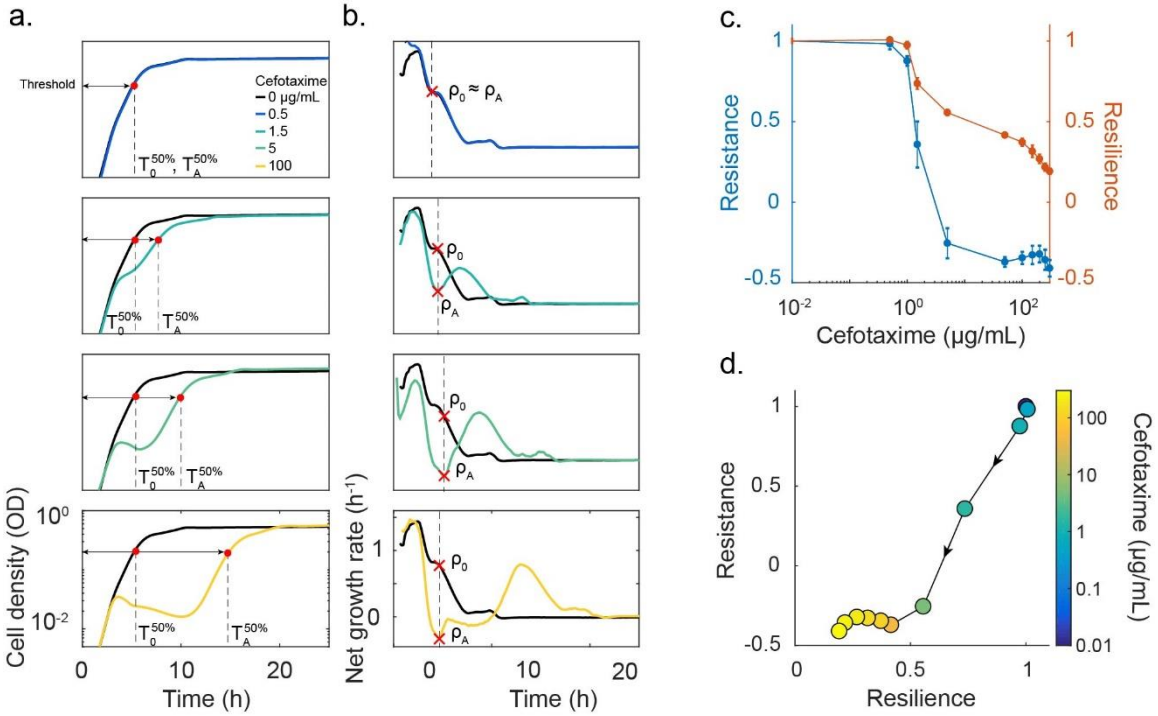

Figure 7: Quantifying resistance and resilience (a) Time courses are used to quantify a population's resilience. When no antibiotic was added (black curve), the population grew up unperturbed and reached a target threshold density (here 50% of the carrying capacity) in time = $\boldsymbol{T^{50\%}}$. If the antibiotic concentration added was very low (blue curve, A=0.5 μg/mL cefotaxime), then the population reached the threshold density in a similar time to the untreated population. As the antibiotic concentration increased, the degree of lysis increased and affected the time necessary for the treated population to reach the threshold ($\boldsymbol{T_A^{50\%}}$). We characterized the population's resilience for a range of antibiotic concentrations as the inverse ratio of the times to the half maximal carrying capacity ($\boldsymbol{T_0^{50\%}/T_A^{50\%}}$). **(b) Net growth rate quantifies population's resistance.** When no antibiotic was added, the population's net growth rate decreased over time as it consumed the available nutrients and approached stationary phase. When a low dose of antibiotic was added, the net growth was not significantly altered (blue curve). In this instance, the treated population's maximum net growth rate is recorded as ρ_A and compared to the untreated population's net growth rate at the same time (ρ_0). As the antibiotic concentration increased, the net growth rate curve of the treated population deviated more from the untreated curve. For each antibiotic concentration, ρ_A was recorded as the net growth rate at the point of maximum negative deviation from the untreated population and normalized by ρ_0. We characterized a population's resistance as the ratio of recovery times (ρ_A/ρ_0). **(c) Resistance and resilience as functions of the cefotaxime concentration. At low doses of cefotaxime, the population was resistant and resilient,** showing little disturbance after exposure (see **Figure 7A-B**). As the antibiotic concentration was increased, resistance and resilience decreased due to the increase in cell lysis causing the net growth to decrease and the time to the half max density increased. Once the population

underwent a crash, the resistance was minimized and resilience became the dominating factor for survival. **(d) The resistance-resilience map defines a phenotypic signature.** Using the same data as in **Figure 7A-C**, the resistance-resilience framework can visualize the shift in a population's antibiotic response. When the antibiotic concentration was 0 or very low, the population's response displayed high resistance and resilience. Once the antibiotic concentration increased to 5 μg/mL, the population's response shifted to a position where resistance was minimized and resilience dominated the antibiotic response. With further increase in antibiotic concentration, the resistance level continued to decrease. An effective treatment should minimize both resistance and resilience. Dot color references the antibiotic concentration used at that point, arrows indicate direction of increasing antibiotic concentration.

3.2.3 Determinants of resistance and resilience

To help further our investigation, we developed a kinetic model to describe the temporal response of a bacterial population constitutively expressing Bla to a β-lactam antibiotic. When no antibiotic is present, the population grows to carrying capacity without delay; however, once the antibiotic concentration is high enough, the population density undergoes a crash as a significant portion of the population is lysed by the antibiotic, and a recovery, as the released Bla degrades the antibiotic (**Figure 8a, Figure 13**).

Global sensitivity analysis was used to determine which parameters influenced resistance and resilience under a range of antibiotic concentrations. Briefly, the Sobol method calculates resilience and resistance for a range of parameter values and breaks down the variation for each into fractions that can be attributed to one or more parameters[122]. Here, we reported the total effect index, ST, which reflects how much a parameter and all its interactions with any other parameters contributes to the variation in resistance and resilience at a particular antibiotic concentration (**Figure 8b, Figure 10**). Comparing the ST for each parameter when A=100 μg/mL reveals that resistance is only sensitive to the maximum lysis rate (ST_γ = 1±0.02). The sensitivity analysis revealed that all parameters affect resilience to varying degrees, depending on the antibiotic

concentration. Resilience is sensitive to the maximum lysis rate (ST_{γ}= 0.9 ± 0.02), Bla activity (ST_{κ_b}= 0.13 ± 0.01), the turnover rate of Bla (ST_{d_b}= 0.05 ± 0.003), and the amount of nutrients recycled from cell lysis ($ST_{\xi} =$ 0.03 ± 0.01). These parameters determine the collective ability of the population to remove the antibiotic, underscoring the notion that resilience is a population-level trait.

We tested the influence of Bla activity computationally by varying κ_b , and experimentally by using clavulanic acid, a well-characterized Bla inhibitor (**Figure 8c**, **Figure 14)**. With increased Bla inhibition, the population became more sensitive to the antibiotic, thus resulting in the antibiotic response shifting from relying on both resistance and resilience to just resilience at a lower concentration of antibiotic. Furthermore, the population with significantly reduced Bla activity did not survive exposure to the higher concentrations of antibiotic (resistance and resilience were both reduced).

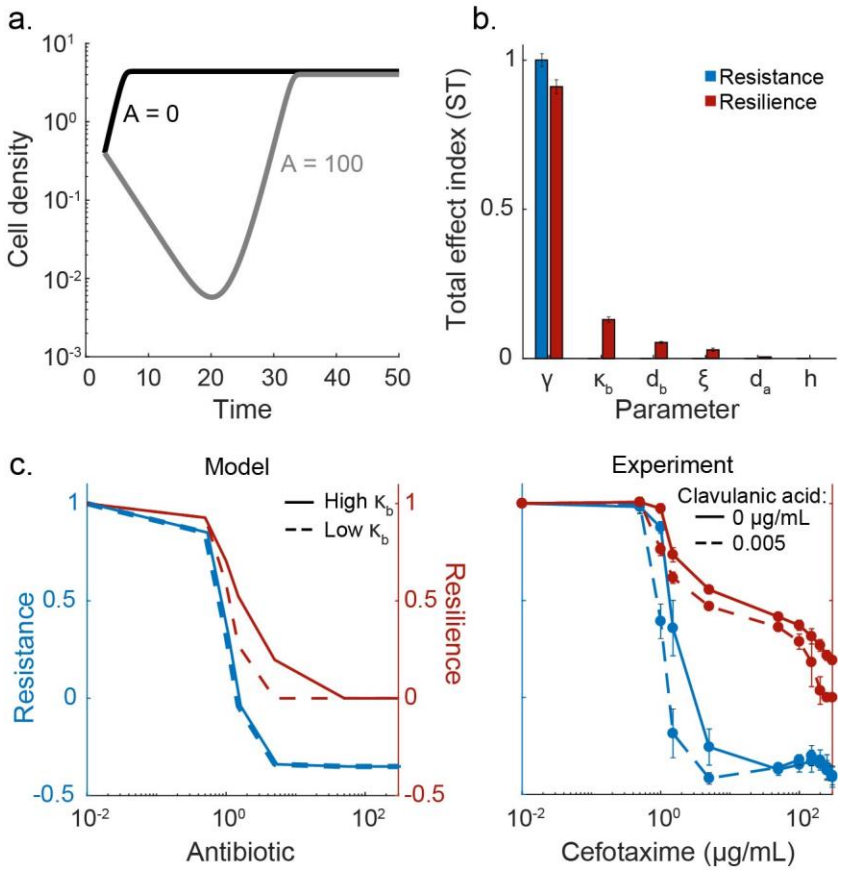

Figure 8. Modeling reveals key determinants of resistance and resilience. (a) Simulated time courses of an ESBL-producing isolate with and without an antibiotic. The characteristic "crash and recovery" is generated once the antibiotic concentration is high enough. **(b) Sensitivity analysis reveals determinants of resistance and resilience.** Total effect indices (ST) for resistance and resilience are reported for each parameter (A = 100 µg/mL). Resistance is most affected by the lysis rate (γ). The remaining parameters did not significantly affect the system's resistance, but did affect resilience. The most influential parameters included the maximum lysis rate ($\boldsymbol{\gamma}$), Bla activity ($\boldsymbol{\kappa_b}$), the turnover rate of Bla ($\boldsymbol{d_b}$), and the amount of nutrients released during lysis ($\boldsymbol{\xi}$). **(c) Modulating resistance and resilience by tuning Bla activity.** We altered Bla activity in the model (left column) or experimentally added clavulanic acid (right column) in combination with a range of antibiotic concentrations. Here, a low Bla activity corresponds to $\boldsymbol{\kappa_b = 0}$ in the model or 0.005µg/mL clavulanic acid in the experiment. A high Bla activity corresponds to $\boldsymbol{\kappa_b = 0.35}$ in the model or no clavulanic acid in the experiment. Reducing Bla activity increased the population's sensitivity, causing both resistance and resilience to decrease at lower concentrations of antibiotic.

3.2.4 Phenotypic signatures of bacterial responses in the resistance-resilience framework

Given that Bla inhibitors are commonly used to restore sensitivity to some β-lactam antibiotics[119], we explored the implications of using the resistance-resilience framework to optimize combination treatments by analyzing the response of four different ESBL-producing isolates (**Table 1**).

Table 1: ESBL-producing isolates screened

Label	**Isolate I**	**Isolate II**	**Isolate III**	**Isolate IV**
Isolate ID	DICON-005	DICON-029	DICON-047	DICON-049
MicroScan ID	*K. pneumoniae*	*E. coli*	*K. oxytoca*	*E. coli*
CTX (mm)	21	21	24	28
CTX + CLA (mm)	31	33	26	32
CAZ (mm)	30	28	24	28
CAZ + CLA (mm)	32	31	24	38
MicroScan ESBL	POSITIVE	POSITIVE	POSITIVE	POSITIVE
Disk Diffusion ESBL	POSITIVE	POSITIVE	NEGATIVE	POSITIVE

We exposed each isolate to different combinations of antibiotic and Bla inhibitor concentrations and recorded their antibiotic responses. The resistance and resilience for each scenario were calculated and plotted against each other (**Figure 9a**). The framework revealed how a small dose of antibiotic (5 µg/mL cefotaxime) could minimize resistance for Isolate I, but larger doses were needed to minimize resilience. However, resilience could be minimized with a small dose of Bla inhibitor (0.05 µg/mL clavulanic acid), when in combination with the antibiotic. A similar trend was observed in Isolates II and IV, with treatments using higher concentrations of Bla inhibitor requiring less antibiotic to minimize resistance and resilience. Isolate III, however, was not affected by increasing

concentrations of Bla inhibitor, as seen by the overlapping resistance-resilience curves. Only the highest concentration of Bla inhibitor (0.5 μg/mL) in combination with a high concentration of antibiotic (150 μg/mL) prevented the population from recovering.

Using the resistance-resilience framework, we determined that the minimum inhibitory concentration (MIC) of antibiotic for each level of Bla inhibitor was unique for each isolate (**Figure 9b**). Here, the MIC is defined as the concentration necessary to prevent the population from recovering within 48 hours of being exposed to treatment. For example, when 0.05 μg/mL clavulanic acid was used, the MIC was 5, 1.5, 1 and > 300 μg/mL cefotaxime for Isolates I, II, III, and IV, respectively. This diversity in the treatment responses can be explained by the expression of different or additional types of Bla that exhibit different sensitivity to inhibition by clavulanic acid. For instance, isolates producing cephalosporinases or chromosomally mediated Bla have been shown to be poorly inhibited by clavulanic acid[119,123,124]. These results underscore a critical caveat in using predetermined formulations of β-lactam/Bla inhibitor combinations to combat ESBL-producing pathogens, which is currently a standard practice[119,125,126]. Given the diversity of the phenotypic responses by the different isolates, quantitative measurements on how a strain responds to an antibiotic and a Bla inhibitor are necessary to predict the outcome of a particular combination treatment.

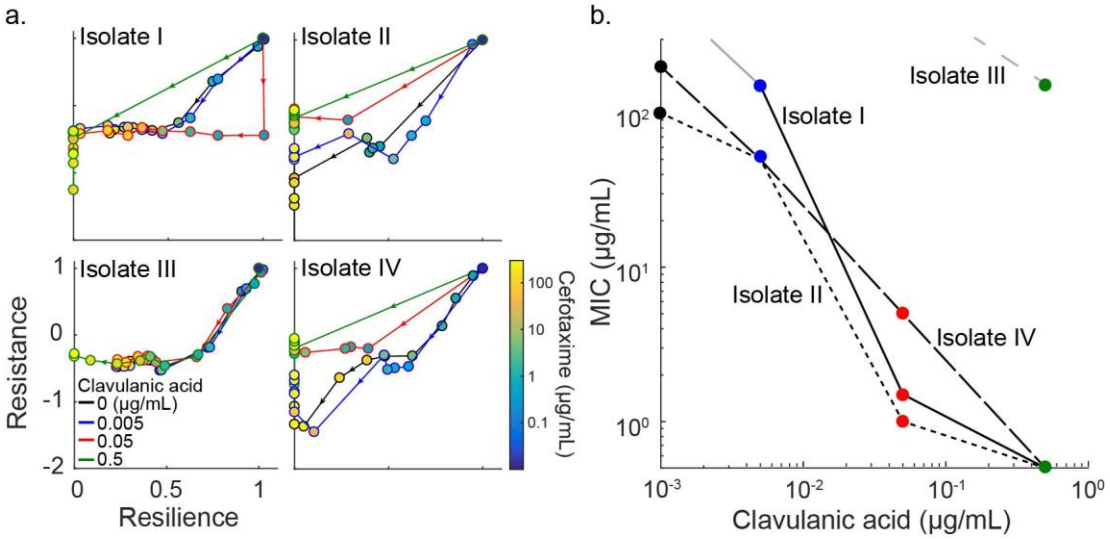

Figure 9. Diverse phenotypic responses by different ESBL-producing isolates. (a) Responses to combinations of Bla inhibitor and antibiotic concentrations. In general, with increasing antibiotic concentrations, the population responses start out as both resistant and resilient (top right of each subplot). The resistance is minimized with low doses of antibiotic, giving way to a response driven by resilience. As antibiotic concentration increased, the corresponding resilience decreased. With the addition of clavulanic acid, the concentration at which the response lost its resistance and then resilience is lowered. For Isolates I, II and IV, the highest clavulanic acid concentration (0.5 µg/mL, green curve) causes the antibiotic response to shift directly from resistant and resilient to sensitive with the lowest dose of cefotaxime (0.5 µg/mL). Isolate III was not as affected by clavulanic acid. Color of the curves indicates concentration of clavulanic acid. Color of the dots indicates concentration of cefotaxime and arrowheads indicate direction of increasing antibiotic concentration. **(b) Dependence of MIC on Bla inhibition.** For each ESBL-producing isolate, the MIC corresponds to the lowest concentration of cefotaxime needed to prevent recovery in 48 hours. One isolate, Isolate III, was not very susceptible to clavulanic acid, suggesting this intervention method would not be optimal in this case. Here, different line patterns represent the isolate and the symbol color represents the concentration of clavulanic acid, as defined in (**Figure 9**Error! Not a valid bookmark self-reference.**a**). The greyed lines indicate that the population recovered under all tested concentrations of cefotaxime tested at that concentration of clavulanic acid, therefore the MIC could not be calculated (Isolate I: clavulanic acid < 0.005 µg/mL; Isolate IV: clavulanic acid < 0.5 µg/mL).

3.3 Discussion

Resistance and resilience provide a powerful framework to dissect the contributions of different factors underlying a population's response to a disturbance. Despite their appeal, resistance and resilience have had limited applications due to differing definitions[95,96] and a lack of quantitative studies. Our analysis of an ESBL-producing

clinical isolate's response to a β-lactam antibiotic serves as a concrete example that illustrates the dichotomy between resistance associated with single cells and resilience associated with populations. That is, resilience can be considered a cooperative trait by a group of bacteria (clonal or mixed).

This dichotomy is applicable to other systems. Some bacteria are resistant to xeric stress due to the disturbance triggering their adaptive mechanisms[127]. Specifically, a xerotolerant cell survives a dry spell by decreasing its energy consumption, protecting its DNA from damaging reactive oxygen species, stabilizing its membrane, and preventing intracellular water loss. Another example of resistance being a single cell level response is the production of heat-shock proteins to enable the cell's survival of stressful conditions, such as extreme temperatures[128,129]. As for resilience, a population of cyanobacteria has been shown to depend on its density to survive high levels of light that are damaging to single cells. Mutual shading is a density dependent phenomenon achieved when the damaged cyanobacteria that are closer to the light source provide shade to their lower neighbors, thus allowing the population to regrow in lower, less damaging levels of light[130,131]. Additionally, the microbiome is resilient to diet changes, antibiotic exposure and invasion by new species due to population level attributes such as species richness and function response diversity[132].

In our analysis, the framework is applied to the dynamics of a homogenous population, where the resistance and resilience both depend on the average properties of cells. However, this framework is applicable for dissecting bacterial responses to

antibiotics for more complex (heterogeneous) populations. For example, some population's antibiotic response is driven by a small subpopulation of persisters, or slow-growing or dormant bacteria that are not sensitive to antibiotics[9,133]. Upon antibiotic exposure, most of the population is killed, leaving the persisters behind. Once the antibiotic has been removed, the persisters, which are genetically identical to their sensitive counterparts, spontaneously switch back into the normal, growing state and reestablish the colony. Therefore, this antibiotic response would be characterized with low resistance and high resilience due to the presence of persisters.

Alternatively, bacteria that have mutated forms of a given antibiotic's target are resistant to that antibiotic[134]. For instance, vancomycin-resistant *Enterococcus faecalis* (VRE) has mutated the end of a peptidoglycan strand, a component necessary for cell wall synthesis and the target for vancomycin[135]. This mutation reduces the peptidoglycan's binding affinity for vancomycin by 1000fold. Because a single bacterium of VRE has this mutation and ability to withstand much higher antibiotic concentrations, an entire population's antibiotic response would be characterized as high resistance.

In addition to dissecting an antibiotic response into its components and corresponding attributes, the resistance-resilience framework has demonstrated the need to modulate combination treatments. Comparing the resistance-resilience fingerprint of different isolates under varied concentrations of cefotaxime and clavulanic acid revealed how varied their responses are to Bla inhibition. As one way to extend the efficacy of a β-lactam is by pairing it with a Bla inhibitor [61,136,137], this observation is relevant for guiding

the optimization of combination treatments. Currently, there are a few versions of the treatment combining clavulanic acid and amoxicillin for clinical use; however, the concentration of clavulanic acid is kept constant between the versions while the amoxicillin concentration is changed[138-140]. Early studies suggest this clavulanic acid concentration was selected to minimize patient side effects and maintain a sufficiently high serum concentration of clavulanic acid [119,125,126]. Nevertheless, our finding suggests that the clavulanic acid concentration can be optimized within a safe range to reduce the amount of antibiotic necessary and minimize the resistance and resilience of a given isolate. This would allow for treatments to be customized to the situation and reduce over-prescribing.

3.4 Methods

3.4.1 Bacterial strains, growth media, and culturing conditions:

We characterized bacterial isolates from a library assembled by the Duke Hospital Infectious Disease department. This library consists of approximately 80 isolates that have been identified as ESBL producers. Unless otherwise noted, *K. pneumoniae* isolate DICON 005 was used. As a sensitive bacteria control, *E. coli* MC4100 cells were used. Unless otherwise indicated, experiments were conducted in M9 medium [1× M9 salts (48 mM Na2HPO4, 22 mM KH2PO4, 862 mM NaCl, 19 mM NH4Cl), 0.4% glucose, 0.2% casamino acids (Teknova), 0.5% thiamine (Sigma), 2 mM MgSO4, 0.1 mM CaCl2]. For overnight cultures, we inoculated single colonies from an agar plate into 2 mL M9 and incubated them for 12 hours at 30°C.

3.4.2 Measuring time courses:

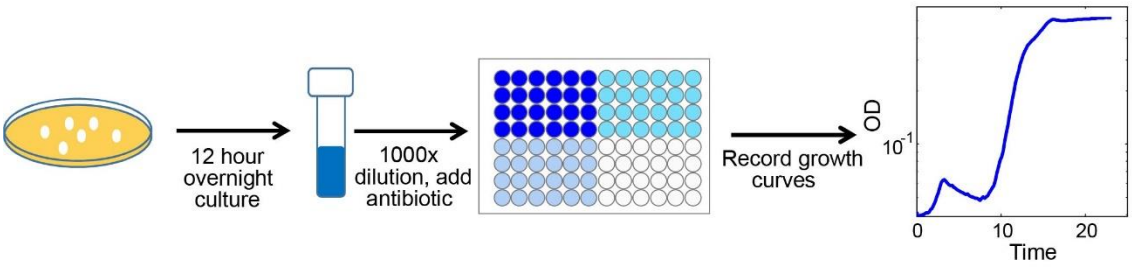

1 mL overnight culture was washed (centrifuged for 5 minutes at 13000rpm, discarded supernatant, and resuspended in 1 mL fresh M9) and the optical density (OD) was adjusted to 0.5 OD_{600} by adding the appropriate volume of M9. The culture was then diluted 1000fold in fresh M9 and the appropriate amount of cefotaxime (Sigma) was added to achieve a range of concentrations from 0-300 µg/mL. A 96-well plate (Costar) was loaded with 200 µL of culture per well and topped with 50 µL mineral oil (Sigma) to prevent evaporation. The plate was loaded into a Tecan Infinite M200 PRO microplate reader (chamber temperature maintained at 30°C) and OD_{600} readings were measured every 10 minutes for 48 hours with intermittent plate shaking. Unless otherwise noted, n=4 for each condition tested.

3.4.3 Cefotaxime activity level:

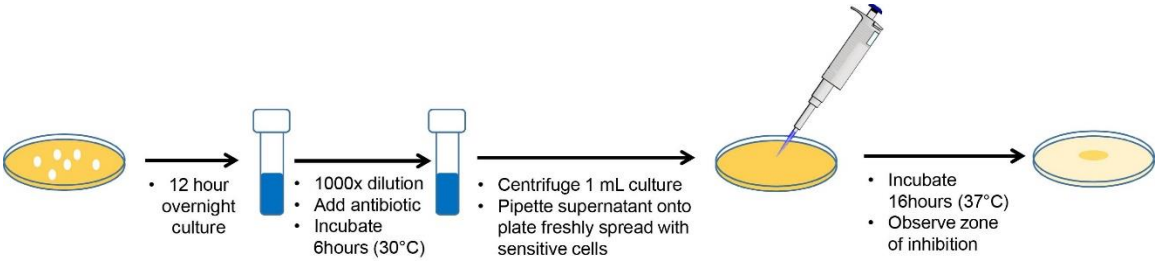

ESBL-producing Isolate I and sensitive strain MC4100 were cultured in M9 for 12 hours at 30°C. One mL of each overnight culture was washed (centrifuged for 5 minutes at 13000rpm, discarded supernatant, and resuspended in 1 mL fresh M9) and the OD was adjusted to 0.5 OD_{600} by adding the appropriate volume of M9. The culture was then diluted 1000fold in 4 mL of fresh M9 and the appropriate amount of cefotaxime was added to achieve final concentrations of 0, 10 or 100 µg/mL. The cultures were incubated at 37°C for 6 hours. At this time, lawns of sensitive cells were prepared by spreading 5 µL of the 1000fold diluted MC4100 culture onto agar plates. Supernatant from the cultures incubated with cefotaxime were prepared by spinning down 0.5 mL culture with 5 µg/mL clavulanic acid (to prevent further Bla activity). 4 µL of the supernatant were dropped into the center of the agar plates, which were then incubated for 16 hours at 37°C. The zones of inhibition were recorded by camera.

3.4.4 Selective pressure:

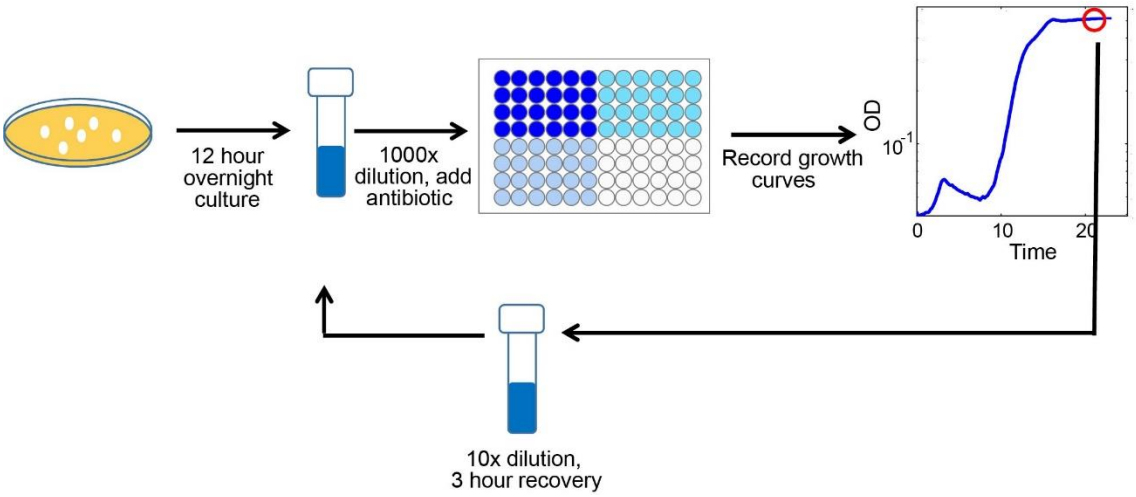

After conducting a 24-hour time course, as described in (Methods 2.4.2), culture that had been exposed to 0, 2 µg/mL, and 200 µg/mL of cefotaxime were diluted 10fold in fresh M9 (antibiotic free) and incubated at 37°C for 3 hours. The recovered cultures were then used to run another time course using the same antibiotic concentrations used in the previous round of treatment.

3.4.5 Quantifying Bla activity:

1 mL overnight culture was washed (centrifuged for 5 minutes at 13000rpm, discarded supernatant, and resuspended in 1 mL fresh M9) and diluted 1000x in fresh M9. The appropriate amount of cefotaxime (Sigma) was added to achieve 0, 1, 10, and 100 µg/mL. The cultures were incubated for 3 hours at 30°C. For each culture, 1 mL was kept on ice to preserve the population density at the 3 hour time point. 2 mL were spun down (5 minutes, 13000rpm) and resuspended in 2 mL

water before being sonicated (20 amp, duration 1 minute in 4°C room) to release periplasmic Bla. The sonicated culture was diluted 10fold in water and then treated with 0 or 1 uM of Fluorocillin. A 96-well plate was loaded with 200 µL of each culture (whole cells), sonicate with and without Fluorocillin, and topped with 50 µL mineral oil. The plate was loaded into a Tecan Infinite M200 PRO microplate reader (chamber temperature maintained at 25°C) and OD_{600} and GFP readings were measured every 10 minutes for 1.5 hours. The GFP measurements of the sonicated samples were plotted over time and the slope was calculated. The slope was normalized by the relevant culture's OD measurement. A one-way ANOVA was used to determine any significant differences between the conditions.

3.4.6 Varying Bla inhibition:

The preparation of cells, antibiotic, and 96-well plate were prepared as in (Methods 2.4.2). When the cefotaxime was added, clavulanic acid potassium salt (Sigma) was also added to achieve final concentrations ranging from 0-5 µg/mL.

3.4.7 Varying initial cell density:

Culture was prepared as in (Methods 2.4.2) except culture dilution ranged from 100 to 100,000fold. Cultures were exposed to 0 or 100 µg/mL cefotaxime and time courses were measured by plate reader and the final cell density after 30 hours was recorded.

3.4.8 Plate reader data analysis:

MATLAB (Version 9.2.0.556344, R2017a) was used to plot and characterize the time courses obtained from the plate reader (i.e. recovery time, growth rate, and change in GFP over time).

3.4.9 Modeling:

The interaction between a β-lactam and a bacterial population expressing a β-lactamase (Bla) can be simplified to the interactions between four main components: population density, antibiotic concentration, nutrient level, and Bla concentration. To model bacteria that constitutively produce Bla and lyse due to antibiotics degrading the cell wall, we modified Tanouchi et al.'s ordinary-differential-equation model [14] for the nondimensional dynamics of bacterial density (n), extracellular Bla concentration (B), nutrient level (S), and β-lactam concentration (A).

$$\frac{dn}{d\tau} = (g - l)n, \quad 3$$

$$\frac{db}{d\tau} = ln - d_B b\ , \quad 4$$

$$\frac{da}{d\tau} = -\kappa_b ba - d_a a, \quad 5$$

$$\frac{ds}{d\tau} = (\xi l - g)n\ , \quad 6$$

$$g = \frac{S}{1+S}\ , \quad 7$$

$$l = \gamma \frac{a^h}{1+a^h} g. \quad 8$$

Initial conditions of $n(0) = 0.4$, $b(0) = 0$, $a(0) = 0{:}300$, and $s(0) = 4$ were used for all the simulations. We assume that the growth rate of cells (g) is limited by s, following the Monod kinetics. We assume the lysis rate (l) can reach a maximum of γ, depends on a following the Hill kinetics, and g. d_B and d_A are the natural decay rates of extracellular Bla and antibiotic, respectively. κ_b is the rate at which Bla degrades the antibiotic. ξ is a weighting factor for how much nutrients is recycled upon cell lysis, and h is the Hill coefficient. See **3.5 Model development** for parameter values and full model development.

3.5 Model development

We model the dynamics of a system of 4 variables: cell density (N), nutrient concentration (S), antibiotic concentration (A) and external Bla concentration (B).

Reactions

$$N + S \xrightarrow{Monod} 2\,N \qquad N \xrightarrow{L(A,S)} B_{in}B + \xi S \qquad (1)$$

$$A \xrightarrow{d_A} \emptyset \qquad B \xrightarrow{d_B} \emptyset \qquad (2)$$

$$B + A \underset{k_2}{\overset{k_1}{\rightleftharpoons}} BA \qquad BA \xrightarrow{k_3} B \qquad (3)$$

1. Left: A cell, plus an equal mass of nutrients, produces another cell with a Monod dynamics. Right: Cells lyse at a rate L (which depends on A and S), releasing a quantity B_{in} of Bla and a proportion of nutrients ξ.

2. The antibiotic and Bla decay respectively at rates d_A and d_B.

3. Enzymatic degradation of the antibiotic by Bla (outside the cells).

Units: To derive differential equations from this reaction network, adequate units need to be chosen for the state variables and parameters. We will count N and S in the same unit, number of (equivalent) bacteria per liter, and A and B in moles per liter. In the following, as a visual aid, we will note |X| all quantities in the unit of N, and [X] all quantities in the unit of A.

$$\frac{d|N|}{dt} = G|N| - L|N| \qquad G = \mu \frac{|S|}{|K_S|+|S|}$$

$$\frac{d|S|}{dt} = -G|N| + \xi L|N| \qquad L = \gamma \frac{[A]^h}{[K_A]^h+[A]\hat{}h} G$$

$$\frac{d[A]}{dt} = -k_1[B][A] + k_2[BA] - d_A[A]$$

$$\frac{d[B]}{dt} = B_{in}L[N] - d_B[B] - k_1[B][A] + k_2[BA] + k_3[BA]$$

$$\frac{d[BA]}{dt} = k_1[B][A] - k_2[BA] - k_3[BA]$$

A quasi-steady-state approximation on the transitory complex BA yields $[BA] = \frac{k_1}{k_2+k_3}[B][A]$. Replacing this expression into the system gives

$$\frac{d|N|}{dt} = (G - L)|N| \qquad G = \mu \frac{|S|}{|K_S|+|S|}$$

$$\frac{d|S|}{dt} = (\xi L - G)|N| \qquad L = \gamma \frac{[A]^h}{[K_A]^h+[A]\hat{}h} G$$

$$\frac{d[A]}{dt} = -k_b[B][A] - d_A[A] \qquad k_b = \frac{k_1 k_3}{k_2+k_3}$$

$$\frac{d[B]}{dt} = B_{in}L[N] - d_B[B]$$

Dimensionless model: In order to make the model more suitable for simulations, and factor out some unidentifiable parameters, we made it dimensionless by the following change of variables:

$$n = \frac{|N|}{|K_S|} \qquad s = \frac{|S|}{|K_S|}$$

$$a = \frac{[A]}{[K_A]} \qquad b = \frac{[B]}{B_{in}|K_S|}$$

$$\kappa_b = \frac{k_b B_{in}|K_S|}{\mu} \qquad \tau = t\mu$$

$$d_a = \frac{d_A}{\mu} \qquad d_b = \frac{d_B}{\mu}$$

Resulting in this dimensionless model:

$$\frac{dn}{d\tau} = (g - l)n \qquad g = \frac{s}{1+s}$$

$$\frac{ds}{d\tau} = (\xi l - g)n \qquad l = \gamma \frac{a^h}{1+a^h} g$$

$$\frac{da}{d\tau} = -\kappa_b b a - d_a a$$

$$\frac{db}{d\tau} = ln - d_b b$$

Parameter values and typical ranges

Initial values. In all the experiments, a 3-hour delay is observed before the crash becomes visible (see **Figure 13** for example). We didn't model this delay, but assumed that the growth was nominal during this initial phase, and started all the simulations from the state reached after 3 hours of normal exponential growth. Because of collective antibiotic tolerance, to conserve a potent antibiotic on a higher cell density, we had to underestimate the efficiency of the antibiotic hydrolysis by Bla (κ_b). This is indeed the parameter that deviates the most from the literature values.

Table 2. Values for dimensioned and dimensionless variables

Dimensioned model				Dimensionless model		
Variable	Typical range	Initial value	Unit	Variable	Typical range	Initial value
|N|	10^3 to 10^{12}	$7 \cdot 10^{10}$	cell/L	$n = \frac{\|N\|}{\|K_S\|}$	10^{-8} to 10	0.4
|S|	10^3 to 10^{12}	$4 \cdot 10^{10}$	cell/L	$s = \frac{\|S\|}{\|K_S\|}$	10^{-8} to 10	4
[A]	0 to 10^{-3}	0 to 10^{-3}	mol/L	$a = \frac{[A]}{[K_A]}$	0 to 500	0 to 500
[B]	0 to 10^{-7}	0	mol/L	$b = \frac{[B]}{B_{in}[K_S]}$	0 to 3	0

Table 3: Values and units for dimensioned and dimensionless parameters

Dimensioned model				Dimensionless model	
Param.	Literature value	Unit	Ref.	Parameter	Fitted value
μ	0.8	1/h	[14]	-	-
$\lvert K_S \rvert$	$4 \cdot 10^9$ to 10^{11}	ċell/L	[141]	-	-
ξ		1	[142]	ξ	0.8
γ	1.8 to 4	1	[143]	γ	1.35
$[K_A]$	$2 \cdot 10^{-6}$	mol/L	[144]	-	-
H	3	1	[145]	h	3
k_b	10^{10}	L/(mol·h)	[146]	$\kappa_b = k_b \frac{B_{in} \lvert K_S \rvert}{\mu}$	0.35
d_A	0.015	1/h	[147]	$d_a = \frac{d_A}{\mu}$	0.02
d_B	0.02 to 0.5	1/h	[148]	$d_b = \frac{d_B}{\mu}$	0.1
B_{in}	$3 \cdot 10^{-19}$	mol/cell	[149]	-	-
D	$1 \cdot 10^{-12}$	OD/(cell/L)	[150]	-	-

Analytical expression of resistance. It is possible to derive from this model an analytical expression for the resistance. Indeed, the resistance is defined as $\frac{\rho_A}{\rho_0}$, where ρ_A is the net lysis rate observed at the point of greatest deviation from the untreated population, and ρ_0 is the net growth rate observed without antibiotic. The maximum lysis rate is always observed at the introduction of the antibiotic (after the 3-hour delay), when the antibiotic concentration in the medium is still unaltered. The net lysis rate is then $\rho_A = G - L = G - \gamma \frac{[A]^h}{[K_A]^h + [A]^h} G$, and taking $\rho_0 = G$ we finally obtain

$$\text{Resistance} = 1 - \gamma \frac{[A]^h}{[K_A]^h + [A]^h} = 1 - \gamma \frac{a^h}{1 + a^h}$$

A simple analytical expression does not seem to exist for resilience.

3.6 Sensitivity analysis

Sobol sensitivity analysis was used to determine which parameters influenced resistance and resilience under a range of antibiotic concentrations (see the tutorial by Zhang[122] for a good explanation). Briefly, the total-order sensitivity index, ST, reflects how much a parameter contributes to the variation of resistance or resilience, alone or in coordination with any number of others (**Figure 10**). The sensitivity analysis was performed on the dimensionless model, on a parameter space spanning a factor of 4 centered around each parameter's default value ($x \in [\frac{x_0}{2}, 2x_0]$). The sampling of the parameter space and analysis of the results was done with the open-source Python library SALib[151].

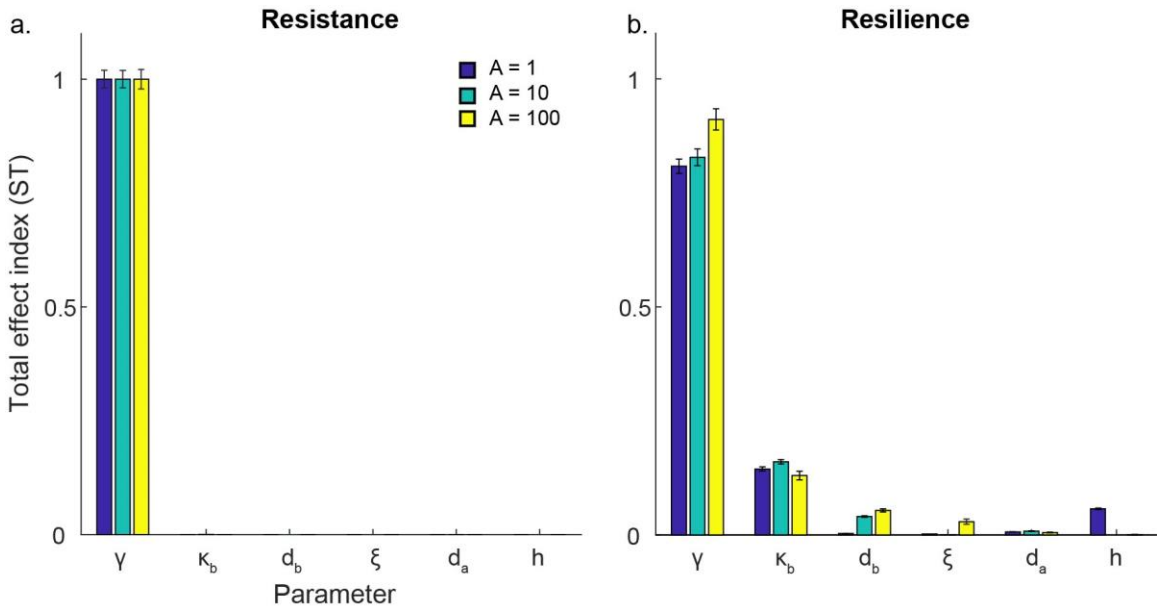

Figure 10. Sensitivity analysis reveals parameters affecting resistance and resilience. (a) **Resistance is most sensitive to the maximum lysis rate** (γ) for all antibiotic concentrations tested. (b) **Resilience is affected by numerous parameters**. Regardless of antibiotic concentration, lysis rate has the greatest impact followed by Bla activity level (κ_b). As antibiotic concentration increases, the turnover rate of Bla (d_b) and nutrient recycling (ξ) become more influential and the Hill coefficient (h) becomes less influential. Of interest are the parameters affecting Bla activity, κ_b and d_b, because they can be targeted clinically by a Bla inhibitor.

3.6.1 Resistance

The main effector of resistance is the maximum lysis rate γ, which is given a total-effect index of 1 at 1, 10 and 100 μg/mL (**Figure 10a**). From the expression derived earlier,

$$\text{Resistance} = 1 - \gamma \frac{a^h}{1+a^h}$$

When a << 1, resistance will be 1, regardless of parameter variation. When a >> 1, resistance becomes dependent on γ as resistance approaches $1 - \gamma$. When a ≈ 1, h should have a minor influence, which is shadowed by γ's. These parameters are characteristic of single cell level behavior, suggesting that resistance is a single cell level trait.

3.6.2 Resilience

Results from the sensitivity analysis for resilience revealed that all parameters contributed to varying degrees, depending on the antibiotic concentration (**Figure 10b**). At low concentrations of antibiotic, the most influential parameters are the maximum lysis rate (ST_{γ}= 0.81 $\pm$ 0.02) and the catalytic activity of Bla (ST_{κ_b}= 0.145$\pm$0.005). At higher concentrations, γ and κ_b's total-effect indexes persist as the two mainly influential parameters, with the addition of the decay rate of Bla which appears at ST_{d_b} = 0.040 $\pm$ 0.002 at A = 10 µg/mL and at ST_{d_b} = 0.053 $\pm$ 0.003 at A = 100 µg/mL. Although γ is the main effector, κ_b and d_b are related to population-level behaviors, suggesting that resilience could be a population-level trait.

3.7 Supplementary figures

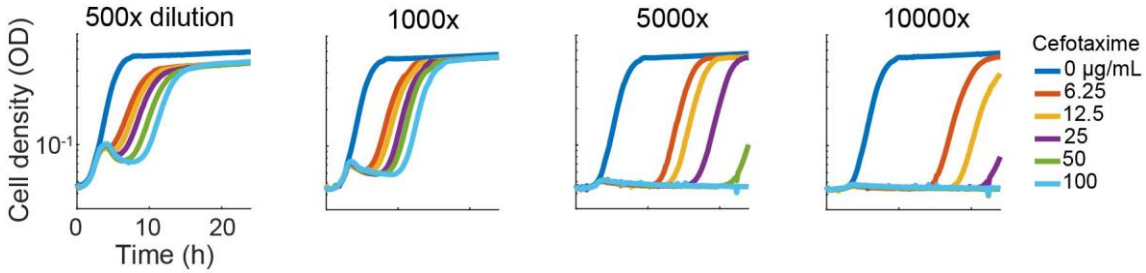

Figure 11. Collective antibiotic tolerance. The population survival to antibiotic exposure depends on the initial cell density. The starting density was diluted from 500 to 10000 times and then exposed to a range of cefotaxime doses. The time courses show that increasing the antibiotic concentration resulted in a longer recovery time because more cells were lysed. If the cell density is too low, then there will be too few cells to produce the amount of Bla needed to degrade the antibiotic and allow the population to recover.

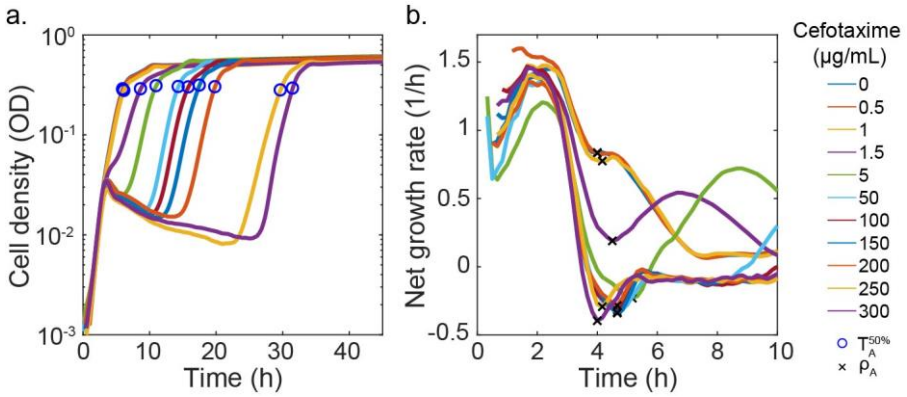

Figure 12: Time course and rate of change curves of Isolate I. (a) Resilience was calculated from the time courses (antibiotic added at time = 0). At low concentrations (A < 1:5 μg/mL), the growth curves looked very similar to the control (A = 0) and are considered to be "resistant" to these conditions. At A = 1:5 μg/mL, the growth curve starts to deviate from the control due to an increase in cell lysis, showing a decrease in resistance. Once the concentration was high enough (A = 5 μg/mL), the population started displaying the crash and recovery dynamics. The time to half maximum density ($T^{50\%}$, blue circle) was determined for each concentration and used to calculate resilience. **(b) Resistance was calculated from the net growth rate**. $\boldsymbol{\rho_A}$ is calculated as the point of maximum deviation from the untreated population, as indicated by the black crosses. The initial 3 hours were not included because the ratio of noise to actual measurement was too high.

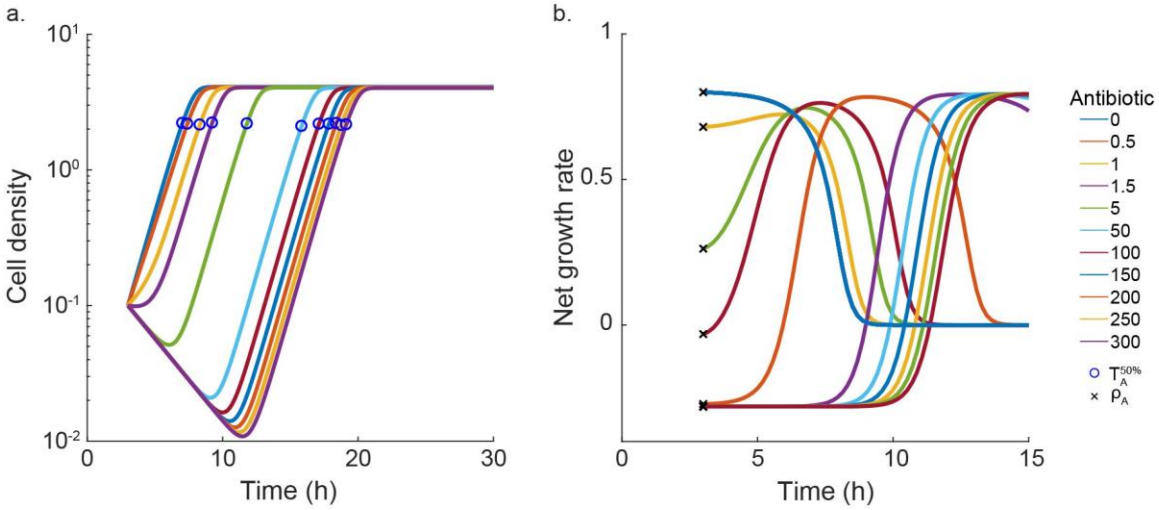

Figure 13. Time courses and rate of change curves generated by the model. (a) Simulated time courses. Similar to the experimental data, the cell density undergoes a crash and recovery once the antibiotic concentration is high enough. With increasing antibiotic concentration, the amount of time necessary for the population to recover increases. $T^{50\%}$ was calculated as in **Figure 12a**. **(b) Simulated net growth rate.** The net growth rate was used to determine ρ_A, calculated similarly to **Figure 12b**.

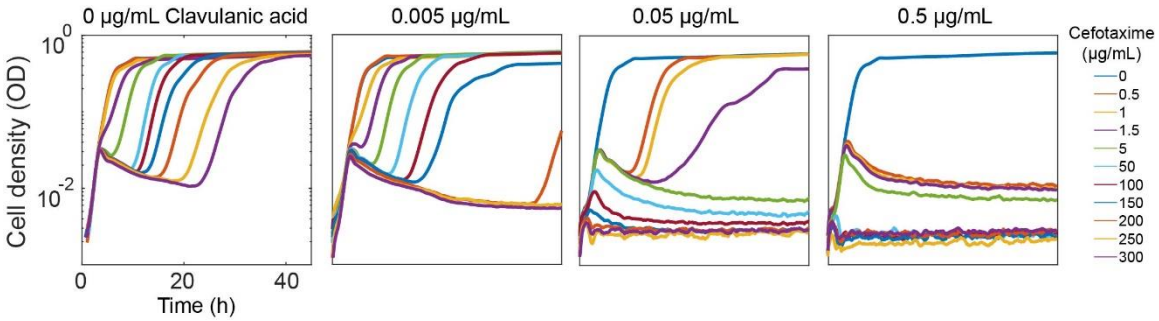

Figure 14: Time courses showing the effects of Bla inhibition. Isolate I was exposed to the same range of cefotaxime (0 : 300 µg/mL) in combination with clavulanic acid ranging from 0 : 0.5 µg/mL. With increasing clavulanic acid concentrations, the isolate became increasingly sensitive to the cefotaxime as more Bla activity was inhibited.

4. Bacterial temporal dynamics enable optimal design of antibiotic treatment[3]

There is a critical need to better use existing antibiotics due to the urgent threat of antibiotic resistant bacteria coupled with the reduced effort in developing new antibiotics. β-lactam antibiotics represent one of the most commonly used classes of antibiotics to treat a broad spectrum of Gram-positive and -negative bacterial pathogens. However, the rise of extended spectrum β-lactamase (ESBL) producing bacteria has limited the use of β-lactams. Due to the concern of complex drug responses, many β-lactams are typically ruled out if ESBL-producing pathogens are detected, even if these pathogens test as susceptible to some β-lactams. Using quantitative modeling, we show that β-lactams could still effectively treat pathogens producing low or moderate levels of ESBLs when administered properly. We further develop a metric to guide the design of a dosing protocol to optimize treatment efficiency for any antibiotic-pathogen combination. Ultimately, optimized dosing protocols could allow reintroduction of a repertoire of first-line antibiotics with improved treatment outcomes and preserve last-resort antibiotics.

[3] The content of this chapter has been published. Meredith H.R, Lopatkin A.J., Anderson D.J., & You L. Bacterial temporal dynamics enable optimal design of antibiotic treatment. PLoS Computational Biology. 2015 Apr 23; 11(4).
Author contributions: HRM and LY wrote the manuscript.

4.1 Introduction

Bacteria eventually develop resistance to all antibiotics they encounter [152-154]. Unfortunately, the evolution of antibiotic resistant bacteria is accelerating due to the widespread use of antibiotics [155,156]. As the antibiotic pipeline is drying up and the threat of antibiotic resistance is becoming more urgent [2,116], it is critical that we better utilize the antibiotics already on the market [3,15,157].

One of the largest and most commonly used classes of antibiotics for treating both Gram-positive and Gram-negative bacteria is the β-lactams [117,158,159]. Many β-lactams, such as penicillin V, amoxicillin, and first-generation cephalosporins, are first-line antibiotics; they are recommended for initial therapy because they are highly effective against non-resistant pathogens, have a lower risk of side effects, and are less expensive, relative to second-line antibiotics [160-162]. However, the rapid emergence of extended spectrum β-lactamase (ESBL) producing pathogens has greatly limited the use of β-lactam antibiotics [113,117]. ESBL-producing pathogens have significant adverse effects on clinical outcomes due to their ability to hydrolyze penicillins, broad-spectrum cephalosporins, and monobactams [114-116]. Patients infected with ESBL-producing pathogens have worse prognoses and, if given the incorrect treatment, mortality rates of 42-100% greater than patients receiving the correct treatment [114,163]. Additionally, β-lactams could promote horizontal gene transfer of virulence factors [164] and could be responsible for the spread of ESBL genes. As a precaution, most first-line β-lactams are ruled out if ESBL-producing pathogens are detected, even for ESBL-producing pathogens that appear to be sensitive to

a particular β-lactam [165-168]. This is done largely out of concern for complicating drug responses that have been observed *in vitro*, such as the inoculum effect, a phenomenon in which the minimum inhibitory concentration (MIC) of an antibiotic increases as the bacterial density increases [10,167,169-172].

With first-line β-lactams ruled out, second-line antibiotics, such as carbapenems, fluoroquinolones, β-lactam/β-lactamase inhibitor combinations, glycopeptides, and cephamycins, are typically administered [173]. Although this practice is based on a valid concern, it has limitations. Specifically, second-line antibiotics are associated with higher costs and more adverse effects [174-179]. Additionally, the more frequently bacteria are exposed to second-line antibiotics, the faster the pathogens are likely to develop resistance to our last resort antibiotics [153,156]. Given the dearth of new antibiotics entering the market and the limited number of effective antibiotics already available, we cannot afford to disregard potentially effective antibiotics.

First-line β-lactams could represent a missed opportunity for treating pathogens producing moderate levels of ESBLs. Individual bacteria that produce moderate levels of ESBL can remain sensitive to the antibiotic due to insufficient production or activity of ESBL; however, if enough bacteria are present, then the population's collective ESBL concentration will be sufficient to render the population resistant to the antibiotic [17,180]. In other words, a low density population of moderate ESBL producers would lyse entirely because its collective ESBL concentration would be insufficient to inactivate the β-lactam, while a high density population would only experience partial lysis before its collective

ESBL concentration can inactivate the β-lactam and promote the recovery of the surviving bacteria. This collective population recovery is time dependent [14]. Shortly after the antibiotic is first applied, the population will be reduced due to lysis and appear susceptible because it will not have yet benefited from the activity of ESBLs. Ideally, a treatment could pinpoint the time window when the most lysis has occurred and the least benefit has been experienced.

Extensive studies have been carried out to devise methods to optimize treatment efficacy of antibiotics by changing the dosing period and amplitude. These studies typically examine which metric(s) can capture the pharmacokinetic/pharmacodynamics (PK/PD) of an antibiotic and be used to predict antibiotic efficacy [181-184]. Current metrics adopted in the clinical setting, such as the MIC, do not account for the time course of antimicrobial activity and are not sufficiently predictive of treatment efficacy [165,185-187].

Therefore, there is a need for a simple metric that characterizes this pathogen-antibiotic interaction that can be easily measured and used to design dosing protocols that will effectively clear an infection. Here, we use quantitative modeling to demonstrate a strategy for customizing regimens for particular bacteria and antibiotic combination without needing to know the full mechanistic basis for the bacteria-antibiotic interaction. Specifically, we focus on optimizing a dosing protocol to enable β-lactams to effectively treat a moderate ESBL-producing pathogen. To help guide the design of effective protocols, we develop a metric, the recovery time, which is easy to measure and quantifies the pathogen-antibiotic interaction. Even though we assumed specific

molecular mechanisms underlying this collective antibiotic response, our model illustrates that the predictive power of the recovery time is maintained for different specific molecular mechanisms and for different initial conditions. Through optimized antibiotic regimens, our strategy could extend the use of first-line antibiotics, improve treatment outcome, and preserve last-resort antibiotics.

4.2 Results

4.2.1 Model development and characterization

We developed a kinetic model comprising a set of ordinary differential equations (ODEs) to capture the population dynamics of collectively tolerant, ESBL-producing bacteria being treated by a β-lactam (**4.5.1. Model development.**) [14]. We further nondimensionalized the model to facilitate analysis. In this model, introduction of the antibiotic inhibits bacterial growth and causes lysis. β-lactamase (Bla) is naturally found in the periplasm of Gram-negative bacteria, where it can benefit the host bacterium by hydrolyzing the β-lactams that diffuse into the periplasm [119]. However, moderate amounts of periplasmic Bla are insufficient to protect a bacterium from high concentrations of antibiotic [17,188]. Conversely, sufficient amounts of Bla can accumulate to protect a population if enough bacteria are initially present. With a dense enough population, the collective intracellular and extracellular Bla, due to lysis or leaky secretion [120], will be sufficient to degrade the antibiotic to a sublethal concentration before all cells are eliminated (**Figure 15a**). Thus, the survival of the population depends on establishing a collective antibiotic tolerance (CAT)[172]. In general, Bla expression can be constitutive or

inducible by the antibiotic [149,189-191]. Here, we focus on constitutive Bla expression, which is most clinically relevant to the pathogens that express plasmid-mediated ESBLs [180,192]. However, our conclusions also apply to the case where Bla expression is inducible. They will likely apply to bacterial responses to other antibiotics if the antibiotic causes an initial decline in the population density by killing a subpopulation of cells and the population can recover when the antibiotic is subsequently degraded by an enzyme produced by the cells (whether or not the enzyme is released into the culture).

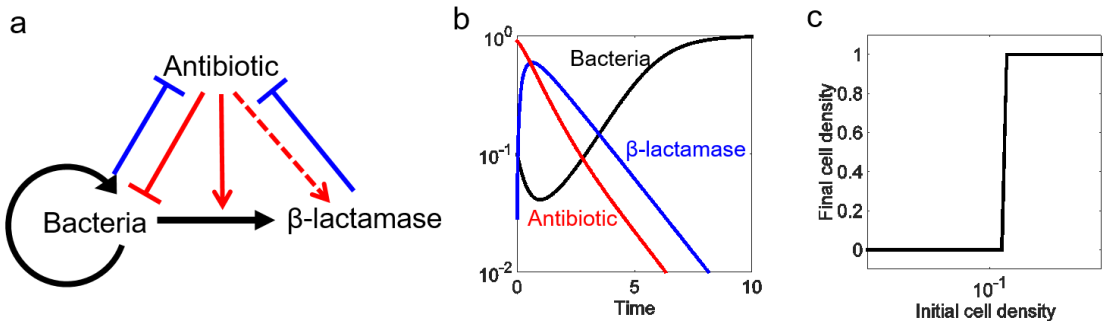

Figure 15: Mechanism and dynamics of antibiotic-mediated death. (a) Antibiotic-mediated death. Black represents bacterial actions, blue represents Bla actions, and red represents antibiotic actions. Arrows denote induction or activation; T-lines indicate inhibition; the dashed arrow represents the ability for the model to simulate inducible or constitutive Bla production. **(b) Typical time courses** of bacterial density, antibiotic, and Bla after one dose of antibiotic treatment. The antibiotic can cause cell lysis, which triggers the release of Bla into the environment. Sufficient degradation of the antibiotic by the Bla allows the surviving bacteria to recover. **(c) Collective tolerance.** A bacterial population can only recover from an antibiotic dose if enough bacteria are present for sufficient Bla to be produced.

Using physiologically relevant parameters, our model generates PK/PD profiles that are characteristic of Bla-mediated CAT. Starting from a sufficiently high initial density, the population exhibits an initial decline upon antibiotic treatment, followed by eventual recovery due to intrinsic and Bla-mediated degradation of the antibiotic (**Figure 15b**). Sufficient time is needed to observe this apparent drug tolerance. If examined

shortly after antibiotic treatment, the population will have just experienced significant lysis and will appear susceptible because the effects of Bla have not yet been fully recognized.

For a fixed initial antibiotic concentration, the model predicts a switch-like dependence of population survival over the initial population density: the population can only survive if starting at a sufficiently high density (**Figure 15c**). If too few bacteria are present, the total expression of Bla from the entire population is insufficient to degrade the antibiotic fast enough to allow the population to recover. If enough bacteria are present, however, the population can endure the initial crash in density for a longer period. As such, some bacteria remain when the antibiotic concentration decreases sufficiently, due to Bla-mediated degradation, to allow the population to recover. The density-dependent survival of the population is the defining feature of the inoculum effect [10,193].

4.2.2 Recovery time as a metric to quantify bacterial response

Our results illustrate the defining features of a CAT bacterial response involving antibiotic-triggered death. In particular, the population will appear resistant when its initial density is sufficiently high and it is given enough time to recover. These features form the basis for the preemptive practice of disregarding β-lactams when an ESBL-pathogen is identified. However, our model also indicates that the population is sensitive when its initial density is sufficiently low or when it is examined in a short time window. Given these properties, we reason that optimal antibiotic dosing may remain effective in

eliminating bacteria. If so, an immediate next question is how to best design the treatment protocol.

This task would be straightforward if we could determine the specific molecular mechanisms and defining parameters for each pathogen-antibiotic pair: under such a scenario, we could in theory use a model specific to the pair to examine efficacy of different dosing protocols. This is impractical, however, as many ESBL pathogens are poorly characterized at the molecular level and there are many different ESBL enzymes [194]. A more practical option would be to identify an easy-to-measure, *lumped metric* based on a bacterial population's response to a single dose of antibiotic that will allow us to reliably predict its response to periodic antibiotic treatment without needing to know the underlying molecular-level parameters.

A typical metric to quantify efficacy of an antibiotic is the minimum inhibitory concentration (MIC), which can be measured by disk diffusion and microbroth dilution methods after a certain duration of antibiotic treatment [195]. However, the MIC measured at a particular time point does not capture the rich temporal dynamics of bacterial responses due to antibiotic-triggered death. Instead, we propose to use another lumped metric: the recovery time; specifically, this defines the time it takes a population to return to its initial density after being exposed to a dose of antibiotic (**Figure 16**). By definition, the recovery time captures the dominant dynamic features of bacterial temporal response. As such, it may be a more predictive metric for the long-term outcome of periodic antibiotic treatment.

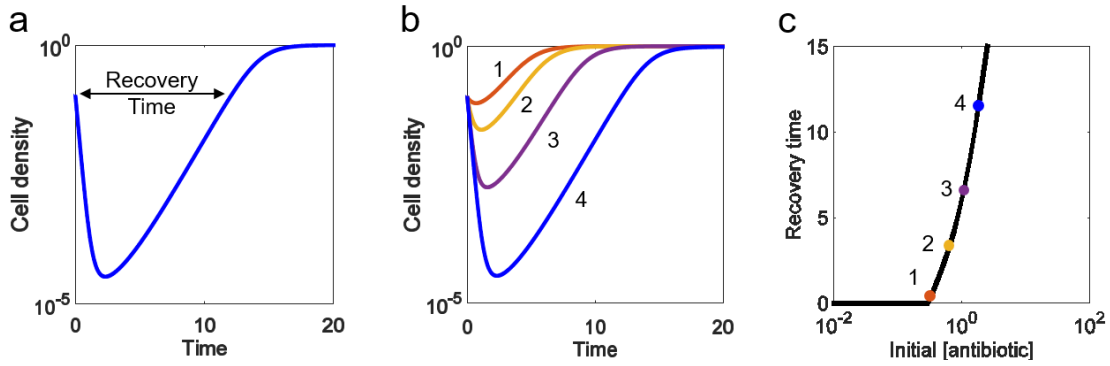

Figure 16: Defining the recovery time. (a) Recovery time defined. The recovery time is the time it takes for a population to return to its starting density after being exposed to a dose of antibiotic. **(b) Each antibiotic concentration has a recovery time.** To capture both the time- and concentration-dependent relationship between an antibiotic and the bacterial population, the recovery time is measured for a range of an antibiotic's concentrations. (Increasing numbers labeling the curves correspond to increasing concentrations of antibiotic: 1 = weakest, 4 = strongest). **(c) The recovery time curve links pathogen to an antibiotic.** The recovery times for a range of antibiotic concentrations produce an informative curve that represents the interaction between a pathogen and a particular antibiotic.

4.2.3 Predictive power of the recovery time for injection-based protocols

We first tested the predictive power of the recovery time in injection-based dosing protocols. With the base-parameter set, our model predicts a monotonic dependence of the recovery time on the antibiotic concentrations for single-dose treatment (**Figure 17a**). Once the initial antibiotic concentration is high enough to cause cell lysis ($a_0 > 0.5$), the recovery time increases exponentially with the initial antibiotic concentration until the antibiotic concentration is too high ($a_0 > 10$) and the recovery time becomes infinite. This dependence is an intrinsic property of antibiotic-mediated lysis. Under low concentrations of antibiotic ($0.5 < a_0 < 10$), the recovery time is primarily determined by how fast the antibiotic is degraded by Bla. Under increasing concentrations of antibiotic ($a_0 > 10$), the rate of antibiotic degradation is essentially saturated (limited by

the population size and the constant production rate of Bla) and the recovery time is primarily determined by the lysis rate. β-lactams' killing rate is time-, not dose-, dependent and is reflected in the model's lysis rate's non-linear dependence on the antibiotic concentration (Hill coefficient = 3) [196]. Once the antibiotic concentration is high enough, further increasing the concentration does not increase the lysis rate.

As noted above, the recovery time could represent a simple, yet reliable, metric in predicting outcomes from periodic treatment. To test this notion, we examined the consequence of periodic dosing of varying antibiotic concentrations. For each concentration, we varied the dosing periods from 0.1 to 2 times the corresponding recovery time, and obtained the final population density after 100 doses. Our modeling results confirmed the predictive power of the recovery time: as long as the initial antibiotic concentration is sufficiently high to cause significant initial lysis, the population will reach a high final density if the period is greater than the recovery time; the population goes extinct otherwise **(Figure 17b)**.

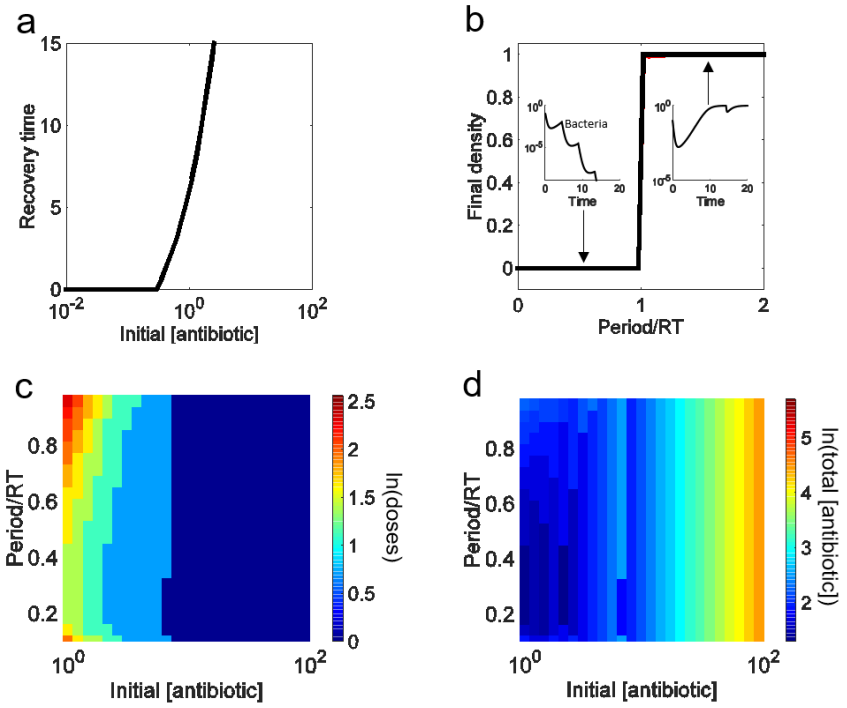

Figure 17: Recovery time guides design of effective injection based regimen. (a) Dependence of the recovery time on the initial antibiotic concentration. If the initial antibiotic concentration is too low, then the population will not be affected and its recovery time will be zero. However, after the initial antibiotic concentration is high enough, increasing the concentration results in an increase in the time it takes for a population to recover from a single dose. **(b) Predictive power of recovery time for the outcome of long-term periodic antibiotic dosing.** For each antibiotic concentration-period combination, we calculate the final population density after 100 antibiotic doses. Subplots demonstrate the outcomes for the first couple of doses of regimens using periods less than one recovery time (bacteria final density is below the defined threshold of 10^{-10}) versus regimens using periods greater than one recovery time (bacteria final density returns to carrying capacity). **(c) Dependence of treatment efficiency on the antibiotic concentration and the dosing period**. Each combination using an antibiotic concentration with a recovery time > 0 ($\boldsymbol{a_0 > 0.5}$) and any period less than 1 recovery time can eventually eliminate the population. Different combinations will reduce the population density to a pre-defined threshold (10^{-10}) with varying efficiency: the combination is more efficient if fewer doses are needed to reach the threshold. $\boldsymbol{a_0 < 0.5}$ could not clear the infection in 100 doses. **(d) Dependence of total antibiotic usage on** the antibiotic concentration and dosing period. The total usage is calculated as the antibiotic concentration multiplied by number of doses needed to reduce population density to a predefined threshold.

Of the regimens leading to eventual population extinction (period < recovery time), different combinations of antibiotic concentrations and dosing periods eliminate a population with varying efficacy. To quantify this efficacy, we calculated the minimum

number of doses necessary to reduce the population density to below 10^{-10} (**Figure 17c**). The resulting landscape shows a strong dependence on antibiotic concentration and the corresponding recovery time. When the antibiotic concentration is too low and the recovery time is close to 0, the number of doses required to clear the infection is very large, regardless of the dosing frequency. When the antibiotic concentration is very high and the corresponding recovery times approach infinite, then the number of doses is very low. However, there is an intermediate range of antibiotics with intermediate recovery times that show variation in the number of doses necessary to clear the infection. Concentrations producing the longer recovery times require fewer doses because they can reduce the bacterial density more severely than concentrations with shorter recovery times.

For intermediate antibiotic concentrations ($1 < a_0 < 10$) to be most effective, the model suggests they should be delivered at low-to-intermediate period lengths (period = 20-50% recovery time) at which the population is most vulnerable. At the end of each period, the bacteria are still lysing, have almost reached minimum density, but have not yet experienced the benefits of Bla. At this point, the antibiotic has not been completely removed; thus the population will be subjected to a slightly higher concentration of antibiotic at each additional dose. If the antibiotic is delivered too frequently, the accumulated antibiotic increases the rate of lysis, thus causing higher amounts of Bla to be released, ultimately leading to the faster removal of the antibiotic. However, Bla cannot fully degrade the antibiotic before the next dose is added and the population

quickly dies off. Although the population is cleared, a higher number of doses is necessary because the degree of lysis per dose is not maximized. In other words, subsequent doses are applied before the full extent of lysis from the previous dose is observed. However, if the antibiotic is delivered too infrequently, then the population will have the chance to recover between doses. Once again, these conditions do not maximize the degree of lysis per dose and more doses are necessary to achieve the same amount of population decrease associated with doses applied more frequently.

A final aspect to consider when designing a regimen is the total amount of antibiotic delivered (**Figure 17d**). Although some of the model's regimens using higher concentrations of antibiotic ($a_0 > 10$) are associated with fewer doses, they have the highest net antibiotic concentration. These concentrations may not be optimal, due to potential adverse effects associated with using excessive amounts of antibiotic, such as the destruction of the normal microbial flora, interference with the immune response, increased nephrotoxicity, and selection for antibiotic resistant mutants [174,197-200]. Also, efficient use of antibiotics can help reduce treatment cost [160,177]. Using dose number and total antibiotic delivered, an effective and realistic regimen can be designed by minimizing the number of doses, the delivery frequency, and the total antibiotic delivered.

We note that the predictive power of the recovery time is maintained for low or moderate inoculum sizes. In particular, our modeling demonstrates that a multi-dose regimen will clear a population if the time between doses is less than one recovery time,

regardless of effective antibiotic concentration and inoculum size **(Figure 18)**. Similar to the base case, the regimen can be optimized to have the fewest doses and the lowest net antibiotic concentration delivered by selecting the lowest concentration of antibiotic associated with the longest recovery time.

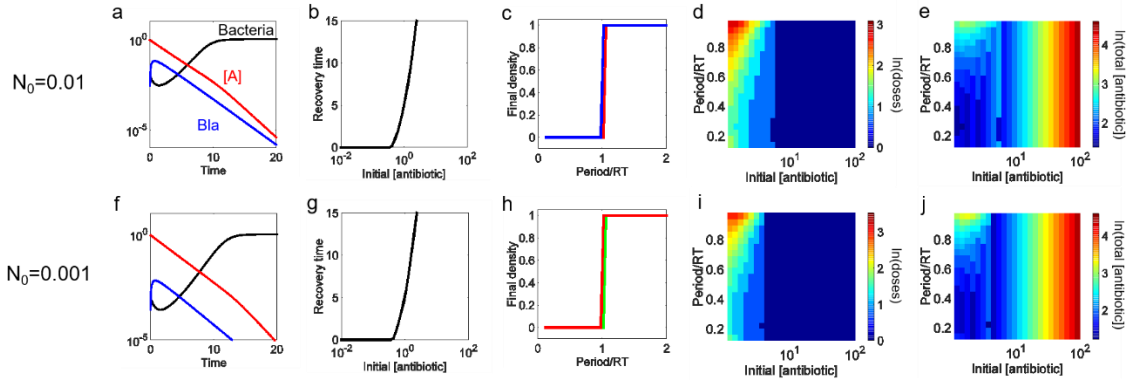

Figure 18. The effect of initial cell density on the predictive powers of recovery time. (a,f) Time courses for populations with initial densities that are 10x and 100x smaller than the base model. (b,g) Recovery time curves for populations with initial densities that are 10x and 100x smaller than the base model. (c,h) Final density depends on dosing frequency. Despite the lower initial densities, both models followed the trend where periods less than one recovery time eliminate the population as long as the initial antibiotic concentration is sufficiently high to cause significant initial decline. This indicates that the recovery time is a viable tool for predicting treatment outcomes for a range of population sizes. **(d,i) Dose number necessary to reduce a population below critical threshold depends on antibiotic concentration and period length.** The fewest number of doses corresponds to the antibiotic concentrations with the longest recovery times; however, intermediate concentrations can be effective when applied at low to intermediate period lengths. **(e,j) Total antibiotic concentration delivered depends on single dose concentration.** The regimens applying doses of lower concentrations of effective antibiotic will eliminate the population just as effectively as the regimens using high concentrations, but with less total antibiotic.

Additionally, the predictive power of the recovery time is maintained for an antibiotic with dose-dependent killing (Hill coefficient = 1) or an antibiotic with time-dependent killing (Hill coefficient = 10): a multi-dose regimen will clear a population if the time between doses is less than one recovery time, regardless of effective antibiotic concentration and degree of antibiotic-mediated killing (**Figure 19**).

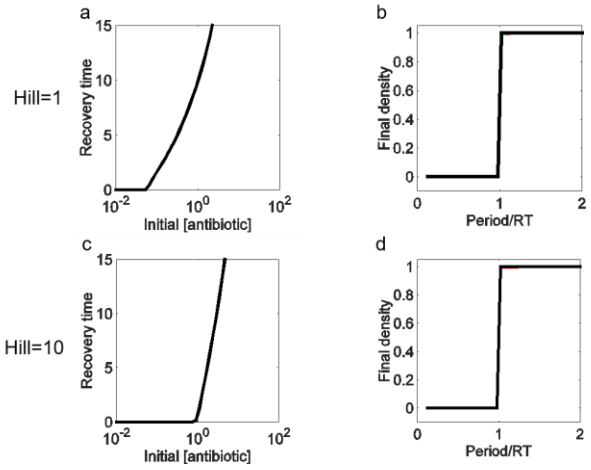

Figure 19. The effect of the Hill coefficient on the predictive powers of recovery time. (a,c) Recovery time depends less on antibiotic concentration if the Hill coefficient (H) is high enough. When H=1, the recovery time is dose dependent, increasing as the antibiotic concentration increases. When H=10, the recovery time quickly transitions from being 0 to infinite (the population has been wiped out). Once past the threshold, increasing the antibiotic concentration will not continue to increase the recovery time. **(b,d) Final density depends on dosing frequency.** Despite the different Hill coefficients, both models followed the trend where periods less than one recovery time eliminate the population as long as the initial antibiotic concentration is sufficiently high to cause significant initial decline. This indicates that the recovery time is a viable tool for predicting treatment outcomes for a range of antibiotics with different modes of killing (time vs. dose dependent).

The predictive power of the recovery time can be applied to bacteria with varying rates of Bla synthesis and accumulation as long as the antibiotic concentration applied has an effective recovery time **(Figure 20 A-T).** When the bacteria are producing and accumulating Bla at a very fast rate **(Figure 20 P-T)**, most individual bacteria can sufficiently protect themselves (CAT is no longer necessary) and the population experiences little or no decline in density. Consequentially, the model predicts that effective treatment protocols would shift to higher antibiotic concentrations capable of inducing significant lysis in more resistant bacteria.

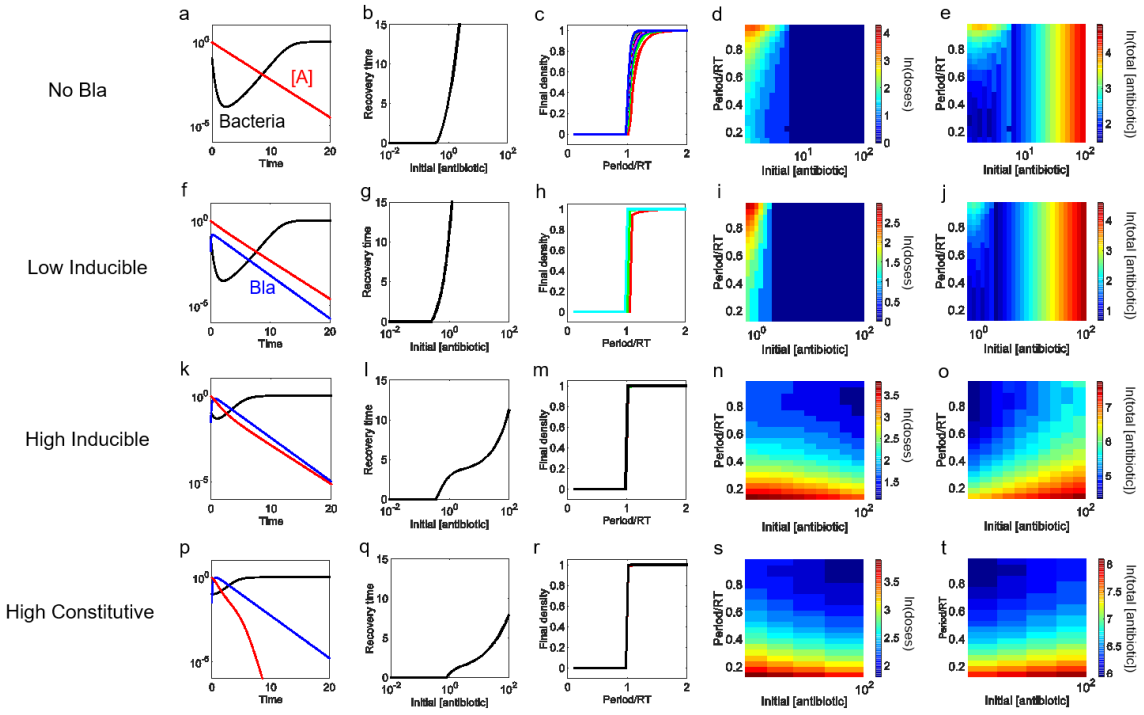

Figure 20. The effect of Bla production levels on the predictive powers of recovery time. **(a-e) No Bla production. (a) Time course.** The recovery of bacteria that do not produce Bla depends on the intrinsic removal of the antibiotic caused by natural degradation and turnover by the body's fluid. **(b) Recovery time curve.** Because the bacteria still undergo the process of lysing before recovering, the dosing protocol based on recovery time is still applicable. Without the production of Bla to aid in the recovery of the population, the recovery time is longer and monotonically dependent on the antibiotic concentration. **(c) Final density.** Protocols using periods of less than one recovery time are effective at eliminating the population, regardless of antibiotic concentration. **(d) Dose number.** For each antibiotic concentration and period combination, the corresponding number of doses necessary to eliminate the population was calculated. The regimens using antibiotics associated with longer recovery times require the fewest doses; however, low concentrations of antibiotic ($\boldsymbol{a_0 \approx 1}$) can be effective if applied at period lengths of 0.10-0.50 period/RT. **(e) Total antibiotic delivered.** Despite many different regimens requiring the same number of doses to clear an infection, the regimens could be differentiated by the total amount of antibiotic delivered. When comparing regimens with the same number of doses, the amount of antibiotics delivered decreases as the dose concentration decreases.

(f-j) Low inducible Bla production. (f) Time course. The population recovers faster than a population that does not produce Bla because it generates sufficient Bla to degrade the antibiotic; however, the recovery time is slower than a population that constitutively produces Bla because more bacteria lyse before sufficient Bla accumulates to effectively remove the antibiotic. **(g) Recovery time.** The recovery time increases as the initial antibiotic concentration increases. **(h) Final density.** Protocols using periods of less than one recovery time are effective at clearing an infection, regardless of antibiotic concentration. **(i) Dose number.** A larger range of antibiotic concentrations require the lowest number of doses because the population is more sensitive to lower antibiotic concentrations, relative to constitutive producers. **(j) Total**

antibiotic delivered. Despite the higher number of doses, the least amount of antibiotic is delivered for regimens using lower antibiotic concentrations.

(k-p) High Inducible Bla Production. (k) Time course. Increased Bla production results in less lysis, faster antibiotic degradation, and, consequently, a faster population recovery. **(l) Recovery time curve.** The non-monotonic dependence reflects the generation of the Eagle effect: a higher antibiotic concentration can generate faster population response.**(m) Final density.** Protocols using periods of less than one recovery time are effective at clearing an infection, regardless of antibiotic concentration. **(n) Dose number**. The dose number is highly complex in terms of the dependence on the initial antibiotic concentration and period length. The dependence on the recovery time, however, appears simpler: the fewest number of doses is needed for antibiotic concentrations with the longest recovery times that are delivered at intermediate-to-long dosing frequencies. Concentrations producing the longer recovery times require fewer doses because they can reduce the bacterial density more severely than concentrations with shorter recovery times. **(o) Total antibiotic delivered**. Despite the higher dose numbers, the least antibiotic is delivered for regimens applying low concentrations of antibiotics at intermediate-to-long periods.

(p-t) High constitutive Bla production. (p) Time course. Here, bacteria constitutively produce Bla at a rate an order of magnitude greater than the bacteria that constitutively produce low amounts of Bla. As a result, the bacteria produce sufficient Bla such that the private Bla present in the periplasm can provide sufficient protection against the antibiotic. As such, the overall population growth rate is always greater than the lysis rate; thus the population will always increase in density. **(q) Recovery time.** Because the bacteria produce such high amounts of Bla, the population experiences no or little initial decrease in density. Thus, the recovery time is close to 0 until stronger antibiotic concentrations are applied. **(r) Final density.** Protocols using periods of less than one recovery time are effective at clearing an infection, as long as the antibiotic concentration induces a sufficiently long recovery time (see **S5 Figure**). **(s) Dose number.** The shorter periods are associated with increased number of doses because there would be less time between when cells lyse and the Bla will not have the chance to naturally degrade before the next round of lysis adds more Bla to the environment. Higher concentrations and longer period lengths result in lower dose numbers. **(t) Total antibiotic delivered.** The least amount of antibiotic delivered is associated with regimens using lower dose concentrations and intermediate-to-long periods. This supports the notion that longer periods allow for the large amounts of Bla to degrade before the next dose, thus allowing each dose to be as effective as possible.

The predictive power is upheld as long as the recovery times associated with subsequent doses are sufficiently similar to the original recovery time measured from a single dose. Recovery times of subsequent doses depend on two main factors: the activity of Bla in the environment and the concentration of antibiotic. On one hand, if there is insufficient time for Bla to degrade between doses, then it will compound with each dose until the population is being protected by higher concentrations of Bla, relative to when the first dose was administered. As a result, the increasing pool of Bla will degrade the

antibiotic faster, the recovery time of subsequent doses will decrease, and the population can recover when dosed at period lengths less than the original recovery time **(Figure 21 A-B).** This would happen in scenarios where the antibiotic concentration applied is insufficient to counterbalance the Bla that is either expressed at high levels or has an increased rate for hydrolyzing an antibiotic. The loss of predictive power in this case can be avoided by using a sufficiently strong antibiotic concentration. On the other hand, if there is insufficient Bla to degrade the antibiotic between doses, then the antibiotic will compound with each dose until the population is being exposed to higher concentrations of antibiotic, relative to when the first dose was administered. As a result, the increasing concentration of antibiotic will kill more cells, the recovery time of subsequent doses will increase, and the population will not be able to recover when dosed with period lengths equal to the original recovery time **(Figure 21 C-D)**.

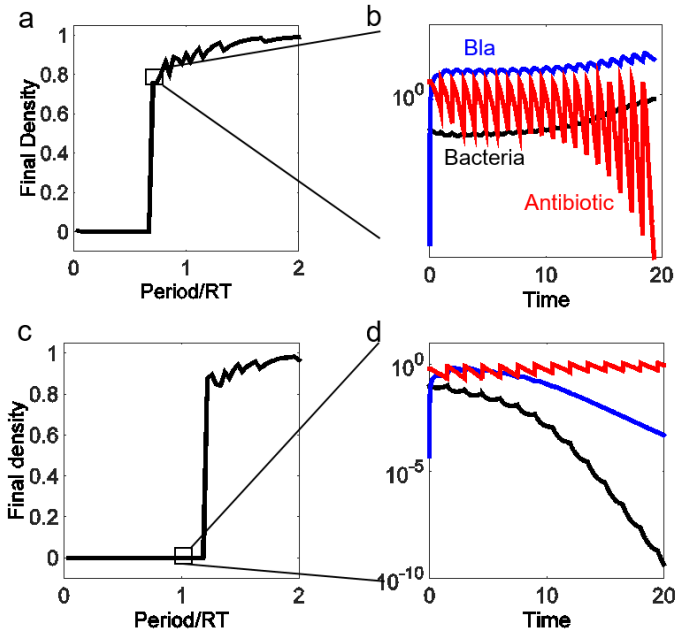

Figure 21. Predictive power is lost when single dose recovery time does not predict recovery time of subsequent doses. (a-b) Population recovers at periods < 1 recovery time (a) Final Density. Populations can recover from an antibiotic applied at periods less than one recovery time if the bacteria are producing extreme levels of Bla and the antibiotic concentration is too weak to induce sufficient lysis (i.e. has a short recovery time). If the recovery time is too short, then the time between doses is too short for the Bla to return to a baseline level. As a result, the net Bla compounds with each subsequent dose, allowing populations to survive an antibiotic applied at periods less than one recovery time. **(b)**. **Time curves for cell density, Bla, and antibiotic concentration.** Because each subsequent dose of antibiotic causes more cells to lyse and release Bla before the Bla from the previous dose is degraded, there is an increase in the base amount of Bla always present. As a result, the cells can clear the antibiotic faster on subsequent doses compared to the first dose. Consequentially, the observed recovery time from the multi-dose regimen is actually shorter than the expected response time calculated from the single dose. Here, A = 1.4 and period = 0.60 RT. **(c-d) Population fails to recover at periods = 1 recovery time (c) Final Density.** Populations fail to recover from a low antibiotic concentration applied at periods less than one recovery time if the bacteria are producing low levels of Bla. Because the antibiotic concentration is low, the recovery time and its derived dosing periods are short. The time between doses is insufficient for the Bla to degrade enough of the antibiotic to recover. As a result, the antibiotic concentration compounds with each subsequent dose, preventing populations from recovering at periods greater than one recovery time. **(d) Time curves for cell density, Bla, and antibiotic concentration.** With each subsequent dose of antibiotic, more cells lyse and release Bla; however, the cells produce insufficient Bla to degrade the current dose of antibiotic before the next dose is delivered. As a result, the antibiotic accumulates with each subsequent dose and the cells are killed. Here, A = 0.63 and period = 1.33 RT.

4.2.4 Predictive power of recovery time for intravenous-drip protocols

Many antibiotics, such as β-lactams, are most effective when applied continuously for long periods of time [201,202]. Thus, we also modeled the predictive power of the recovery time in intravenous (IV)-drip based protocols, where a set concentration of antibiotic is delivered over a set duration during each dosing period. Here, we delivered the antibiotic dose over three time units and measured the corresponding recovery time (**Figure 22a**). Similar to the injection recovery times, the IV-drip recovery times increase monotonically as the concentration of the dose increases, more Bla is required to remove the antibiotic, and more of the population lyses. In contrast, the IV-drip therapy has a narrower range of intermediate antibiotics with 0 < recovery time < 100. Some of the lower concentrations that are effective for injection treatment ($0.5 < a_0 < 1$) are ineffective for IV drip treatment because the dose is too weak when delivered over a longer period of time. However, when the dose concentration is sufficiently high, the IV-drip recovery time is longer than the injection recovery time because the IV-drip is exposing the bacteria to a higher concentration for a longer period of time (**Figure 22b**).

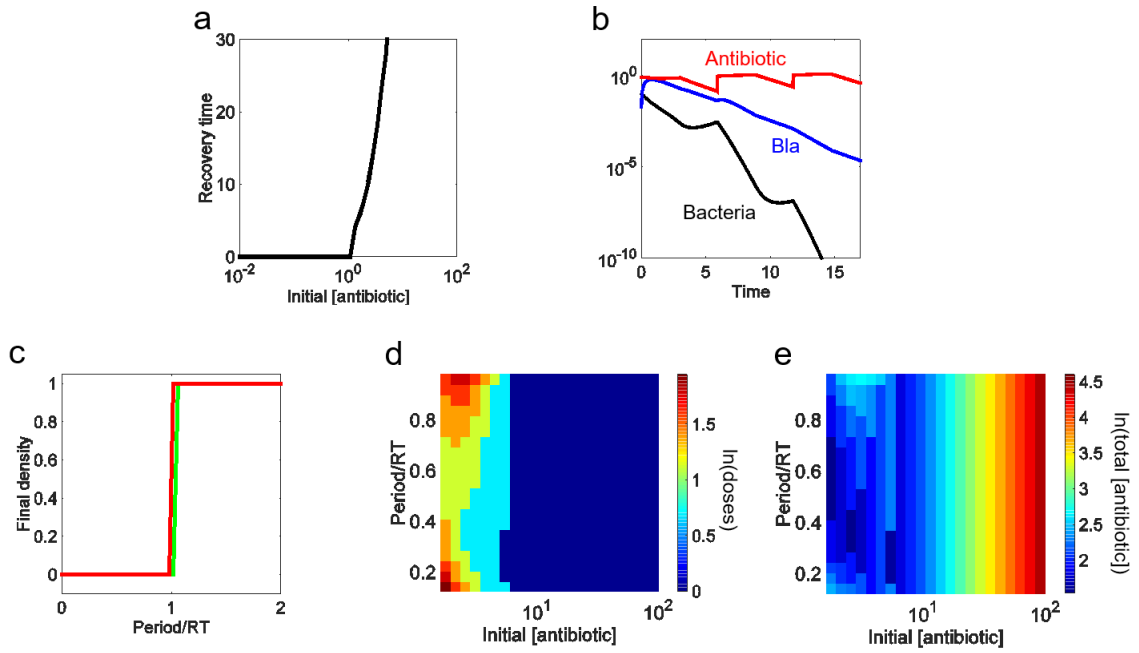

Figure 22: Recovery time guides design of effective intravenous drip based regimen. (a) Dependence of the recovery time on the antibiotic concentration during IV. We maintain each concentration for a fixed duration (time = 3) and then calculate the corresponding recovery time. **(b) Time course of an IV-drip regimen.** The antibiotic was delivered for a fixed duration until the bacteria density dropped below a pre-defined threshold (10^{-10}). **(c) Predictive power of recovery time for the outcome of long-term periodic antibiotic dosing.** For each antibiotic concentration-period combination, we calculate the final population density after applying 100 antibiotic doses. **(d) Dependence of treatment efficiency on the antibiotic concentration and the dosing period.** The efficacy is determined in the same manner as in **Figure 17**. **(e) Dependence of total antibiotic usage on the antibiotic concentration and the dosing period.** The total usage is calculated as in **Figure 17**.

Again, we use the recovery time from a single IV dose to establish the range of dosing frequencies able to eliminate the bacterial population. At each dosing concentration (for a fixed time duration of 3), we applied 100 doses of the antibiotic at periods ranging from the infusion duration (τ = 3) to 2 times the corresponding recovery time and calculated the resulting final bacterial density. The model shows that the predictive power of the recovery time is maintained when the antibiotic dosing

concentration is sufficiently large with a long enough recovery time ($a_0 > 1.5$): a multi-IV-dose regimen will eventually eliminate the population if the dosing period is less than one recovery time, regardless of effective antibiotic concentration (**Figure 22c**). There is slight deviation from this for $a_0 < 1.5$ due to the corresponding recovery times being too short for the Bla to be reduced to a baseline concentration before the next round of lysis and Bla release occurs. As a result, periods less than one recovery time could fail to eradicate the infection because the Bla concentration compounds with each subsequent dose, the antibiotic is degraded more quickly, fewer cells lyse, and the population can recover (**Figure 21**).

Similar to the injection based therapy, the IV-drip reduced a population constitutively producing high concentrations of Bla as long as the period was less than one recovery time and the initial antibiotic concentration was sufficiently high to cause significant initial decline **(Figure 23)**. However, the IV-drip protocols retained a larger range of effective antibiotic concentrations than the injection based protocols. This robustness is due to the antibiotic concentration continuously being replenished from the IV-drip. If a high enough concentration is maintained for sufficient time, the population's Bla concentration will not be able to remove the antibiotic fast enough to prevent lysis and the population will decrease with each subsequent round of IV-drip infusion. Thus, these results suggest that IV-drip based regimens could serve as a platform for effectively applying first-class β-lactams to clear constitutive producers of high levels of ESBLs.

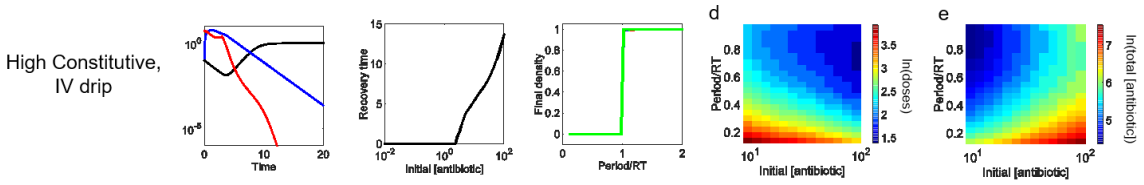

Figure 23. High constitutive Bla production, IV-drip treatment (a) Time course. The antibiotic was infused into the system over 3 time units, resulting in a sustained high concentration that led to a sustained decline in the population density. The Bla produced was insufficient to effectively degrade the antibiotic while it was being infused, so the population could not start to recover until after the infusion had ended. **(b) Recovery time**. A higher concentration of antibiotic was necessary to elicit a recovery time. Relative to the population constitutively producing Bla that was treated with an injection regimen, the IV-drip treatment produced longer recovery times. **(c) Final density**. IV-drip therapy results support the predictive power of the recovery time for populations constitutively producing high levels of Bla. Doses delivered at periods less than 1 recovery time clear the infection whereas doses delivered at periods longer than 1 recovery time fail. **(d) Dose number.** The fewest doses are required for regimens using high antibiotic concentrations delivered at intermediate-long periods. **(e) Total antibiotic delivered.** The least amount of antibiotic was delivered for regimens delivering the intermediate concentrations of antibiotic at intermediate-to-long periods.

We next evaluated the efficacy of each effective concentration-period combination by calculating the minimum number of doses necessary to reduce the population density to below 10^{-10} **(Figure 22d)**. Relative to the injection protocol, the IV-drip therapy has a narrower region of intermediate dose numbers, reflecting the narrow region of intermediate recovery times. Similarly to the injection based regimens, the intermediate antibiotic concentrations ($1 < a_0 < 5$) require the least doses when delivered at low-to-intermediate period lengths (period = 20-60% recovery time) because that is when the population is most vulnerable. Again, the initial antibiotic concentrations too low to have a recovery time ($a_0 < 1$) do not clear the infection, regardless of the dosing interval or number of doses applied. The concentrations with an infinite recovery time ($a_0 > 5$) require only a single dose and thus the dosing frequency does not matter.

Although the number of doses necessary to clear an infection might be the same for a range of antibiotic concentrations and periods, the least amount of total antibiotic is needed for intermediate antibiotic concentrations applied at 20-60% of the associated recovery time **(Figure 22e**).

4.2.5 Predictive power of the recovery time in mixed populations

A bacterial population often consists of phenotypically or genetically heterogeneous subpopulations[203,204]. For instance, different cells may express different levels of Bla, have different growth rates, or exhibit different sensitivities to the same antibiotic. This heterogeneity could compromise the predictive power of the recovery time. To examine this notion, we extended our injection-based model to account for two cases, each dealing with a mixture of two subpopulations (**4.5 Supplementary materials**). In one case, one subpopulation grows much more slowly and exhibits much greater tolerance to the antibiotic. In the other, two subpopulations display different degrees of collective antibiotic tolerance.

4.2.5.1 Case I: A mixture consisting of normal cells and persister cells

The first case accounts for the impact of persisters. Persisters are non- or slow-growing bacteria that are genetically identical to susceptible cells, but are highly tolerant to antibiotics [5-9,133]. Because persisters are generated at low frequencies and can only start to reestablish the population upon removal of the antibiotic [6,205,206], the overall dynamics of persisters will happen at a much slower time scale than for normal cells. Here, we

assume persisters form a small fraction of the initial population (< 1%), transition to and from normal cell phenotypes when the antibiotic concentration is low enough, and grow and lyse at rates 100 to 1000 times slower than normal cells [7,9]. When antibiotic concentrations are low ($a_0 < 0.3$), the recovery time is 0, regardless of the presence of persisters. As antibiotic concentration starts to increase ($0.3 < a_0 < 26$), the population of normal cells starts to undergo the population crash and recovery while the persisters grow and die very slowly (**Figure 24 a,f**). Once the antibiotic has been sufficiently degraded, then the persisters start being generated from and returning to the normal population. This ability to transition between phenotypes is what allows for a population containing persisters to recover under antibiotic concentrations ($a_0 > 26$) that would normally kill a population without persisters (**Figure 24 b, g**). The predictive power of the recovery time is upheld for the population with persisters growing and dying 100fold more slowly, but not 1000fold more slowly (**Figure 24 c, h**). Although the normal population is reduced below the threshold after a few doses, the persisters' net death rate determines the duration that the antibiotics need to be applied. The persisters growing and lysing 100fold more slowly than normal cells have a death rate high enough to reduce the persisters to 0 before the 100 doses of antibiotic have been applied at periods less than 1 recovery time (**Figure 24 d**). The fewest doses are needed for regimens applying higher concentrations of antibiotic ($a_0 > 26$) at period lengths > 0.3 recovery time. The persisters growing and lysing 1000fold more slowly are still present at a low density at the end of most of the different regimens tested. Here, the successful regimens are those

delivering high concentrations of antibiotic ($a_0 > 10$) with long period lengths (period > 0.65 recovery time) (**Figure 24 i**). Similar to the previous models, the persister model shows that regimens applying higher dose concentrations deliver a higher overall concentration of antibiotic (**Figure 24 e, j**). These results suggest that, while the recovery time can help optimize regimens for relatively slow- growing and lysing persisters, the power is lost for extremely slow- or non- growing persisters. This further confirms that if our model's central assumption, that the population is collectively antibiotic tolerant, is violated, then the predictive power of the recovery time will diminish.

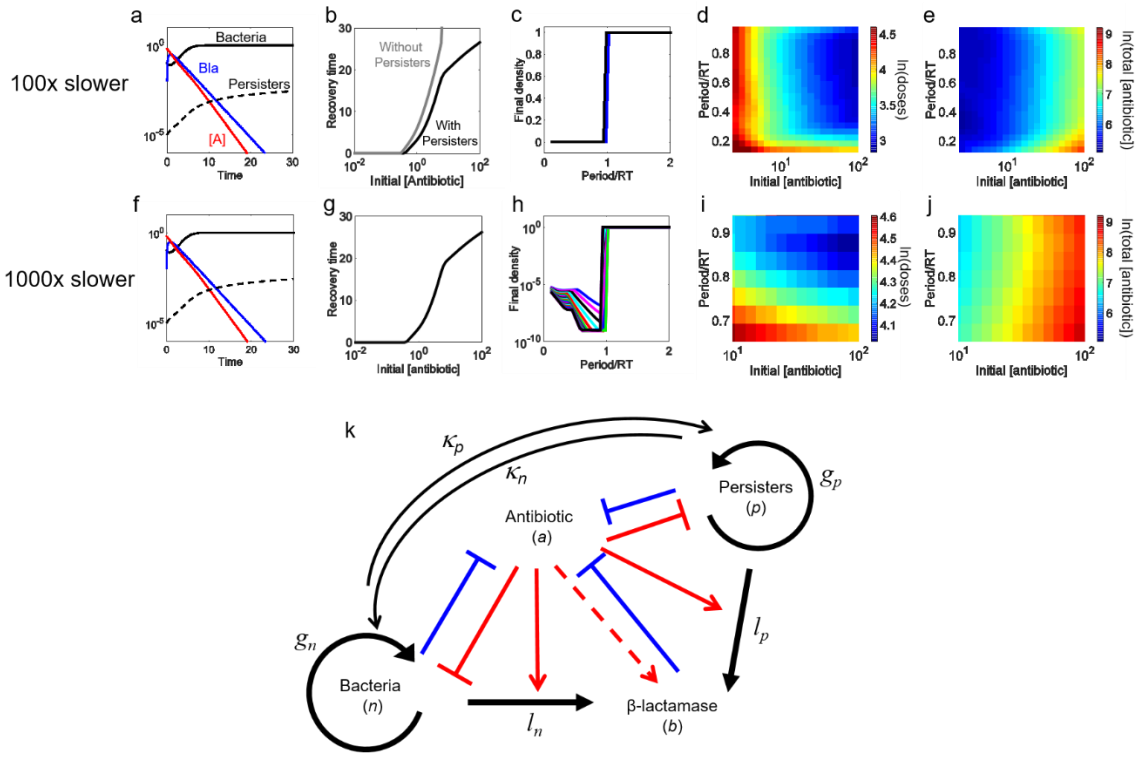

Figure 24. The effect of persisters on the predictive powers of recovery time. Our model assumes that persisters form a small fraction of a population, grow and lyse at rates much slower than normal cells ($g_p \ll g_N, l_P \ll l_N$), and, when the antibiotic concentration is low enough ($a < \sigma_1$), they are generated from and revert to a normal cell phenotype at the slow rates of κ_P and κ_N, respectively. **(a-e) Population with persisters that grow and lyse at rates 100 times more slowly than normal cells (a) Time course.** The bacteria lyse due to the antibiotic, release Bla to degrade the antibiotic, and then recover once the antibiotic concentration is low enough. At this point, persisters (dashed black line) are generated from and return to the normal cell population (solid black line). Here, the initial density of persisters and normal cells are 0.00001 and 0.1, respectively. **(b) Recovery time.** The recovery times are the same between the population containing persisters (black line) and the population containing no persisters (grey line) until $a_0 > 0.3$. From $0.3 < a_0 < 26$, both populations take longer to recover with increasing antibiotic concentration; however, the population containing persisters recovers slightly faster. When $a_0 > 26$, then the population without persisters fails to recover, whereas the population with persisters is able to re-establish the population. **(c) Final Density.** After 100 doses of antibiotic, the final total density was measured. Periods greater than 1 recovery time resulted in the full recovery of the population; however, periods less than 1 recovery time appeared to suppress the population's recovery. **(d) Dose number.** For each antibiotic concentration and period combination, the corresponding number of doses necessary to reduce the total population density to a critical threshold was calculated. The regimens using antibiotics associated with longer recovery times and longer periods require the fewest doses. **(e)Total antibiotic delivered.** Despite many different regimens requiring the same number of doses, the regimens could be differentiated by the total amount of antibiotic delivered. When comparing regimens with the same number of doses, the amount of antibiotics delivered would decrease as the dose concentration decreased. **(f-j) Population with persisters that grow and lyse at rates 1000 times more slowly than normal cells (f) Time course.** Similar to **(a)**. **(g) Recovery time.** Similar to **(b)**. **(h) Final Density.** Similar to general trend of **(c)**, where

final densities are high when using periods > 1 recovery time and are low otherwise. However, many of the low final densities achieved after 100 doses with periods < 1 recovery time are close to, but not exactly, 0. This means that once the regimen is completed and sufficient time has passed, the population will be able to regrow**. (i) Dose number.** For each antibiotic concentration and period combination, the corresponding number of doses necessary to reduce the total population density to a critical threshold was calculated. The regimens using antibiotics associated with longer recovery times and longest periods require the fewest doses. The regimens using lower concentrations of antibiotic ($a_0 < 10$) and/or shorter dosing periods (period < 0.65 recovery time) were not successful at reducing the population below the threshold after 100 doses. This is due to the presence of persisters. **(j) Total antibiotic delivered.** The total amount of antibiotic delivered for each regimen was calculated and suggests that an injection based regimen would need very high concentrations of antibiotic to sufficiently reduce a population with persisters. **(k) Schematic for how a population with persisters responds to antibiotic.** Black represents bacterial actions, blue represents Bla actions, and red represents antibiotic actions. Arrows denote induction or activation; T-lines indicate inhibition; the dashed arrow represents the ability for the model to simulate inducible or constitutive Bla production.

4.2.5.2 Case II: A mixture consisting of two distinct subpopulations that are both sensitive to the antibiotic

Here, the divergence between the two subpopulations is much less than that between normal and persister cells. The more resistant subpopulation has thresholds of growth inhibition and lysis five times greater than the moderately resistant subpopulation. As a result, the more resistant subpopulation does not lyse as much and recovers faster than the moderately resistant subpopulation (**Figure 25 a, f**). If the subpopulations can switch between states[207,208], the more resistant subpopulation can re-establish the moderately resistant subpopulation once the antibiotic concentration is sufficiently low. Otherwise, the moderately resistant subpopulation will not recover. Because both subpopulations still undergo the process of lysing before recovering, the dosing protocol based on recovery time is still applicable (**Figure 25 b, g**). For $0.3 < a_0 < 2.3$, both subpopulations recover at similar rates, thus the population as a whole recovers quickly. For $2.3 < a_0 < 26$, the more resistant subpopulation recovers faster and determines the

population level recovery time. For $a_0 > 26$, neither subpopulation can recover. The predictive power is upheld for this mixed population: a multi-dose regimen will clear a population if the time between doses is less than one recovery time, regardless of effective antibiotic concentration and degree of antibiotic-mediated killing (**Figure 25 c, h**). Similar to other scenarios, the dosing number and total antibiotic delivered can be determined and optimized, based on the antibiotic concentration and period length (**Figure 25 d-e, i-j**). These results suggest that the recovery time could be used to optimize treatments for heterogeneous populations with more than two subpopulations, as long as the phenotypic difference between these subpopulations is not drastic.

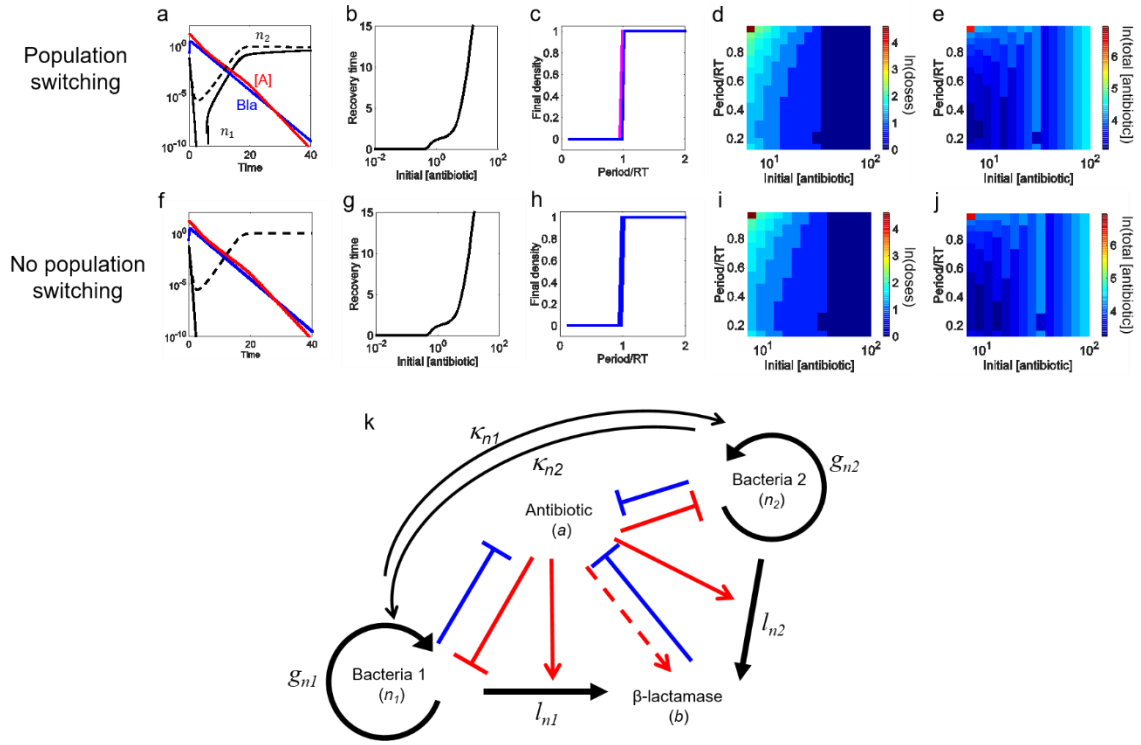

Figure 25. The effect of a mixed population on the predictive powers of recovery time. The model represents a mixed population with equal starting densities of two subpopulations (n_1 and n_2) with different levels of antibiotic resistance. n_1 has the same parameter values as the base case from the homogeneous model; however, n_2 has increased thresholds for antibiotic effects. Particularly, n_2 requires higher concentrations of antibiotic to inhibit growth ($\sigma_5 = 5\sigma_1$) and induce lysis ($\sigma_6 = 5\sigma_2$). Although this model accounts for two distinct subpopulations, it could be extended to multiple populations displaying some degree of collective antibiotic tolerance. **Subpopulation can switch between states (a-e). (a) Time course.** Both subpopulations start at the same starting density (0.05) and start to lyse due to antibiotic. One subpopulation (n_2) is more resistant than the other (n_1), with thresholds for growth inhibition (σ_5) and lysis (σ_6) 5 times higher. Both populations contribute Bla to degrade the antibiotic. Once the antibiotic concentration is sufficiently low, then the subpopulations can start to recover. Since n_1 and n_2 can switch between states, n_2 can help n_1 recover under concentrations that would otherwise be lethal. **(b) Recovery time curve.** Because both populations still undergo the process of lysing before recovering, the dosing protocol based on recovery time is still applicable. When $0.3 < a_0 < 2.3$, both n_1 and n_2 are recovering at similar rates, thus the population as a whole recovers quickly. Once $2.3 < a_0 < 26$, then n_2 recovers faster and determines the population level recovery time. When $a_0 < 26$, then both subpopulations cannot recover. **(c) Final density.** Protocols using periods of less than one recovery time are effective at eliminating the population, regardless of antibiotic concentration. **(d) Dose number.** For each antibiotic concentration and period combination, the corresponding number of doses necessary to eliminate the population was calculated. The regimens using antibiotics associated with longer recovery times require the fewest doses; however, lower concentrations of antibiotic ($10 < a_0 < 26$) can be effective if applied at

period lengths of 0.10-0.50 period/RT. **(e) Total antibiotic delivered.** Despite many different regimens requiring the same number of doses to clear an infection, the regimens could be differentiated by the total amount of antibiotic delivered. When comparing regimens with the same number of doses, the amount of antibiotics delivered would decrease as the dose concentration decreased. **(f-j). Subpopulations cannot switch between states (f) Time course.** Same as in **(a)** except n_1 and n_2 do not switch back and forth. Thus the more resistant subpopulation, n_2, is selected to recover. **(g) Recovery time curve.** Same as in **(b)**. **(h) Final density.** Same as in **(c)**.**(i) Dose number.** Same as in **(d). (j) Total antibiotic delivered.** Same as in **(e)**. **(k) Schematic for a mixed population's response to antibiotic.** Black represents bacterial actions, blue represents Bla actions, and red represents antibiotic actions. Arrows denote induction or activation; T-lines indicate inhibition; the dashed arrow represents the ability for the model to simulate inducible or constitutive Bla production.

4.3 Discussion

Most antibiotic regimens are based on empirical observations of how bacterial infections responded to an antibiotic [109,174,209]. However, these regimens may be suboptimal both because they were not initially designed to handle resistant bacteria and because the current diagnostic assays cannot accurately predict how resistant pathogens will respond to them. It is critical that we develop a new strategy for using the existing antibiotics more effectively or our medical care will return to a state equivalent to that of a pre-antibiotic era. Ideally, the new strategies would be based on the molecular mechanisms underlying antibiotic resistance. However, this is impractical, given that many pathogens' resistance mechanisms have not been characterized and they evolve rapidly. To this end, we propose using the recovery time as a lumped metric that can characterize a pathogen's response to an antibiotic without requiring knowledge of the underlying mechanism.

We used a kinetic model to test the ability of the recovery time to predict ESBL-producing pathogens' responses to periodic dosing of β-lactams. Our simulation results

suggest that the recovery time of a single dose can be used to design optimal multi-dose regimens for multiple delivery methods, including injections and continuous IV drip, various inoculum sizes, bacteria with a range of Bla production levels, and certain heterogeneous populations. Optimal dosing regimens for treating Bla-producing bacteria with a β-lactam would apply intermediate concentrations of antibiotic that have long recovery times at time intervals corresponding with when the bacterial density has been minimized. Furthermore, our modeling results suggest that regimens using lower, yet still lethal, concentrations of antibiotic can be as effective as regimens using higher concentrations. Reducing the amount of antibiotic the host is exposed to may be important to minimize the perturbation of the host's microbiota and other defense mechanisms [174,197-199,210], which could have long-lasting detrimental effects. Also, under certain conditions, a higher concentration of antibiotic can lead to selection of more resistant subpopulation of bacterial pathogens [93].

Although this model considers the population level response to an antibiotic, there is a significant amount of gene-expression noise at the single cell level [203,204]. If an antibiotic were applied such that the population would have the chance to recover between doses, then the antibiotic would select for the bacteria expressing higher levels of resistance genes (as demonstrated in **Figure 25 f**). Ultimately, this would direct the evolution of the population towards an inherently more resistant infection than before the antibiotic treatment was applied. Our proposed method would minimize this problem by

delivering subsequent doses of antibiotic before a more resistant population grew to a significant density.

The recovery time of a pathogen under a single dose of antibiotic is a metric that is easy to measure and could guide the choice of an appropriate multi-dose antibiotic regimen for a wide range of infections. Measurements of the recovery time can be carried out in high resolution using commercially available microplate readers [211]. A critical step entails the construction of a comprehensive recovery time database for various pathogens under different antibiotics (**Figure 26**). When a new bacterial pathogen is identified, its recovery times to a range of antibiotic concentrations will be recorded *in vitro* for different starting densities. Based on these measurements, regimens with varied concentrations and period lengths will be tested for different inoculum sizes. From these results, the period length, dose number, and antibiotic concentration can be optimized for a particular pathogen *in vitro*. Before entering this information into the database, the PK/PD of the particular antibiotic will be necessary to determine the concentration of antibiotic that should be delivered such that the concentration at the site of infection matches the concentration selected from the *in vitro* experiments. Given this database, a proper diagnosis of a pathogen, and an estimate of the severity of the infection (e.g. inoculum size), one can readily identify the scenarios in which first- and second-line antibiotics may still be applied and chose the most effective treatment protocol. Whenever a new pathogen arises, it can be evaluated and added to the library.

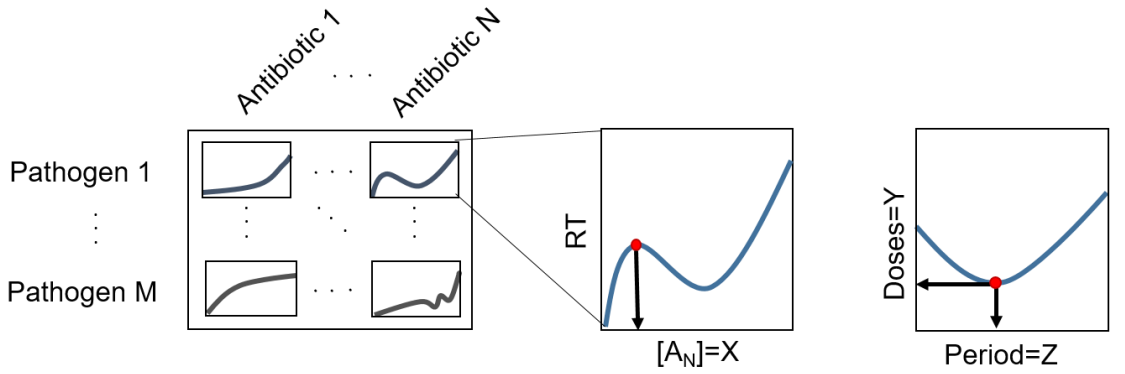

Pathogen	Antibiotic	Concentration	Period & Doses
1	1 ⋮ N	X_1 ⋮ X_N	Y_1 doses every Z_1 hours ⋮ Y_N doses every Z_N hours

4. Add regimen details to database

Figure 26: Potential use of recovery time to guide clinical practice. A critical step entails the construction of a comprehensive database of the recovery time curves of various pathogens under different antibiotics. Based on the recovery time curve, the optimal antibiotic concentration (X), dose number (Y), and period length (Z) can be calculated for each pathogen-antibiotic combination and entered into a database. Given this database and a proper diagnosis of a pathogen, one can readily identify the most effective treatment protocol.

The ability to predict the outcome of a multi-dose treatment without knowing the underlying resistant mechanism would remove the uncertainty that prevents clinicians from using first-line β-lactams when an ESBL-producing pathogen is detected. Given ESBL-producing bacteria's prevalence [115,212-214], our proposed strategy could help to minimize the rate at which these bacteria develop resistance to more extreme antibiotics by ensuring that we do not overlook effective first-line antibiotics before moving on to more extreme antibiotics.

4.4 Methods

The interaction between a β-lactam and a bacterial population expressing Bla can be simplified to the interactions between three main components: population density (*n*), antibiotic concentration (*a*), and Bla concentration (*b*). Our base model consists of the following ordinary differential equations:

$$\frac{dn}{d\tau} = (g - l)n \quad (9)$$

$$\frac{db_{out}}{d\tau} = \boldsymbol{l b_{in}^{*} - \gamma_2 b_{out} - \kappa_{IV}(\tau) b_{out}} \quad (10)$$

$$\frac{da}{d\tau} = \boldsymbol{\kappa_{IV}(\tau) a_{inject} - (b_{out} + \alpha b_{in}^{*}) \left(\frac{a}{1+a}\right) - \gamma_3 a - \kappa_{IV}(\tau) a} \quad (11)$$

$$g = (1 - n)\left(\frac{\sigma_1}{\sigma_1 + a}\right) \quad (12)$$

$$\boldsymbol{l = \gamma_1 \left(\frac{a^H}{\sigma_2^H + a^H}\right)\left(\frac{\sigma_4}{\sigma_4 + b_{in}}\right)} \quad (13)$$

$$\boldsymbol{b_{in} = \kappa \left(\frac{r}{g + \gamma_4}\right)} \quad (14)$$

$$\boldsymbol{b_{in}^{*} = \beta n b_{in}} \quad (15)$$

$$\boldsymbol{r = \frac{a}{\sigma_3 + a}} \quad (16)$$

where *g* and *l* represent bacteria growth and lysis, respectively. Initial conditions of $n(0)=0.1$, $b(0)=0$, and $a(0)=0.01$-100 were used for all simulation results, except for S2 Figure where $n(0)=0.01$ or 0.001. The rest of the parameters are defined in a table in Table 4. See section **4.5 Supplementary materials** for further details of the model development and for the extended models that account for heterogeneous populations.

Minor modifications are introduced to account for the IV drip protocol or dynamics of a mixture consisting of two subpopulations.

4.5 Supplementary materials

4.5.1. Model development.

The interaction between a β-lactam and a bacterial population expressing a β-lactamase (Bla) can be simplified to the interactions between three main components: population density, antibiotic concentration, and Bla concentration. To model bacteria that inducibly or constitutively produce Bla and lyse due to antibiotics degrading the cell wall, we used an ordinary-differential-equation model for the dynamics of bacterial density (*N*), Bla concentration (*B*), and β-lactam concentration (*A*).

Dimensional EQs:

$$\frac{dN}{dt} = (G - L)N \quad (17)$$

$$\frac{dB_{out}}{dt} = LB_{in}^{*} - d_{B_{out}}B_{out} - k_{IV}(t)B_{out} \quad (18)$$

$$\frac{dA}{dt} = k_{IV}(t)A_{inject} - k_{B_{out}}(B_{out} + \alpha B_{in}^{*})\left(\frac{A}{K_A + A}\right) - d_A A - k_{IV}(t)A \quad (19)$$

$$G = \left(1 - \frac{N}{N_m}\right)\left(\frac{\mu K_1}{K_1 + A}\right) \quad (20)$$

$$L = \left(\frac{d_N A^H}{K_2^H + A^H}\right)\left(\frac{K_4}{K_4 + B_{in}}\right) \quad (21)$$

$$B_{in} = \frac{k_{B_{in}}R}{G + d_{B_{in}}} \quad (22)$$

$$B_{in}^{*} = B_{in}V_{cell}N \quad (23)$$

$$R = \frac{A}{K_3 + A} \quad (24)$$

Our key modeling assumptions are:

- The dynamics of cell density (N) depend on the growth rate (G) and the lysis rate (L).
- G is a function of N, the bacterial carrying capacity (N_m), the specific growth rate of the cells (μ), the half-maximal constant for growth inhibition by the antibiotic (K_1), and the antibiotic concentration (A).
- L is a function of the maximum lysis rate constant (d_N), the antibiotic concentration (A), the half maximal constant cell lysis by the antibiotic (K_2), the Hill coefficient (H), the half-maximal constant for antibiotic degradation by the periplasmic Bla (K_4), and the concentration of periplasmic Bla (B_{in}).
- The dynamics of extracellular Bla present in the culture (B_{out}) depends on how much Bla is released, degraded (with a rate constant, d_{Bout}), and washed out of the system (with an IV flow rate, k_{IV} (e.g. $\frac{1}{pulse\ length}$), when applicable). Bla release depends on L, the concentration of intracellular Bla (B_{in}), N, and the volume of a cell (V_{cell}).
- The dynamics of the intracellular Bla (B_{in}) is a function of the maximum production rate of Bla per cell (k_{Bin}), the rate of Bla induction (P), G, and the intracellular degradation rate constant of Bla (d_{Bin}). P is a function of A and the half maximal constant for antibiotics inducing the production of Bla (K_3). If K_3 is set to 0, Bla

production is constitutive; if K_3 is greater than 0, the Bla production is inducible by *A*.

- The different methods of antibiotic delivery (injection versus IV drip) were differentiated by the time dependent flow rate, $k_{IV}(t)$. It would be 0 for injections (delivered instantaneously) and non-zero for IV drips (delivered over a set time). It was assumed that the rate of antibiotic being introduced by IV would be the same rate at which the antibiotic would be pushed out of the region. The IV drip duration was determined by a step function dependent on time.
- The dynamics of antibiotic concentration in the environment is dependent on the amount of Bla present (both B_{out} and B_{in}), how quickly Bla degrades the β-lactam (k_{Bout}), A, the half-maximal constant for degradation of the antibiotic by Bla (K_A), and the degradation rate constant of the antibiotic (d_A).
- To convert periplasmic Bla from a per cell basis (B_{in}) to a per population basis (B_{in}^*), B_{in} was multiplied by the number of cells present at a given time and the volume of a cell. The efficacy of periplasmic Bla is altered by a weighting variable (α).
- In these models, the antibiotic has two main effects: inhibiting cell growth and promoting lysis. In the inducible model, antibiotics also serve to activate the production of a Bla.

Non-dimensionalizing the equations by $n = \frac{N}{N_m}, b_{out} = \frac{B_{out}k_{Bout}}{\mu K_A}, a = \frac{A}{K_A}, and\ \tau = t\mu$ gives

$$\frac{dn}{d\tau} = (g - l)n \quad (25)$$

$$\frac{db_{out}}{d\tau} = lb_{in}^{*} - \gamma_2 b_{out} - \kappa_{IV}(\tau)b_{out} \quad (26)$$

$$\frac{da}{d\tau} = \kappa_{IV}(\tau)a_{inject} - (b_{out} + \alpha b_{in}^{*})\left(\frac{a}{1+a}\right) - \gamma_3 a - \kappa_{IV}(\tau)a \quad (27)$$

$$g = (1 - n)\left(\frac{\sigma_1}{\sigma_1 + a}\right) \quad (28)$$

$$l = \gamma_1\left(\frac{a^H}{\sigma_2^H + a^H}\right)\left(\frac{\sigma_4}{\sigma_4 + b_{in}}\right) \quad (29)$$

$$b_{in} = \kappa\left(\frac{r}{g+\gamma_4}\right) \quad (30)$$

$$b_{in}^{*} = \beta n b_{in} \quad (31)$$

$$r = \frac{a}{\sigma_3 + a} \quad (32)$$

where $\sigma_1 = \frac{K_1}{K_A}, \sigma_2 = \frac{K_2}{K_A}, \sigma_3 = \frac{K_3}{K_A}, \sigma_4 = \left(\frac{K_4 k_{B_{out}}}{K_A \mu}\right), \gamma_1 = \frac{d_N}{\mu}, \gamma_2 = \frac{d_{B_{out}}}{\mu},\ \gamma_3 = \frac{d_A}{\mu},\ \gamma_4 = \frac{d_{B_{in}}}{\mu},\ \beta = N_m V_{cell}, \kappa_{IV} = \frac{k_{IV}}{\mu}, \text{and } \kappa = (\frac{k_{b_{in}} k_{b_{out}}}{\mu^2 K\_A})$.

4.5.1.1 Heterogeneous population model:

To model a heterogeneous population, we modified the model described above to account for a second population. By adjusting the maximum lysis (γ_5) and growth ($\nu\nu$) rates of the second subpopulation, this model can account for the dynamics of persisters (*P*), a small fraction of persisters that grow and lyse significanlty more slowly than

normal cells and revert back to/generate from normal cells once the antibiotic concentration is sufficiently low [7,9]. This same model can also be used to represent a population consisting of bacteria with different levels of antibiotic resistance by adjusting the thresholds for growth inhibition (σ_5) and lysis (σ_6). This model could ultimately be expanded to account for multiple subpopulations, given that they all displayed some level of collective antibiotic tolerance:

$$\frac{dN}{dt} = (G - L)N + k_N P - k_p N \quad (33)$$

$$\frac{dP}{dt} = (G_P - L_P)P + k_P N - k_N P \quad (34)$$

$$\frac{dB_{out}}{dt} = (L + L_P)B_{in}^* - d_{B_{out}} B_{out} - k_{IV}(t) B_{out} \quad (35)$$

$$\frac{dA}{dt} = k_{IV}(t) A_{inject} - k_{B_{out}}(B_{out} + \alpha B_{in}^*)\left(\frac{A}{K_A + A}\right) - d_A A - k_{IV}(t) A \quad (36)$$

$$G = \left(1 - \frac{N_T}{N_m}\right)\left(\frac{\mu K_1}{K_1 + A}\right) \quad (37)$$

$$G_P = \left(1 - \frac{N_T}{N_m}\right)\left(\frac{\mu_p K_5}{K_5 + A}\right) \quad (38)$$

$$L = \left(\frac{d_N A^H}{K_2^H + A^H}\right)\left(\frac{K_4}{K_4 + B_{in}}\right) \quad (39)$$

$$L_P = \left(\frac{d_P A^H}{K_6^H + A^H}\right)\left(\frac{K_4}{K_4 + B_{in}}\right) \quad (40)$$

$$B_{in} = \frac{k_{B_{in}} R}{G + G_p + d_{B_{in}}} \quad (41)$$

$$B_{in}^* = B_{in} V_{cell} N_T \quad (42)$$

$$R = \frac{A}{K_3 + A} \quad (43)$$

$$N_T = N + P \quad (44)$$

Our key modeling assumptions for the persister model are:

- The dynamics of cell density (*N*) depends on the growth rate (*G*), the lysis rate (*L*), the rate at which persisters (*P*) are generated from the normal cell population (k_P), and the rate at which persisters return to the normal cell phenotype (k_N). We assume that $k_N = k_P = 0$ until *A* is sufficiently low enough ($a < \sigma_1$), after which $k_N \gg k_P$.
- The dynamics of persister cell density (*P*) depend on the persisters' growth rate (G_P), lysis rate (L_P), rate of generation (k_P) from normal cells (N), and rate of reversion back to *N* (k_N).
- The dynamics of extracellular Bla present in the culture (B_{out}) is now a function of both the normal cell lysis rate (L) and the persister cell lysis rate (L_P), the concentration of intracellular Bla (B_{in}), the total number of cells (N_T), and the volume of a cell (V_{cell}).
- G_P is a function of N_T, N_M, the specific growth rate of the cells (μ_P), the half-maximal constant for growth inhibition by the antibiotic (K_5), and the antibiotic concentration (*A*). For persisters, we assume that the threshold for growth inhibition is the same as the normal cell's ($K_1 = K_5$) and that the growth rate is the distinguishing factor.
- L_P is a function of the maximum lysis rate constant of persisters (d_p), the antibiotic concentration (*A*), the half maximal constant cell lysis by the antibiotic (K_6), the

Hill coefficient (*H*), the half-maximal constant for antibiotic degradation by the periplasmic Bla (K_4), and the concentration of periplasmic Bla (B_{in}). For persisters, we assume that the threshold for lysis is the same as the normal cell's ($K_2 = K_6$) and that the lysis rate is the distinguishing factor.

- $B_{in}$and B_{in}^* have been updated to reflect both populations' contributions.

Our key modeling assumptions for a mixed population model are:

- To model a mixed population with distinct subpopulations, set $k_P = k_N = 0$.
- We assume that the distinguishing features between populations are the thresholds for growth inhibition (σ_1, σ_5) and lysis (σ_2, σ_6). By altering the relative values of these parameters ($\sigma_1 < \sigma_5,\ \sigma_2 < \sigma_6$), the dynamics of populations with different resistance levels can be modeled.

Non-dimensionalizing the equations by $P = \frac{P}{N_m}$ gives

$$\frac{dn}{d\tau} = (g - l)n + \kappa_N p - \kappa_P n \quad (45)$$

$$\frac{dp}{d\tau} = (g_P - l_p)p + \kappa_p n - \kappa_N p \quad (46)$$

$$\frac{db_{out}}{d\tau} = (l + l_P)b_{in}^* - \gamma_2 b_{out} - \kappa_{IV}(\tau)b_{out} \quad (47)$$

$$\frac{da}{d\tau} = \kappa_{IV}(\tau)a_{inject} - (b_{out} + \alpha b_{in}^*)\left(\frac{a}{1+a}\right) - \gamma_3 a - \kappa_{IV}(\tau)a \quad (48)$$

$$g = (1 - n_T)\left(\frac{\sigma_1}{\sigma_1 + a}\right) \quad (49)$$

$$\boldsymbol{g_p = (1 - n_T)\left(\frac{\sigma_5}{\sigma_5 + a}\right)v} \quad 50$$

$$\boldsymbol{l = \gamma_1\left(\frac{a^H}{\sigma_2^H + a^H}\right)\left(\frac{\sigma_4}{\sigma_4 + b_{in}}\right)} \quad 51$$

$$\boldsymbol{l_p = \gamma_5\left(\frac{a^H}{\sigma_6^H + a^H}\right)\left(\frac{\sigma_4}{\sigma_4 + b_{in}}\right)} \quad 52$$

$$\boldsymbol{b_{in} = \kappa\left(\frac{r}{g + g_p + \gamma_4}\right)} \quad 53$$

$$\boldsymbol{b_{in}^* = \beta b_{in} n_T} \quad 54$$

$$\boldsymbol{r = \frac{a}{\sigma_3 + a}} \quad 55$$

$$\boldsymbol{n_T = n + p} \quad 56$$

where $\sigma_5 = \frac{K_5}{K_A}, \sigma_6 = \frac{K_6}{K_A}, \gamma_5 = \frac{d_P}{\mu},\ \kappa_N = \frac{k_N}{\mu}, \kappa_P = \frac{k_P}{\mu}, and\ \upsilon = \frac{\mu_p}{\mu}$.

Table 4: Definition and the value of parameters used in the model

Parameter	Description and Source	Value
α	Weighting factor for periplasmic β-lactamase, which provides less protection against antibiotic than extracellular β-lactamase.	0.01
H	Hill coefficient for determining lysis rate. A low Hill coefficient (H=1) represents an antibiotic with a dose-dependent lysis rate, whereas a higher Hill coefficient (H=3) represents an antibiotic with a time-dependent lysis rate. [196]	3 (1)
$\beta = (N_m V_{cell})$	Parameter used to convert from single cell level to population level where N_m = 10^9 cells/mL and V_{cells}= 10^{-12} mL/cell. [215]	0.001
$\gamma_1 = \left(\frac{d_N}{\mu}\right)$	Maximum lysis rate by antibiotic given that μ=0.8/hour.[14] Tuomanen et al. suggest that 50-90% of a population can lyse per hour (d_N).[143]	62
$\gamma_2 = \left(\frac{d_{B_{out}}}{\mu}\right)$	Maximum degradation rate of extracellular Bla given that $d_{B_{out}}$=0.46/hour. [148]	0.58
$\gamma_3 = \left(\frac{d_A}{\mu}\right)$	Maximum degradation rate of β-lactam antibiotic, given that d_A=0.35/hour. [216,217]	0.51
$\gamma_4 = \left(\frac{d_{b_{in}}}{\mu}\right)$	Maximum degradation rate of periplasmic Bla given that $d_{B_{in}}$=0.2/hour. [218]	0.25
$\gamma_5 = \left(\frac{d_P}{\mu}\right)$	Maximum lysis rate of the second population by antibiotic given that μ=0.8/hour. The persister model assumes that d_P is 2-3 orders of magnitude smaller than d_N. The mixed population model assumes that $d_P = d_N$.	0.062:62
$\nu = \left(\frac{\mu_P}{\mu}\right)$	Maximum growth rate of the second population, given that μ=0.8/hour. The persister model assumes that μ_P is 2-3 orders of magnitude smaller than μ for the situations when persisters are practically not growing and 0.02 for the situations when persisters are slowly growing[7,9]. The mixed population model assumes that $\mu_P = \mu$.	0.001:1
$\kappa_{IV} = \left(\frac{k_{IV}}{\mu}\right)$	Rate of IV drip given that the dose is delivered over a set pulse length (here, pulse length was arbitrarily set to 2.4 hours).	0.33
$\kappa = \left(\frac{k_{b_{in}} k_{B_{out}}}{\mu^2 K_A}\right)$	Efficiency of Bla is determined by how quickly Bla is produced and how efficiently Bla can hydrolyze a β-	5.44E3

	lactam antibiotic. The maximum rate Bla can be produced (k_{Bin}) is on the order of 0.1 μM/hour [149], the maximum rate of (k_{Bout}) is on the order of 1E10[5]-1E10[6]/hour (variable, depending on which antibiotic used) [144,149].	
$\sigma_1 = \left(\frac{K_1}{K_A}\right)$	Half maximal constant for growth inhibition, given that K_1= 0.2-16 μM [219]and K_A=33-150 μM [144] (depending on the antibiotic).	0.24
$\sigma_2 = \left(\frac{K_2}{K_A}\right)$	Half maximal constant for lysis by antibiotic, assuming that K_2 is larger than K_1 (there is a small range of concentrations under which cells have stopped growing, but are not lysing).	1.29
$\sigma_3 = \left(\frac{K_3}{K_A}\right)$	Half maximal constant for inducing Bla production, assuming that it takes much higher concentrations for bacteria to produce Bla than it would for bacteria to stop growing or start lysing. [33]	5.17 or 0
$\sigma_4 = \left(\frac{K_4 k_{B_{out}}}{K_A \mu}\right)$	Half maximal constant for periplasmic Bla protection, assuming that very little periplasmic Bla is necessary for a single cell to experience a small amount of protection from the antibiotic.	2.08E3
$\sigma_5 = \left(\frac{K_5}{K_A}\right)$	Half maximal constant for growth inhibition of the second population. Persister cells are assumed to have a similar threshold as normal cells ($K_5 = K_1$), whereas as more resistant population would have a higher threshold ($K_5 = 5K_1$).	0.24:1.2
$\sigma_6 = \left(\frac{K_6}{K_A}\right)$	Half maximal constant for lysis by antibiotic of the second population Persister cells are assumed to have a similar threshold as normal cells ($K_6 = K_2$), whereas as more resistant population would have a higher threshold ($K_6 = 5K_2$).	1.29:6.45

5. Concluding remarks and future directions

5.1 Concluding remarks

The central theme to this thesis is understanding the antibiotic response of resistant bacteria to better guide the way antibiotics are applied.

In Chapter 2, I discussed how collective antibiotic tolerance (CAT) is an important mechanism behind bacteria surviving antibiotic treatment. Unlike previous studies that focus on how bacteria resist antibiotic on a single-cell basis, we highlighted **bacteria that are sensitive at the single-cell level but can survive treatment if the population density is sufficiently high**. We reviewed several different CAT mechanisms, namely antibiotic mediated altruistic death, quorum sensing, and bistable inhibition of bacterial growth. Oftentimes, multiple CAT mechanisms work together within a single population or a mixed population of bacteria relies on social interactions to survive. In addition to facilitating the recovery of a population to an antibiotic dose, **CAT is of concern because it provides otherwise susceptible bacteria the opportunity to acquire single-cell level resistance**. To avoid this, we proposed treatment strategies that could be used to negate CAT. For instance, CAT could be minimized by timing the dosing of antibiotic treatments to coincide with when the population is at a lower density and thus more susceptible or preventing the production and/or function of effector proteins responsible for CAT. This review differs from, yet compliments, the existing studies characterizing antibiotic responses and improves the understanding of different mechanisms bacteria use for survival.

In Chapter 3, I introduced the resistance-resilience framework as a tool for dissecting the bacterial antibiotic response of an ESBL-producing bacteria to a β-lactam antibiotic. Through dissecting the antibiotic response with this framework, we note that **resilience and resistance are not absolute properties**, but shift as a function of antibiotic concentration. With increasing concentrations of antibiotic, resistance is the first component to be minimized, followed by a gradual decrease in resilience. Sensitivity analysis of the kinetic model revealed that **the main effectors of resistance were single cell level traits, whereas the main effectors of resilience were population level traits**. To validate this observation, we dissected the isolate's antibiotic response to a combination treatment of antibiotic and a Bla inhibitor. We noted that the antibiotic alone was effective at minimizing resistance, but that the Bla inhibitor was necessary to sufficiently minimize the resilience. We further applied this framework to other isolates and observed that each system was unique in its response to the combination treatment. These results underscore a critical caveat in using fixed formulations of β-lactam/Bla inhibitor combinations to combat ESBL-producing pathogens, which is currently a standard practice. Given the diversity of the phenotypic responses by the different isolates, **quantitative measurements on how a strain responds to an antibiotic and a Bla inhibitor are necessary to predict the outcome of a particular combination treatment**. Generally, this framework can be applied to dissecting responses and designing treatment strategies for other systems.

While resistance and resilience have been defined in the literature for decades, this is the first time to our knowledge that the resistance-resilience approach has been applied to antibiotic responses. It differs significantly from the current methods used to characterize bacteria susceptibility, which analyze the outcome of a population at a single time point after being exposed to a single concentration of antibiotic. This study also offers a concrete, quantitative example of how to measure resistance and resilience that can be applied to numerous fields ranging from microbiology to ecology.

In Chapter 4, I used a kinetic model to illustrate how the antibiotic response from a single dose of antibiotic could be used to predict the outcome of a multi-dose regimen. As long as the antibiotic concentration was sufficiently high to induce a crash in the population, a regimen would eliminate a bacterial population if it dosed at intervals shorter than a 1 recovery time. This conclusion was supported for a number of different simulations, including populations with homogeneous or heterogeneous growth rates, populations with inducible or constitutive Bla expression, populations containing persisters, and treatments using a bolus injection or continuous infusion of an antibiotic.

This work highlights the importance of temporal dynamics, which are often overlooked when characterizing a population by its minimum inhibitory concentration (MIC). Specifically, populations that initially crash in population density before recovering to a high density have a “window” of increased susceptibility that is not observed when a population is characterized based on a single time point. The strategy of using the recovery time to determine the dosing frequency differs from current dosing

strategies that have been empirically decided. Additionally, as the recovery time is based on a phenotypic response, the underlying mechanism(s) do not need to be known to design an effective treatment. This new method would provide a way to use existing antibiotics more effectively and guide how and when to reintroduce antibiotics that are currently disregarded as ineffective treatment options.

5.2 Future Directions

5.2.1 Validating multi-dosing predictions *in vitro*

To date, my work has focused on characterizing bacteria's single-dose response *in vitro* and testing multi-dosing regimens *in silico*. In future work, my colleagues and I will validate the predictions of Chapter 4: the recovery time of a population to a single dose of antibiotic can predict the population outcome of a multi-dose treatment. Preliminary data suggests either the experimental set-up or the model need to be optimized. Currently, the concentrations of antibiotic that induced the characteristic crash and recovery did not adhere to the recovery-time based predictions (**Figure 27**).

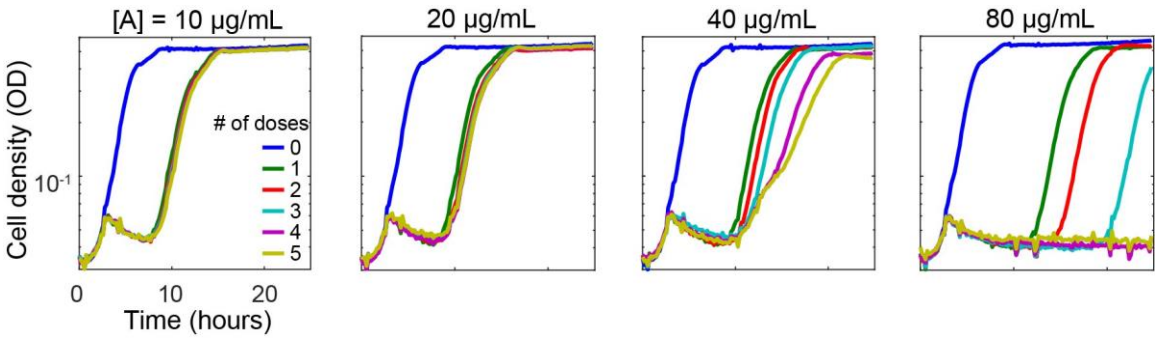

Figure 27. Multi-dosing is effective once antibiotic concentration is high enough. Here, doses of 10, 20, 40, or 80 µg/mL cefotaxime were added 0-5 times to the culture every 3 hours. Since the recover times of a single dose were 5.7, 6.1, 7.2, and 7.5 hours for A = 10, 20, 40 and 80 µg/ml cefotaxime, respectively, a dosing period of 3 hours should have successfully eradicated the populations in each of the scenarios. Instead, there were no observable differences in the recovery times for populations receiving 1 or 5 doses of 10 or 20 µg/ml cefotaxime. Once the antibiotic concentration was high enough ($A \geq 40$ µg/ml cefotaxime), then the recovery time started to be affected by subsequent doses.

This is likely due to the accumulation of Bla in the micro-well, which would degrade subsequent doses of low concentrations of antibiotic before they had a chance to induce another population crash. The model assumes a significant turnover rate of Bla in the media, but preliminary data suggests the decrease in Bla activity over 48 hours is not significant at the $p < 0.05$ level [$F(2, 9) = 2.23$, $p = 0.16$] (**Figure 28**). One possible set-up would be a microfluidic chip where the bacteria would be cultured in chambers that have a constant flow of media running through it that would prevent the accumulation of Bla over time. This device has been successfully implemented in our lab before, so I do not expect it would be difficult to optimize for this future work. Another option is to alter the model to reflect batch culture characteristics such that the criterion selected to capture the antibiotic response is a more accurate predictor of multi-dosing outcomes.

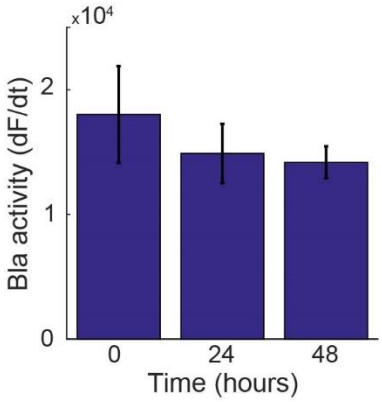

Figure 28. Turnover rate of Bla is not significant in the 96 well-plate. Using a similar protocol as in **3.4.5 Quantifying Bla activity:**, Bla was isolated from the culture and kept at 30°C for 48 hours in a rotating incubator. At 0, 24, and 48 hours after the Bla was harvested, a sample was removed, mixed with Fluorocillin (final concentration 1 μM), and the change in green fluorescence over time was captured with a plate reader. There was decrease in Bla activity over the 48 hour observation period was insignificant, suggesting that the turnover rate of Bla in this set up was not significant.

5.2.2 Validating optimal combination treatments *in vitro*

The resistance-resilience framework in Chapter 3 demonstrated that different isolates respond uniquely to combination treatments. The next logical step would be to use the framework to identify the optimal formulation of antibiotic and Bla inhibitor for a given isolate. First, this will involve updating the model to include the temporal dynamics of the Bla inhibitor. Second, the new model would be tuned to better fit data collected for single-dose responses to combination treatments. Then, the model will be used to determine the different combinations of antibiotic and Bla inhibitor concentrations that should be tested *in vitro* to verify the optimal formulation strategies.

5.2.3 Generalizing results

These experiments and models were primarily focused on one isolate and one antibiotic. Once the experimental conditions have been established in 5.2.1 and 5.2.2, we plan to generalize our results by testing our predictions on a wider range of isolates that depend on different mechanisms to survive antibiotics and different antibiotics. We are currently collaborating with the Duke Hospital's Antibiotic Stewardship Outreach Network, and will have access to a wide range of clinical isolates that we could test. Our lab owns a robotic arm and liquid handling system that would be crucial for scaling up the methods. The system can be programmed to pipette different antibiotic antibiotics at pre-set intervals to 6 microwell plates running in parallel.

5.2.4 Clinical translation

Ultimately, these predictions would be tested *in vivo*. As the antibiotics being used have already been approved by the Food and Drug Administration, we would be able to move directly to testing in patients. Discussions with Dr. Deverick Anderson revealed that Duke Hospital has a history of implementing new dosing protocols. For instance, Duke Hospital has successfully implemented a new regimen for the dosing of piperacillin-tazobactam (a β-lactam/Bla-inhibitor combination treatment). This is a promising lead for a place to test our predictions once the methods have been optimized and generalized.

References

1 Levy, S. B. & Marshall, B. Antibacterial resistance worldwide: causes, challenges and responses. *Nature medicine* **10**, S122-S129 (2004).

2 Projan, S. J. Why is big Pharma getting out of antibacterial drug discovery? *Current opinion in microbiology* **6**, 427-430 (2003).

3 Fishman, N. Antimicrobial stewardship. *American journal of infection control* **34**, S55-S63 (2006).

4 Davies, J. & Davies, D. Origins and evolution of antibiotic resistance. *Microbiology and Molecular Biology Reviews* **74**, 417-433 (2010).

5 Tuomanen, E., Durack, D. & Tomasz, A. Antibiotic tolerance among clinical isolates of bacteria. *Antimicrobial agents and chemotherapy* **30**, 521 (1986).

6 Lewis, K. Persister cells, dormancy and infectious disease. *Nature Reviews Microbiology* **5**, 48-56 (2006).

7 Johnson, P. J. & Levin, B. R. Pharmacodynamics, population dynamics, and the evolution of persistence in Staphylococcus aureus. *PLoS genetics* **9**, e1003123 (2013).

8 Levin, B. R. & Rozen, D. E. Non-inherited antibiotic resistance. *Nature Reviews Microbiology* **4**, 556-562 (2006).

9 Balaban, N. Q., Merrin, J., Chait, R., Kowalik, L. & Leibler, S. Bacterial persistence as a phenotypic switch. *Science* **305**, 1622-1625 (2004).

10 Tan, C. *et al.* The inoculum effect and band-pass bacterial response to periodic antibiotic treatment. *Molecular systems biology* **8** (2012).

11 Lee, J. H. & Lee, J. Indole as an intercellular signal in microbial communities. *FEMS microbiology reviews* **34**, 426-444 (2010).

12 Hu, B., Du, J., Zou, R.-y. & Yuan, Y.-j. An environment-sensitive synthetic microbial ecosystem. *PloS one* **5** (2010).

13 Pai, A., Tanouchi, Y. & You, L. Optimality and robustness in quorum sensing (QS)-mediated regulation of a costly public good enzyme. *Proceedings of the National Academy of Sciences* **109**, 19810-19815 (2012).

14 Tanouchi, Y., Pai, A., Buchler, N. E. & You, L. Programming stress-induced altruistic death in engineered bacteria. *Molecular systems biology* **8** (2012).

15 Tanouchi, Y., Lee, A. J., Meredith, H. & You, L. Programmed cell death in bacteria and implications for antibiotic therapy. *Trends in microbiology* **21**, 265-270 (2013).

16 Nedelcu, A. M., Driscoll, W. W., Durand, P. M., Herron, M. D. & Rashidi, A. On the paradigm of altruistic suicide in the unicellular world. *Evolution* **65**, 3-20 (2011).

17 Thomson, K. S. & Moland, E. S. Cefepime, piperacillin-tazobactam, and the inoculum effect in tests with extended-spectrum β-lactamase-producing Enterobacteriaceae. *Antimicrobial agents and chemotherapy* **45**, 3548-3554 (2001).

18 Sykes, R. & Matthew, M. The β-lactamases of gram-negative bacteria and their role in resistance to β-lactam antibiotics. *Journal of Antimicrobial Chemotherapy* **2**, 115-157 (1976).

19 Kolodkin-Gal, I., Sat, B., Keshet, A. & Engelberg-Kulka, H. The communication factor EDF and the toxin–antitoxin module mazEF determine the mode of action of antibiotics. *PLoS biology* **6**, e319 (2008).

20 Engelberg-Kulka, H., Sat, B., Reches, M., Amitai, S. & Hazan, R. Bacterial programmed cell death systems as targets for antibiotics. *Trends in microbiology* **12**, 66-71 (2004).

21 McGannon, C. M., Fuller, C. A. & Weiss, A. A. Different classes of antibiotics differentially influence Shiga toxin production. *Antimicrobial agents and chemotherapy* **54**, 3790-3798 (2010).

22 Plunkett, G., Rose, D. J., Durfee, T. J. & Blattner, F. R. Sequence of Shiga Toxin 2 Phage 933W fromEscherichia coli O157: H7: Shiga Toxin as a Phage Late-Gene Product. *Journal of bacteriology* **181**, 1767-1778 (1999).

23 Lainhart, W., Stolfa, G. & Koudelka, G. B. Shiga toxin as a bacterial defense against a eukaryotic predator, Tetrahymena thermophila. *Journal of bacteriology* **191**, 5116-5122, doi:10.1128/JB.00508-09 (2009).

24 Miller, M. B. & Bassler, B. L. Quorum sensing in bacteria. *Annual Reviews in Microbiology* **55**, 165-199 (2001).

25 Hammer, B. K. & Bassler, B. L. Quorum sensing controls biofilm formation in Vibrio cholerae. *Molecular microbiology* **50**, 101-104 (2003).

26 Robicsek, A. *et al.* Fluoroquinolone-modifying enzyme: a new adaptation of a common aminoglycoside acetyltransferase. *Nature medicine* **12**, 83-88 (2005).

27 Ding, X., Baca-DeLancey, R. R. & Rather, P. N. Role of SspA in the density-dependent expression of the transcriptional activator AarP in Providencia stuartii. *FEMS microbiology letters* **196**, 25-29 (2001).

28 Juhas, M., Eberl, L. & Tümmler, B. Quorum sensing: the power of cooperation in the world of Pseudomonas. *Environmental microbiology* **7**, 459-471 (2005).

29 Davies, D. G. *et al.* The involvement of cell-to-cell signals in the development of a bacterial biofilm. *Science* **280**, 295-298 (1998).

30 Ishida, H. *et al.* In vitro and in vivo activities of levofloxacin against biofilm-producing Pseudomonas aeruginosa. *Antimicrobial agents and chemotherapy* **42**, 1641-1645 (1998).

31 Singh, R., Ray, P., Das, A. & Sharma, M. Penetration of antibiotics through Staphylococcus aureus and Staphylococcus epidermidis biofilms. *Journal of antimicrobial chemotherapy* **65**, 1955-1958 (2010).

32 Anderl, J. N., Franklin, M. J. & Stewart, P. S. Role of antibiotic penetration limitation in Klebsiella pneumoniae biofilm resistance to ampicillin and ciprofloxacin. *Antimicrobial agents and chemotherapy* **44**, 1818-1824 (2000).

33 Giwercman, B., Jensen, E., Høiby, N., Kharazmi, A. & Costerton, J. Induction of beta-lactamase production in Pseudomonas aeruginosa biofilm. *Antimicrobial agents and chemotherapy* **35**, 1008-1010 (1991).

34 Costerton, J., Stewart, P. S. & Greenberg, E. Bacterial biofilms: a common cause of persistent infections. *Science* **284**, 1318-1322 (1999).

35 Craig, W. A., Bhavnani, S. M. & Ambrose, P. G. The inoculum effect: fact or artifact? *Diagnostic microbiology and infectious disease* **50**, 229-230 (2004).

36 Udekwu, K. I., Parrish, N., Ankomah, P., Baquero, F. & Levin, B. R. Functional relationship between bacterial cell density and the efficacy of antibiotics. *Journal of antimicrobial chemotherapy* **63**, 745-757 (2009).

37 Tadmor, A. D. & Tlusty, T. A coarse-grained biophysical model of E. coli and its application to perturbation of the rRNA operon copy number. *PLoS computational biology* **4**, e1000038 (2008).

38 Thron, C. Bistable biochemical switching and the control of the events of the cell cycle. *Nonlinear Analysis: Theory, Methods & Applications* **30**, 1825-1834 (1997).

39 VanBogelen, R. A. & Neidhardt, F. C. Ribosomes as sensors of heat and cold shock in Escherichia coli. *Proceedings of the National Academy of Sciences* **87**, 5589-5593 (1990).

40 Sykes, M. T., Shajani, Z., Sperling, E., Beck, A. H. & Williamson, J. R. Quantitative Proteomic Analysis of Ribosome Assembly and Turnover< i> In Vivo</i>. *Journal of molecular biology* **403**, 331-345 (2010).

41 Rice, K. C. *et al.* The Staphylococcus aureus cidAB operon: evaluation of its role in regulation of murein hydrolase activity and penicillin tolerance. *Journal of bacteriology* **185**, 2635-2643 (2003).

42 Rice, K. C. *et al.* The cidA murein hydrolase regulator contributes to DNA release and biofilm development in Staphylococcus aureus. *Proceedings of the National Academy of Sciences* **104**, 8113-8118 (2007).

43 Bayles, K. W. The biological role of death and lysis in biofilm development. *Nature Reviews Microbiology* **5**, 721-726 (2007).

44 Groicher, K. H., Firek, B. A., Fujimoto, D. F. & Bayles, K. W. The Staphylococcus aureus lrgAB operon modulates murein hydrolase activity and penicillin tolerance. *Journal of bacteriology* **182**, 1794-1801 (2000).

45 Köhler, T., Curty, L. K., Barja, F., van Delden, C. & Pechère, J.-C. Swarming of Pseudomonas aeruginosa is dependent on cell-to-cell signaling and requires flagella and pili. *Journal of bacteriology* **182**, 5990-5996 (2000).

46 Butler, M. T., Wang, Q. & Harshey, R. M. Cell density and mobility protect swarming bacteria against antibiotics. *Proceedings of the National Academy of Sciences* **107**, 3776-3781 (2010).

47 Kim, W., Killam, T., Sood, V. & Surette, M. G. Swarm-cell differentiation in Salmonella enterica serovar Typhimurium results in elevated resistance to multiple antibiotics. *Journal of bacteriology* **185**, 3111-3117 (2003).

48 Verstraeten, N. *et al.* Living on a surface: swarming and biofilm formation. *Trends in microbiology* **16**, 496-506 (2008).

49 van Ditmarsch, D. *et al.* Convergent evolution of hyperswarming leads to impaired biofilm formation in pathogenic bacteria. *Cell reports* **4**, 697-708 (2013).

50 Overhage, J., Bains, M., Brazas, M. D. & Hancock, R. E. Swarming of Pseudomonas aeruginosa is a complex adaptation leading to increased production of virulence factors and antibiotic resistance. *Journal of bacteriology* **190**, 2671-2679 (2008).

51 Gunn, J. S. Bacterial modification of LPS and resistance to antimicrobial peptides. *Journal of endotoxin research* **7**, 57-62 (2001).

52 Lee, H. H., Molla, M. N., Cantor, C. R. & Collins, J. J. Bacterial charity work leads to population-wide resistance. *Nature* **467**, 82-85 (2010).

53 Andersen, J. B. *et al.* gfp-based N-acyl homoserine-lactone sensor systems for detection of bacterial communication. *Applied and environmental microbiology* **67**, 575-585 (2001).

54 Moons, P., Michiels, C. W. & Aertsen, A. Bacterial interactions in biofilms. *Critical reviews in microbiology* **35**, 157-168 (2009).

55 Allison, D. & Matthews, M. Effect of polysaccharide interactions on antibiotic susceptibility of Pseudomonas aeruginosa. *Journal of applied bacteriology* **73**, 484-488 (1992).

56 Meredith, H. R., Lopatkin, A. J., Anderson, D. J. & You, L. Bacterial temporal dynamics enable optimal design of antibiotic treatment. *PLoS Computational Biology, in press* (2015).

57 Kurioka, T., Yunou, Y., Harada, H. & Kita, E. Efficacy of antibiotic therapy for infection with Shiga-like toxin-producing Escherichia coli O157: H7 in mice with protein-calorie malnutrition. *European Journal of Clinical Microbiology and Infectious Diseases* **18**, 561-571 (1999).

58 Kumon, H., Ono, N., Iida, M. & Nickel, J. C. Combination effect of fosfomycin and ofloxacin against Pseudomonas aeruginosa growing in a biofilm. *Antimicrobial agents and chemotherapy* **39**, 1038-1044 (1995).

59 Schultz, G., Phillips, P., Yang, Q. & Stewart, P. Biofilm maturity studies indicate sharp debridement opens a time-dependent therapeutic window. *Journal of wound care* **19**, 320 (2010).

60 Jacoby, G. A. AmpC β-lactamases. *Clinical microbiology reviews* **22**, 161-182 (2009).

61 Drawz, S. M. & Bonomo, R. A. Three decades of β-lactamase inhibitors. *Clinical microbiology reviews* **23**, 160-201 (2010).

62 Chaibi, E., Sirot, D., Paul, G. & Labia, R. Inhibitor-resistant TEM β-lactamases: phenotypic, genetic and biochemical characteristics. *Journal of Antimicrobial Chemotherapy* **43**, 447-458 (1999).

63 Mutschler, H. & Meinhart, A. ε/ζ systems: their role in resistance, virulence, and their potential for antibiotic development. *Journal of molecular medicine* **89**, 1183-1194 (2011).

64 Lioy, V. S., Rey, O., Balsa, D., Pellicer, T. & Alonso, J. C. A toxin–antitoxin module as a target for antimicrobial development. *Plasmid* **63**, 31-39 (2010).

65 Berry, A. M., Lock, R. A., Hansman, D. & Paton, J. C. Contribution of autolysin to virulence of Streptococcus pneumoniae. *Infection and immunity* **57**, 2324-2330 (1989).

66 Tateda, K. *et al.* Azithromycin inhibits quorum sensing in Pseudomonas aeruginosa. *Antimicrobial agents and chemotherapy* **45**, 1930-1933 (2001).

67 Van Delden, C. *et al.* Azithromycin to prevent Pseudomonas aeruginosa ventilator-associated pneumonia by inhibition of quorum sensing: a randomized controlled trial. *Intensive care medicine* **38**, 1118-1125 (2012).

68 Dong, Y.-H., Xu, J.-L., Li, X.-Z. & Zhang, L.-H. AiiA, an enzyme that inactivates the acylhomoserine lactone quorum-sensing signal and attenuates the virulence of Erwinia carotovora. *Proceedings of the National Academy of Sciences* **97**, 3526-3531 (2000).

69 O'Loughlin, C. T. *et al.* A quorum-sensing inhibitor blocks Pseudomonas aeruginosa virulence and biofilm formation. *Proceedings of the National Academy of Sciences* **110**, 17981-17986 (2013).

70 Brackman, G., Cos, P., Maes, L., Nelis, H. J. & Coenye, T. Quorum sensing inhibitors increase the susceptibility of bacterial biofilms to antibiotics in vitro and in vivo. *Antimicrobial agents and chemotherapy* **55**, 2655-2661 (2011).

71 Soong, G. *et al.* Bacterial neuraminidase facilitates mucosal infection by participating in biofilm production. *The Journal of clinical investigation* **116**, 2297-2305 (2006).

72 Mehta, R. & Champney, W. S. 30S ribosomal subunit assembly is a target for inhibition by aminoglycosides in Escherichia coli. *Antimicrobial agents and chemotherapy* **46**, 1546-1549 (2002).

73 Maisonneuve, E. & Gerdes, K. Molecular Mechanisms Underlying Bacterial Persisters. *Cell* **157**, 539-548, doi:10.1016/j.cell.2014.02.050 (2014).

74 Dalebroux, Z. D., Svensson, S. L., Gaynor, E. C. & Swanson, M. S. ppGpp Conjures Bacterial Virulence. *Microbiology and Molecular Biology Reviews* **74**, 171-199, doi:10.1128/MMBR.00046-09 (2010).

75 Kohanski, M. A., Dwyer, D. J., Hayete, B., Lawrence, C. A. & Collins, J. J. A Common Mechanism of Cellular Death Induced by Bactericidal Antibiotics. *Cell* **130**, 797-810, doi:10.1016/j.cell.2007.06.049 (2007).

76 Toguchi, A., Siano, M., Burkart, M. & Harshey, R. M. Genetics of swarming motility in Salmonella enterica serovar Typhimurium: critical role for lipopolysaccharide. *Journal of bacteriology* **182**, 6308-6321 (2000).

77 Mireles, J. R., Toguchi, A. & Harshey, R. M. Salmonella enterica Serovar Typhimurium Swarming Mutants with Altered Biofilm-Forming Abilities: Surfactin Inhibits Biofilm Formation. *Journal of Bacteriology* **183**, 5848-5854, doi:10.1128/JB.183.20.5848-5854.2001 (2001).

78 Brook, I., Pazzaglia, G., Coolbaugh, J. C. & Walker, R. I. In-vivo protection of group A β-haemolytic streptococci from penicillin by β-lactamase-producing Bacteroides species. *Journal of Antimicrobial Chemotherapy* **12**, 599-606 (1983).

79 Citorik, R. J., Mimee, M. & Lu, T. K. Sequence-specific antimicrobials using efficiently delivered RNA-guided nucleases. *Nature biotechnology*, 1141-1145 (2014).

80 Bikard, D. *et al.* Exploiting CRISPR-Cas nucleases to produce sequence-specific antimicrobials. *Nature biotechnology*, 1146-1150 (2014).

81 Eagle, H. & Musselman, A. D. The rate of bactericidal action of penicillin in vitro as a function of its concentration, and its paradoxically reduced activity at high concentrations against certain organisms. *The Journal of experimental medicine* **88**, 99-131 (1948).

82 Hentzer, M. *et al.* Attenuation of Pseudomonas aeruginosa virulence by quorum sensing inhibitors. *The EMBO journal* **22**, 3803-3815 (2003).

83 Hentzer, M. & Givskov, M. Pharmacological inhibition of quorum sensing for the treatment of chronic bacterial infections. *Journal of Clinical Investigation* **112**, 1300-1307 (2003).

84 Köhler, T., Perron, G. G., Buckling, A. & Van Delden, C. Quorum sensing inhibition selects for virulence and cooperation in Pseudomonas aeruginosa. *PLoS pathogens* **6**, e1000883 (2010).

85 Nalca, Y. *et al.* Quorum-sensing antagonistic activities of azithromycin in Pseudomonas aeruginosa PAO1: a global approach. *Antimicrobial agents and chemotherapy* **50**, 1680-1688 (2006).

86 Schuster, M., Joseph Sexton, D., Diggle, S. P. & Peter Greenberg, E. Acyl-homoserine lactone quorum sensing: from evolution to application. *Annual review of microbiology* **67**, 43-63 (2013).

87 Sandoz, K. M., Mitzimberg, S. M. & Schuster, M. Social cheating in Pseudomonas aeruginosa quorum sensing. *Proceedings of the National Academy of Sciences* **104**, 15876-15881 (2007).

88 André, J. B. & Godelle, B. Multicellular organization in bacteria as a target for drug therapy. *Ecology Letters* **8**, 800-810 (2005).

89 Dandekar, A. A., Chugani, S. & Greenberg, E. P. Bacterial quorum sensing and metabolic incentives to cooperate. *Science* **338**, 264-266 (2012).

90 Chuang, J. S., Rivoire, O. & Leibler, S. Simpson's paradox in a synthetic microbial system. *Science* **323**, 272-275 (2009).

91 Tanouchi, Y., Smith, R. P. & You, L. Engineering microbial systems to explore ecological and evolutionary dynamics. *Current opinion in biotechnology* **23**, 791-797 (2012).

92 Darch, S. E., West, S. A., Winzer, K. & Diggle, S. P. Density-dependent fitness benefits in quorum-sensing bacterial populations. *Proceedings of the National Academy of Sciences* **109**, 8259-8263 (2012).

93 Yurtsev, E. A., Chao, H. X., Datta, M. S., Artemova, T. & Gore, J. Bacterial cheating drives the population dynamics of cooperative antibiotic resistance plasmids. *Molecular systems biology* **9** (2013).

94 Allen, R. C., Popat, R., Diggle, S. P. & Brown, S. P. Targeting virulence: can we make evolution-proof drugs? *Nature Reviews Microbiology* **12**, 300-308 (2014).

95 Shade, A. *et al.* Fundamentals of microbial community resistance and resilience. (2012).

96 Nimmo, D., Mac Nally, R., Cunningham, S., Haslem, A. & Bennett, A. Vive la résistance: reviving resistance for 21st century conservation. *Trends in ecology & evolution* **30**, 516-523 (2015).

97 Ghedini, G., Russell, B. D. & Connell, S. D. Trophic compensation reinforces resistance: herbivory absorbs the increasing effects of multiple disturbances. *Ecology Letters* **18**, 182-187 (2015).

98 DeRose, R. J. & Long, J. N. Resistance and resilience: A conceptual framework for silviculture. *Forest Science* **60**, 1205-1212 (2014).

99 Halpern, C. B. Early successional pathways and the resistance and resilience of forest communities. *Ecology* **69**, 1703-1715 (1988).

100 Connell, S. D. & Ghedini, G. Resisting regime-shifts: the stabilising effect of compensatory processes. *Trends in ecology & evolution* **30**, 513-515 (2015).

101 Funk, J. L., Cleland, E. E., Suding, K. N. & Zavaleta, E. S. Restoration through reassembly: plant traits and invasion resistance. *Trends in ecology & evolution* **23**, 695-703 (2008).

102 Holling, C. S. Resilience and stability of ecological systems. *Annual review of ecology and systematics* **4**, 1-23 (1973).

103 Todman, L. *et al.* Defining and quantifying the resilience of responses to disturbance: a conceptual and modelling approach from soil science. *Scientific reports* **6** (2016).

104 Allison, S. D. & Martiny, J. B. Resistance, resilience, and redundancy in microbial communities. *Proceedings of the National Academy of Sciences* **105**, 11512-11519 (2008).

105 Hodgson, D., McDonald, J. L. & Hosken, D. J. What do you mean,'resilient'? *Trends in ecology & evolution* **30**, 503-506 (2015).

106 Grimm, V. & Wissel, C. Babel, or the ecological stability discussions: an inventory and analysis of terminology and a guide for avoiding confusion. *Oecologia* **109**, 323-334 (1997).

107 Reller, L. B., Weinstein, M., Jorgensen, J. H. & Ferraro, M. J. Antimicrobial Susceptibility Testing: A Review of General Principles and Contemporary Practices. *Clinical Infectious Diseases* **49**, 1749-1755, doi:10.1086/647952 (2009).

108 Jorgensen, J. H. & Turnidge, J. D. in *Manual of Clinical Microbiology, Eleventh Edition* 1253-1273 (American Society of Microbiology, 2015).

109 CLSI. in *Twenty-Second informational supplement NCCLS document M100-S22. National Committee for Clinical Laboratory Standards* Vol. 32 1-188 (Clinical and Laboratory Standards Institute, Wayne, PA, 2012).

110 Dobrindt, U., Hochhut, B., Hentschel, U. & Hacker, J. Genomic islands in pathogenic and environmental microorganisms. *Nature Reviews Microbiology* **2**, 414-424 (2004).

111 Neu, H. C. The crisis in antibiotic resistance. *Science* **257**, 1064-1073 (1992).

112 Alanis, A. J. Resistance to antibiotics: are we in the post-antibiotic era? *Archives of medical research* **36**, 697-705 (2005).

113 Livermore, D. & Hawkey, P. CTX-M: changing the face of ESBLs in the UK. *Journal of Antimicrobial Chemotherapy* **56**, 451-454 (2005).

114 Rupp, M. E. & Fey, P. D. Extended spectrum β-lactamase (ESBL)-producing Enterobacteriaceae. *Drugs* **63**, 353-365 (2003).

115 Ramphal, R. & Ambrose, P. G. Extended-spectrum β-lactamases and clinical outcomes: current data. *Clinical infectious diseases* **42**, S164-S172 (2006).

116 Centers for Disease Control and Prevention. (ed U.S. Department of Health and Human Services) (2013).

117 Page, M. G. in *Antibiotic Discovery and Development* 79-117 (Springer, 2012).

118 Finkel, S. E. & Kolter, R. DNA as a nutrient: novel role for bacterial competence gene homologs. *Journal of bacteriology* **183**, 6288-6293 (2001).

119 Bush, K. Beta-lactamase inhibitors from laboratory to clinic. *Clinical microbiology reviews* **1**, 109-123 (1988).

120 Livermore, D. M. beta-Lactamases in laboratory and clinical resistance. *Clinical Microbiology Reviews* **8**, 557-584 (1995).

121 Tomasz, A. The mechanism of the irreversible antimicrobial effects of penicillins: how the beta-lactam antibiotics kill and lyse bacteria. *Annual Reviews in Microbiology* **33**, 113-137 (1979).

122 Zhang, X. Y., Trame, M., Lesko, L. & Schmidt, S. Sobol sensitivity analysis: a tool to guide the development and evaluation of systems pharmacology models. *CPT: Pharmacometrics & Systems Pharmacology* **4**, 69-79 (2015).

123 Hunter, P. A., Coleman, K., Fisher, J. & Taylor, D. In vitro synergistic properties of clavulanic acid, with ampicillin, amoxycillin and ticarcillin. *Journal of Antimicrobial Chemotherapy* **6**, 455-470 (1980).

124 Bush, K. & Jacoby, G. A. Updated functional classification of β-lactamases. *Antimicrobial agents and chemotherapy* **54**, 969-976 (2010).

125 Ball, P. The clinical development and launch of amoxicillin/clavulanate for the treatment of a range of community-acquired infections. *International journal of antimicrobial agents* **30**, 113-117 (2007).

126 Weber, D. J., Tolkoff-Rubin, N. E. & Rubin, R. H. Amoxicillin and Potassium Clavulanate: An Antibiotic Combination Mechanism of Action, Pharmacokinetics, Antimicrobial Spectrum, Clinical Efficacy and Adverse Effects. *Pharmacotherapy: The Journal of Human Pharmacology and Drug Therapy* **4**, 122-133 (1984).

127 Lebre, P. H., De Maayer, P. & Cowan, D. A. Xerotolerant bacteria: surviving through a dry spell. *Nature Reviews Microbiology* (2017).

128 Colinet, H., Lee, S. F. & Hoffmann, A. Temporal expression of heat shock genes during cold stress and recovery from chill coma in adult Drosophila melanogaster. *The FEBS journal* **277**, 174-185 (2010).

129 Lindquist, S. & Craig, E. The heat-shock proteins. *Annual review of genetics* **22**, 631-677 (1988).

130 Veraart, A. J. *et al.* Recovery rates reflect distance to a tipping point in a living system. *Nature* **481**, 357 (2012).

131 Faassen, E. J. *et al.* Hysteresis in an experimental phytoplankton population. *Oikos* **124**, 1617-1623 (2015).

132 Lozupone, C. A., Stombaugh, J. I., Gordon, J. I., Jansson, J. K. & Knight, R. Diversity, stability and resilience of the human gut microbiota. *Nature* **489**, 220-230 (2012).

133 Lewis, K. Persister cells. *Annual review of microbiology* **64**, 357-372 (2010).

134 Spratt, B. G. Resistance to antibiotics mediated by target alterations. *Science-AAAS-Weekly Paper Edition-including Guide to Scientific Information* **264**, 388-396 (1994).

135 Bugg, T. D. *et al.* Molecular basis for vancomycin resistance in Enterococcus faecium BM4147: biosynthesis of a depsipeptide peptidoglycan precursor by vancomycin resistance proteins VanH and VanA. *Biochemistry* **30**, 10408-10415 (1991).

136 Watkins, R., Papp-Wallace, K. M., Drawz, S. M. & Bonomo, R. A. Novel β-lactamase inhibitors: a therapeutic hope against the scourge of multidrug resistance. *Frontiers in microbiology* **4**, 392 (2013).

137 Letourneau, A. R., Calderwood, S. B., Hooper, D. C. & Bloom, A. Combination beta-lactamase inhibitors, carbapenems, and monobactams. (2009).

138 U.S. Food and Drug Administration. (2005).

139 White, A. R. *et al.* Augmentin (amoxicillin/clavulanate) in the treatment of community-acquired respiratory tract infection: a review of the continuing development of an innovative antimicrobial agent. *Journal of Antimicrobial Chemotherapy* **53**, 3-20 (2004).

140 Bottenfield, G. W. *et al.* Safety and tolerability of a new formulation (90 mg/kg/day divided every 12 h) of amoxicillin/clavulanate (Augmentin®) in the empiric treatment of pediatric acute otitis media caused by drug-resistant Streptococcus pneumoniae. *The Pediatric infectious disease journal* **17**, 963-968 (1998).

141 Senn, H., Lendenmann, U., Snozzi, M., Hamer, G. & Egli, T. The growth of Escherichia coli in glucose-limited chemostat cultures: a re-examination of the kinetics. *Biochimica et Biophysica Acta (BBA)-General Subjects* **1201**, 424-436 (1994).

142 Park, J. T. & Uehara, T. How bacteria consume their own exoskeletons (turnover and recycling of cell wall peptidoglycan). *Microbiology and Molecular Biology Reviews* **72**, 211-227 (2008).

143 Tuomanen, E., Cozens, R., Tosch, W., Zak, O. & Tomasz, A. The Rate of Killing of Escherichia coli byβ-Lactam Antibiotics Is Strictly Proportional to the Rate of Bacterial Growth. *Journal of general microbiology* **132**, 1297-1304 (1986).

144 Osuna, J., Viadiu, H., Fink, A. L. & Soberón, X. Substitution of Asp for Asn at Position 132 in the Active Site of TEM-Lactamase ACTIVITY TOWARD DIFFERENT SUBSTRATES AND EFFECTS OF NEIGHBORING RESIDUES. *Journal of Biological Chemistry* **270**, 775-780 (1995).

145 Kjeldsen, T. S. B. *et al.* CTX-M-1 β-lactamase expression in Escherichia coli is dependent on cefotaxime concentration, growth phase and gene location. *Journal of Antimicrobial Chemotherapy* **70**, 62-70, doi:10.1093/jac/dku332 (2015).

146 Poirel, L., Gniadkowski, M. & Nordmann, P. Biochemical analysis of the ceftazidime-hydrolysing extended-spectrum β-lactamase CTX-M-15 and of its structurally related β-lactamase CTX-M-3. *Journal of Antimicrobial Chemotherapy* **50**, 1031-1034 (2002).

147 Fabre, H., Eddine, N. H. & Berge, G. Degradation kinetics in aqueous solution of cefotaxime sodium, a third-generation cephalosporin. *Journal of pharmaceutical sciences* **73**, 611-618 (1984).

148 Wu, X.-C., Lee, W., Tran, L. & Wong, S. Engineering a Bacillus subtilis expression-secretion system with a strain deficient in six extracellular proteases. *Journal of bacteriology* **173**, 4952-4958 (1991).

149 Vu, H. & Nikaido, H. Role of beta-lactam hydrolysis in the mechanism of resistance of a beta-lactamase-constitutive Enterobacter cloacae strain to expanded-spectrum beta-lactams. *Antimicrobial agents and chemotherapy* **27**, 393-398 (1985).

150 Wang, H. H. *et al.* Programming cells by multiplex genome engineering and accelerated evolution. *Nature* **460**, 894 (2009).

151 Herman, J. & Usher, W. SALib: An open-source Python library for Sensitivity Analysis. *The Journal of Open Source Software* (2017).

152 Clatworthy, A. E., Pierson, E. & Hung, D. T. Targeting virulence: a new paradigm for antimicrobial therapy. *Nature chemical biology* **3**, 541-548 (2007).

153 Walsh, C. Where will new antibiotics come from? *Nature Reviews Microbiology* **1**, 65-70 (2003).

154 Gilmore, M. S. *et al.* Enterococcal Infection—Treatment and Antibiotic Resistance. (2014).

155 MacGowan, A. & Macnaughton, E. Antibiotic resistance. *Medicine* **41**, 642-648 (2013).

156 Čižman, M., Pokorn, M., Seme, K., Oražem, A. & Paragi, M. The relationship between trends in macrolide use and resistance to macrolides of common respiratory pathogens. *Journal of Antimicrobial Chemotherapy* **47**, 475-477 (2001).

157 Weber, J. T. & Courvalin, P. An emptying quiver: antimicrobial drugs and resistance. *Emerg Infect Dis* **11**, 791-793 (2005).

158 Fisher, J. F., Meroueh, S. O. & Mobashery, S. Bacterial resistance to β-lactam antibiotics: compelling opportunism, compelling opportunity. *Chemical reviews* **105**, 395-424 (2005).

159 Hamad, B. The antibiotics market. *Nature Reviews Drug Discovery* **9**, 675-676 (2010).

160 MacLaughlin, E. J., Saseen, J. J. & Malone, D. C. Costs of beta-lactam allergies: selection and costs of antibiotics for patients with a reported beta-lactam allergy. *Archives of family medicine* **9**, 722-726 (2000).

161 Holten, K. B. Appropriate prescribing of oral beta-lactam antibiotics. *American family physician* **62** (2000).

162 Piccirillo, J. F., Mager, D. E., Frisse, M. E., Brophy, R. H. & Goggin, A. Impact of first-line vs second-line antibiotics for the treatment of acute uncomplicated sinusitis. *Jama* **286**, 1849-1856 (2001).

163 Kang, C.-I., Chung, D. R., Ko, K. S., Peck, K. R. & Song, J.-H. Risk factors for infection and treatment outcome of extended-spectrum β-lactamase-producing Escherichia coli and Klebsiella pneumoniae bacteremia in patients with hematologic malignancy. *Annals of hematology* **91**, 115-121 (2012).

164 Maiques, E. *et al.* β-Lactam antibiotics induce the SOS response and horizontal transfer of virulence factors in Staphylococcus aureus. *Journal of bacteriology* **188**, 2726-2729 (2006).

165 Paterson, D. L. *et al.* Outcome of cephalosporin treatment for serious infections due to apparently susceptible organisms producing extended-spectrum β-lactamases: implications for the clinical microbiology laboratory. *Journal of clinical microbiology* **39**, 2206-2212 (2001).

166 Livermore, D. M. *et al.* Are susceptibility tests enough, or should laboratories still seek ESBLs and carbapenemases directly? *Journal of antimicrobial chemotherapy* **67**, 1569-1577 (2012).

167 Queenan, A. M., Foleno, B., Gownley, C., Wira, E. & Bush, K. Effects of inoculum and β-lactamase activity in AmpC-and extended-spectrum β-lactamase (ESBL)-producing Escherichia coli and Klebsiella pneumoniae clinical isolates tested by using NCCLS ESBL methodology. *Journal of clinical microbiology* **42**, 269-275 (2004).

168 Dudley, M. N. *et al.* Background and rationale for revised Clinical and Laboratory Standards Institute interpretive criteria (breakpoints) for Enterobacteriaceae and Pseudomonas aeruginosa: I. Cephalosporins and aztreonam. *Clinical infectious diseases* **56**, 1301-1309 (2013).

169 Bedenić, B., Beader, N. & Žagar, Ž. Effect of inoculum size on the antibacterial activity of cefpirome and cefepime against Klebsiella pneumoniae strains producing SHV extended-spectrum β-lactamases. *Clinical microbiology and infection* **7**, 626-635 (2001).

170 Brook, I. Inoculum effect. *Review of Infectious Diseases* **11**, 361-368 (1989).

171 Bush, K. Is it important to identify extended-spectrum beta-lactamase-producing isolates? *European Journal of Clinical Microbiology & Infectious Diseases* **15**, 361-364 (1996).

172 Meredith, H. R., Srimani, J. K., Lee, A. J., Lopatkin, A. J. & You, L. Collective antibiotic tolerance: mechanisms, dynamics and intervention. *Nature chemical biology* **11**, 182-188 (2015).

173 Falagas, M. & Karageorgopoulos, D. Extended-spectrum β-lactamase-producing organisms. *Journal of Hospital infection* **73**, 345-354 (2009).

174 Conte, J. E. *Manual of antibiotics and infectious diseases: treatment and prevention*. (Lippincott Williams & Wilkins, 2002).

175 Owens, R. C. & Ambrose, P. G. Antimicrobial safety: focus on fluoroquinolones. *Clinical infectious diseases* **41**, S144-S157 (2005).

176 Stahlmann, R. & Lode, H. M. Risks associated with the therapeutic use of fluoroquinolones. *Expert opinion on drug safety* **12**, 497-505 (2013).

177 Leibovici, L., Shraga, I. & Andreassen, S. How do you choose antibiotic treatment? *BMJ: British Medical Journal* **318**, 1614 (1999).

178 Cunha, B. A. Antibiotic side effects. *Medical Clinics of North America* **85**, 149-185 (2001).

179 Mandell, G., Dolin, R. & Bennett, J. *Mandell, Douglas, and Bennett's principles and practice of infectious diseases*. 309-510 (Elsevier, 2010).

180 Jacoby, G. Genetics of extended-spectrum beta-lactamases. *European Journal of Clinical Microbiology and Infectious Diseases* **13**, S2-S11 (1994).

181 Craig, W. A. Pharmacokinetic/pharmacodynamic parameters: rationale for antibacterial dosing of mice and men. *Clinical infectious diseases*, 1-10 (1998).

182 Craig, W. A. Interrelationship between pharmacokinetics and pharmacodynamics in determining dosage regimens for broad-spectrum cephalosporins. *Diagnostic microbiology and infectious disease* **22**, 89-96 (1995).

183 Burgess, D. S., Hastings, R. W. & Hardin, T. C. Pharmacokinetics and pharmacodynamics of cefepime administered by intermittent and continuous infusion. *Clinical therapeutics* **22**, 66-75 (2000).

184 Reese, A. M., Frei, C. R. & Burgess, D. S. Pharmacodynamics of intermittent and continuous infusion piperacillin/tazobactam and cefepime against extended-spectrum β-lactamase-producing organisms. *International journal of antimicrobial agents* **26**, 114-119 (2005).

185 Lodise, T. P., Lomaestro, B. M. & Drusano, G. L. Application of antimicrobial pharmacodynamic concepts into clinical practice: focus on β-lactam antibiotics. *Pharmacotherapy: The Journal of Human Pharmacology and Drug Therapy* **26**, 1320-1332 (2006).

186 Ebert, S. C. & Craig, W. A. Pharmacodynamic properties of antibiotics: application to drug monitoring and dosage regimen design. *Infection Control and Hospital Epidemiology* **11**, 319-326 (1990).

187 Bhat, S. V. *et al.* Failure of current cefepime breakpoints to predict clinical outcomes of bacteremia caused by gram-negative organisms. *Antimicrobial agents and chemotherapy* **51**, 4390-4395 (2007).

188 Rossolini, G. M., Walsh, T. & Amicosante, G. The Aeromonas metallo-β-lactamases: genetics, enzymology, and contribution to drug resistance. *Microbial drug resistance* **2**, 245-252 (1996).

189 Livermore, D. Clinical significance of beta-lactamase induction and stable derepression in gram-negative rods. *European Journal of Clinical Microbiology & Infectious Diseases* **6**, 439-445 (1987).

190 Minami, S., Yotsuji, A., Inoue, M. & Mitsuhashi, S. Induction of beta-lactamase by various beta-lactam antibiotics in Enterobacter cloacae. *Antimicrobial agents and chemotherapy* **18**, 382-385 (1980).

191 Hanson, N. & Sanders, C. Regulation of inducible AmpC beta-lactamase expression among Enterobacteriaceae. *Current pharmaceutical design* **5**, 881-894 (1999).

192 Shah, A., Hasan, F., Ahmed, S. & Hameed, A. Extended-spectrum β-lactamases (ESBLs): characterization, epidemiology and detection. *Critical reviews in microbiology* **30**, 25-32 (2004).

193 Levin, B. R. & Udekwu, K. I. Population dynamics of antibiotic treatment: a mathematical model and hypotheses for time-kill and continuous-culture experiments. *Antimicrobial agents and chemotherapy* **54**, 3414-3426 (2010).

194 Bradford, P. A. Extended-spectrum β-lactamases in the 21st century: characterization, epidemiology, and detection of this important resistance threat. *Clinical microbiology reviews* **14**, 933-951 (2001).

195 Andrews, J. M. Determination of minimum inhibitory concentrations. *Journal of antimicrobial Chemotherapy* **48**, 5-16 (2001).

196 Czock, D. & Keller, F. Mechanism-based pharmacokinetic–pharmacodynamic modeling of antimicrobial drug effects. *Journal of pharmacokinetics and pharmacodynamics* **34**, 727-751 (2007).

197 Jernberg, C., Löfmark, S., Edlund, C. & Jansson, J. K. Long-term impacts of antibiotic exposure on the human intestinal microbiota. *Microbiology* **156**, 3216-3223 (2010).

198 Labro, M.-T. Interference of antibacterial agents with phagocyte functions: immunomodulation or "immuno-fairy tales"? *Clinical microbiology reviews* **13**, 615-650 (2000).

199 Lodise, T. P., Lomaestro, B., Graves, J. & Drusano, G. Larger vancomycin doses (at least four grams per day) are associated with an increased incidence of nephrotoxicity. *Antimicrobial agents and chemotherapy* **52**, 1330-1336 (2008).

200 Buffie, C. G. *et al.* Profound alterations of intestinal microbiota following a single dose of Clindamycin results in sustained susceptibility to C. difficile-induced colitis. *Infection and immunity*, IAI. 05496-05411v05491 (2011).

201 Craig, W. Choosing an antibiotic on the basis of pharmacodynamics. *Ear, nose, & throat journal* **77**, 7-11; discussion 11-12 (1998).

202 Craig, W. A. Does the dose matter? *Clinical infectious diseases* **33**, S233-S237 (2001).

203 Nevozhay, D., Adams, R. M., Van Itallie, E., Bennett, M. R. & Balázsi, G. Mapping the environmental fitness landscape of a synthetic gene circuit. *PLoS computational biology* **8**, e1002480 (2012).

204 Charlebois, D. A., Balázsi, G. & Kærn, M. Coherent feedforward transcriptional regulatory motifs enhance drug resistance. *Physical Review E* **89**, 052708 (2014).

205 Jõers, A., Kaldalu, N. & Tenson, T. The frequency of persisters in Escherichia coli reflects the kinetics of awakening from dormancy. *Journal of bacteriology* **192**, 3379-3384 (2010).

206 Chang, K. C., Leung, C. C., Yew, W. W., Chan, S. L. & Tam, C. M. Dosing schedules of 6-month regimens and relapse for pulmonary tuberculosis. *American journal of respiratory and critical care medicine* **174**, 1153-1158 (2006).

207 Jia, C., Qian, M., Kang, Y. & Jiang, D. Modeling stochastic phenotype switching and bet-hedging in bacteria: stochastic nonlinear dynamics and critical state identification. *Quantitative Biology* **2**, 110-125 (2014).

208 Kussell, E. & Leibler, S. Phenotypic diversity, population growth, and information in fluctuating environments. *Science* **309**, 2075-2078 (2005).

209 Gilbert, D. N., Moellering, R. C., Eliopoulos, G. M., Chambers, H. F. & Saag, M. S. *The Sanford Guide to Antimicrobial Therapy 2012*. 42 edn, (Antimicrobial Therpy, Inc., 2012).

210 Willing, B. P., Russell, S. L. & Finlay, B. B. Shifting the balance: antibiotic effects on host–microbiota mutualism. *Nature Reviews Microbiology* **9**, 233-243 (2011).

211 Tan, C., Smith, R. P., Tsai, M.-C., Schwartz, R. & You, L. Phenotypic Signatures Arising from Unbalanced Bacterial Growth. *PLoS computational biology* **10**, e1003751 (2014).

212 Freeman, J. T., Sexton, D. J. & Anderson, D. J. Emergence of extended-spectrum β-lactamase-producing Escherichia coli in community hospitals throughout North Carolina: a harbinger of a wider problem in the United States? *Clinical Infectious Diseases* **49**, e30-e32 (2009).

213 Coque, T., Baquero, F. & Canton, R. Increasing prevalence of ESBL-producing Enterobacteriaceae in Europe. *Euro surveillance: bulletin Europeen sur les maladies transmissibles= European communicable disease bulletin* **13**, 5437-5453 (2008).

214 Villegas, M., Kattan, J., Quinteros, M. & Casellas, J. Prevalence of extended-spectrum β-lactamases in South America. *Clinical Microbiology and Infection* **14**, 154-158 (2008).

215 Milo, R. BioNumbers: Useful Fundamental Numbers in Molecular Biology. *Nucleic Acids Research* **38**, 3 (2010).

216 Bergan, T. Pharmacokinetics of beta-lactam antibiotics. *Scandinavian journal of infectious diseases. Supplementum* **42**, 83-98 (1983).

217 Drusano, G. L. Role of pharmacokinetics in the outcome of infections. *Antimicrobial agents and chemotherapy* **32**, 289 (1988).

218 Zlokarnik, G. *et al.* Quantitation of transcription and clonal selection of single living cells with β-lactamase as reporter. *Science* **279**, 84-88 (1998).

219 O'Callaghan, C. H. & Morris, A. Inhibition of β-Lactamases by β-Lactam Antibiotics. *Antimicrobial agents and chemotherapy* **2**, 442-448 (1972).

Biography

Hannah Meredith was born in Richmond, Virginia on February 12, 1990. She began undergraduate school at the University of Virginia in August, 2008 and received her Bachelors of Science in Biomedical Engineering in May, 2012. She joined Dr. Lingchong You's lab in Duke's Biomedical Engineering Department in August, 2012 as a National Science Foundation Graduate Research Fellow. In May, 2017, Hannah completed a Doctoral Certificate in Global Health. She was also selected to be a Whitaker Scholar and will be moving to London, England next to conduct a year of post-doctoral research at the London School of Hygiene and Tropical Medicine. A complete list of publications follows:

1. **Meredith, H.R.**, Andreani, V., Lopatkin, A.J., Lee, A.J., Anderson, D.J., Batt, G., and You, L. (2017) A resistance-resilience framework to dissect bacterial antibiotic responses. *Under Review.*
2. Lee, A.J., Wang, S., **Meredith, H.R.**, Zhuang, B., and You, L. (2017). Growth rates predict β-lactam-mediated lysis rates. *Under Review.*
3. Lopatkin, A.J., **Meredith, H.R.**, Srimani, J.K., Durrett, R., and You, L. (2017). Persistence and reversal of plasmid-mediated antibiotic resistance. *Nature Communications*, in press.
4. **Meredith, H.R.**, Lopatkin, A.J., Anderson, D.J., and You, L. (2015). Bacterial temporal dynamics enable optimal design of antibiotic treatment. *PLoS Computational Biology.*
5. **Meredith, H.R.,** Srimani, J.K., Lee, A.J., Lopatkin, A.J., You, L. (2015). Collective antibiotic tolerance: Mechanisms, dynamics, and intervention. *Nature Chemical Biology,* 11 (3), 182-188.
6. Tanouchi, Y., Lee, AJ, **Meredith, H**, You, L. (2013). Programmed cell death in bacteria and implications for antibiotic therapy. *Trends in Microbiology*, 21 (6), 265-270.